The Sensitivity of the Walker Circulation to Different basic States in a Linear Model

By
Karen H. Rosenlof and Duane E. Stevens

Department of Atmospheric Science
Colorado State University
Fort Collins, Colorado

Colorado State University

Department of Atmospheric Science

Paper No. 385

THE SENSITIVITY OF THE WALKER CIRCULATION TO DIFFERENT BASIC STATES IN A LINEAR MODEL

by

Karen Hepler Rosenlof

and

Duane E. Stevens

Research supported by the

National Science Foundation
under grant
ATM-8305759

Department of Atmospheric Science
Colorado State University
Fort Collins, Colorado

December, 1984

Atmospheric Science Paper No. 385

ABSTRACT

The term Walker Circulation is used to refer to the zonal overturning across the equatorial Pacific driven by enhanced convection over the Indonesian region. In this work, we attempt to simulate the Walker Circulation with a linear model including cumulus friction forced by a stationary tropical heat source. The sensitivity of the model circulation to changes in the basic state is examined. A non-zero mean zonal wind basic state is found to enhance the extratropical response to the tropical heat source. Including a mean Hadley cell in the basic state acts to raise the level of zero wind in the model Walker Circulation. In addition, the advective processes of a mean Hadley cell tend to enhance the extratropical response in the case where the heating is embedded almost entirely in mean easterly winds. When the mean Hadley cell is not included for this case, the main response is confined to the tropics.

Atmospheric Science Department
Colorado State University
Fort Collins, Colorado 80523
Fall 1984

AKNOWLEDGEMENTS

We would like to thank Drs. Wayne Schubert and Paul Duchateau for their reviews of this research. We would also like to thank Dr. John Anderson for several helpful discussions. We would also like to thank Paul Ciesielski for his assistance with computer programming, and Gail Watson for typing the manuscript.

This work was sponsored by the National Science Foundation, under grant ATM-8305759. Computing support was provided by the National Center for Atmospheric Research.

This paper is from a thesis submitted to the Academic Faculty of Colorado State University in partial fulfillment of the requirements for the degree of Master of Science.

TABLE OF CONTENTS

1. Introduction

Bjerknes (1969) introduced the term Walker Circulation to refer to a zonal overturning across the equatorial Pacific driven by the ascent of moist air in the western equatorial Pacific. It was named in honor of Sir Gilbert Walker because of its close ties to Walker's Southern Oscillation. Newell et al. (1974) define the circulation somewhat differently, as the deviation of the wind field from the zonal average. This then results in a series of cells around the globe (Fig. 1.1) rather than the one cell that Bjerknes envisioned. However the predominant cell is the response to the greater latent heating in the Indonesian region of the western Pacific.

The Walker circulation is a thermally direct circulation that rises in the western Pacific and has a wide band of subsidence over the eastern Pacific. Bjerknes' theory was that the circulation is the manifestation of a sea surface temperature gradiant. His idea for the maintenance of the circulation is as follows. In the eastern Pacific, upwelling of cool water keeps the air above it too cold to ascend in a Hadley type circulation. Instead, this air flows to the west towards Indonesia where there exists warmer water and thus the air can warm and rise. Warm sea surface temperatures would then provide condensational heating to drive the rising motion above the heat source. However, a budget study by Cornejo-Garrido and Stone (1977) brings about questions as to whether Bjerknes' theory is correct. They agreed that the main

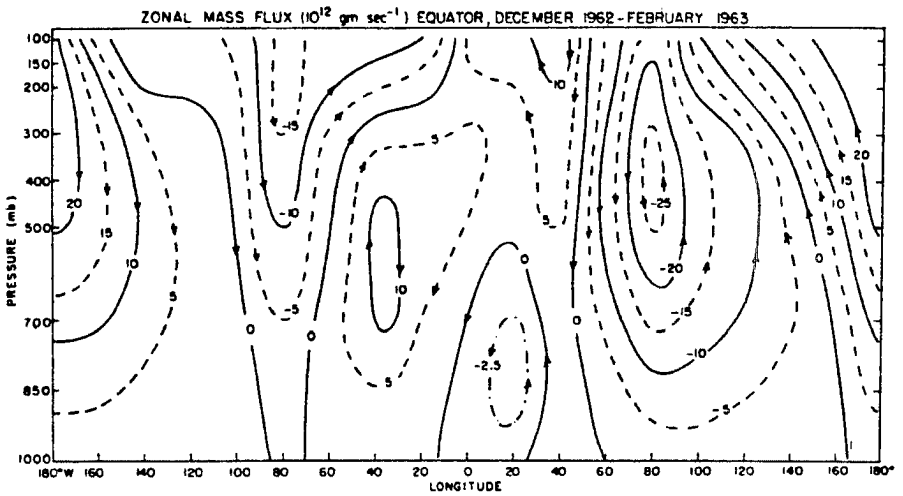

Fig. 1-1. Contours of zonal mass flux in a 10° wide strip centered on the equator. Figure is taken from Newell et al. (1974).

drive for the circulation is the heating due to zonal variations in condensation; however, they observed that where condensation is a maximum, surface evaporation turns out to be a minimum. They concluded that enhanced condensation is a consequence of moisture convergence, not enhanced evaporation. Thus we see that the precise mechanisms for maintaining the Walker Circulation and causing the variability in the circulation are not well understood.

Some of the previous work that has been done directly concerning the Walker circulation has treated the interannual variability of the circulation, especially in conjunction with El Niño events. These studies are significant given the global impact of a major surface warming in the eastern Pacific. Rowntree (1972) used the then current GFDL general circulation model and changed the bottom boundary conditions by putting in different sea surface temperatures. His output showed a direct thermal circulation relative to the increased ocean temperatures in the eastern Pacific. This result resembles what happens to the Walker Circulation during an El Niño event. Julian and Chervin (1978) also did a study with a GCM that included eastern Pacific positive sea surface temperature anomalies to determine their effect on the Walker Circulation. The net result in their model was to weaken the Walker Circulation.

These two studies address changes in the Walker Circulation due to anomalous surface conditions, but do not look at what the mechanisms are for creating the circulation in the first place. A number of studies have addressed the response of the atmosphere to tropical heat sources, giving us a better idea of why the circulation is there in the first place and what gives it the structure it exhibits. These studies have

involved much simpler models than the full blown GCM studies and thus give us a better handle on what parameters in the model calculations bring about certain results.

Gill (1980) did an analytical study on heat-induced tropical circulations. He solved a set of equations on a beta-plane using the long wave approximation. These equations were linearized with respect to a motionless basic state. His solutions for the lower level showed that rising motion occurs directly above the heat source, with easterlies to the east of the heat source and a smaller region of equatorial westerlies west of the heat source. He interpreted this solution in terms of equatorially trapped Kelvin and Rossby waves. When the heating is switched on at an initial time, Kelvin waves carry that information eastward only, which in turn creates easterly trades to the east of the heating. Webster (1972) also interpreted the response to a tropical heating as a Kelvin wave acting east of the heating. Only equatorial Rossby waves which have a phase speed approximately one-third that of the Kelvin wave carry information westward. Because of the slower Rossby wave speed, it does not penetrate as far west in the presence of the constant 2 1/2 day Rayleigh friction used in Gill's study as the Kelvin wave does to the east. So, the region of westerlies is narrower than the region of easterlies (Fig. 1.2).

Webster (1981) used a linear spherical primitive equation model with a zonally symmetric basic state to study the atmospheric response to different heatings. He computed the amount of condensational heating that would result from a specified sea surface temperature anomaly and then ran the model to steady state. For a tropical heat source he found low level convergence with stronger winds to the west of the heat source.

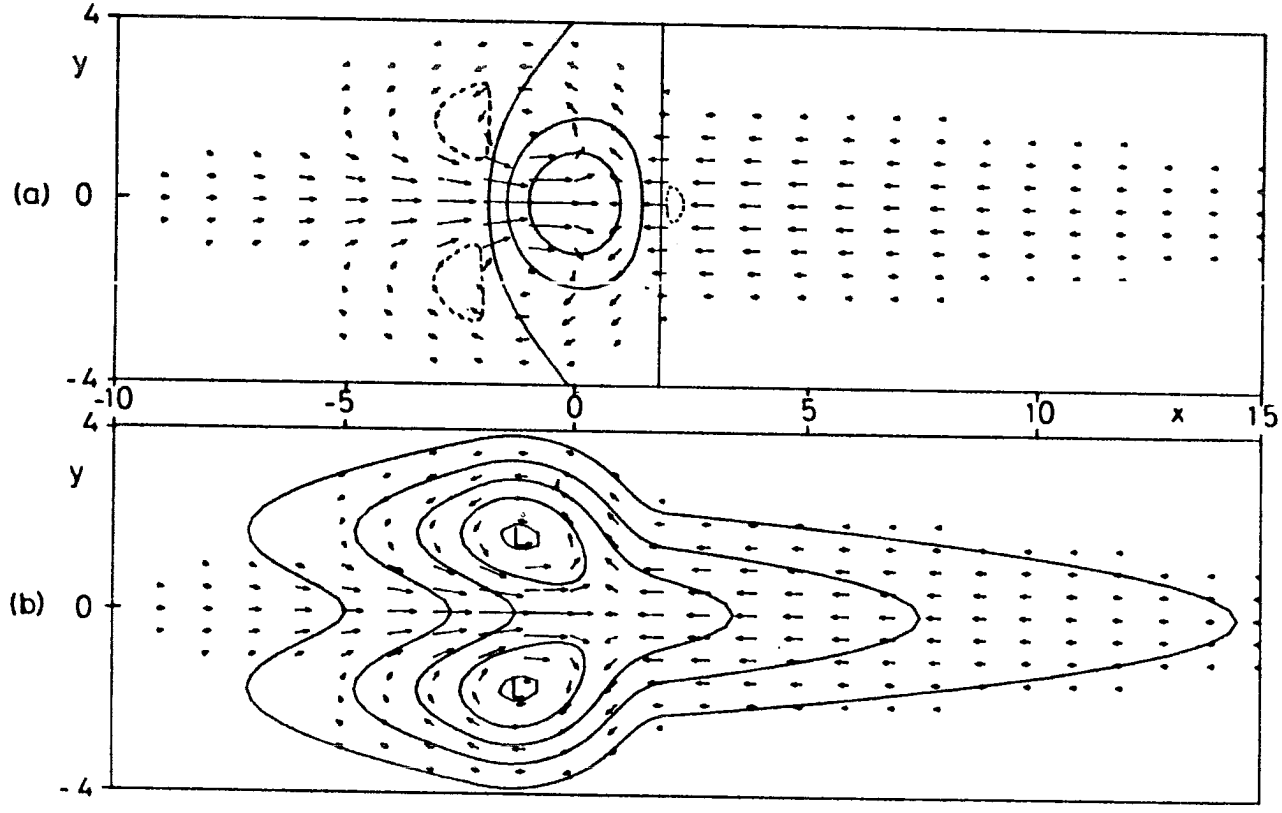

Fig. 1-2. Contours of vertical velocity (a) and perturbation pressure (b) superimposed on the velocity field for the lower layer obtained from the solution for a heating symmetric about the equator from Gill (1980). The heating is confined within $|x| < 2$, with a y dependence given by $\exp(-y^2/4)$.

He found maximum rising motion in the vicinity of the maximum of the condensational heat source as occurs in the observed Walker Circulation.

Lau and Lim (1982) solved the shallow water equations with forcings in different types of mean winds. They concluded that a Walker-type circulation is excited by a heating symmetric about the equator and also identified the response with a Kelvin mode to the east and a Rossby mode to the west of the heating.

Geisler (1981) attempted to isolate a Walker circulation with a linear primitive equation model. Unlike the other studies discussed, his model included momentum rearrangement by cumulus clouds. He forced the model by condensational heating which was the deviation from the zonal average and found the steady state solution. His results show a region of low level easterly winds across most of the Pacific of broader longitudinal extent and weaker than the overturning west of the heat source. This coincides with the observed structure shown in Figure 1.1. However, the level of the zero wind is significantly lower than observed, which may be due to the absence of a mean Hadley cell in the basic state.

Although the studies by Gill, Webster, Lau and Lim, and Geisler produced circulations that qualitatively resemble the observations, there are some aspects that differ from the observed circulation and some potentially significant physical processes that have not been included in these studies. The observed circulation over the Pacific has the zero level of the deviation from the mean zonal wind between 400 and 500 mbs as seen in Figure 1.1. In Geisler's study he tried changing the vertical structure of the heat source in an attempt to determine the effect of that on the zero wind level. Although the zero wind level did

rise when the elevated heat source was used, it was not of much significance since the entire region between 600 and 350 mbs was one of little motion. However, his study did not include a mean vertical velocity in the basic state while it did include a cumulus mass flux. The term $\bar{w} \frac{\partial u}{\partial z}$ and the cumulus friction term probably act to cancel each other out. This would then give a result more like Geisler's case without the cumulus friction which did have a higher zero wind level.

Hartmann et al. (1984) also addressed the question of how important the vertical heating profile is on the structure of the Walker circulation in a linear model. They compared results between using a conventional convective plume heating profile and a mature cloud cluster heating profile which is concentrated in upper layers. They concluded that using the mature cloud cluster heating profile raises the resulting circulation to a height more like that which occurs in the observed circulation. However, they did not include cumulus friction or a mean Hadley cell in their basic state. The presence of a mean Hadley cell may act to raise the height of the resulting circulation without using an elevated heat source.

In this study, we are using a model very similar to the one described in Geisler (1981). As with these other studies, we are using a linear model and are looking at the response to a single tropical heat source. We are adding upon Geisler's study by including first a realistic mean zonal wind field obtained from the FGGE (First GARP Global Experiment) data, and then a prescribed Hadley cell that is computed from an analytical stream function. This study will attempt to determine how important these changes in the basic state are on the

resulting model circulation. Specifically, we will examine how including a mean zonal flow and a mean Hadley cell affect the model response, and what the effects of including cumulus momentum mixing are.

2. Model Description

The model used for this study was developed by Duane Stevens and Paul Ciesielski at Colorado State University. A complete description of the model is given in Stevens and Ciesielski (1984).

The model equations are the primitive equations linearized with respect to an arbitrary basic state. The various basic states used will be discussed in the following sections. The model is formulated on a sphere and employs the hydrostatic approximation. The variables are expanded into a basic state independent of time and longitude and a perturbation which is the deviation from the basic state. The expansion is of the form,

$$X(\lambda, \theta, z, t) = \bar{X}(\theta, z) + X'(\theta, z)e^{i(s\lambda - \sigma t)}$$

where

θ = latitude,

$z = \ln (^{Po}/P)$,

s = wavenumber,

λ = longitude,

σ = frequency,

t = time,

$(\bar{\ })$ = basic state

$(\ )'e^{i(s\lambda - \sigma t)}$ = perturbation on the basic state.

The equations are spectral in longitude; that is, a single Fourier component is assumed in the zonal direction. A frequency is specified by the user; for our study we set the frequency equal to zero and studied the steady state response to a specified perturbation heating. Dissipation is introduced in the form of Rayleigh friction, Newtonian cooling, cumulus friction and vertical diffusion. The linearized equations used are as follows, and a list of symbols used is given in Appendix A.

U momentum equation:

$$\left[-i\sigma + \frac{is\bar{u}}{a\cos\theta} + \alpha_R - \frac{\bar{v}}{a}\tan\theta\right]u' + \frac{\bar{v}}{a}\frac{\partial u'}{\partial\theta} + \bar{w}\frac{\partial u'}{\partial z} - \frac{g}{p}\frac{\partial}{\partial z}(\bar{M}_c u') -$$

$$\frac{g}{p}\frac{\partial}{\partial z}\left(\frac{\mu^\dagger}{H}\frac{\partial u'}{\partial z}\right) + \left[\frac{1}{a}\frac{\partial\bar{u}}{\partial\theta} - \frac{\bar{u}}{a}\tan\theta - f\right]v' +$$

$$\left[\frac{\partial\bar{u}}{\partial z}\right]w' + \left[\frac{is}{a\cos\theta}\right]\phi' = -\frac{g}{p}\frac{\partial}{\partial z}\left[\bar{M}_c u'_c + M_c'(\bar{u}_c - \bar{u})\right] \qquad (2.1)$$

V momentum equation:

$$\left[\frac{2\bar{u}}{a}\tan\theta + f\right]u' + \left[-i\sigma + \frac{is\bar{u}}{a\cos\theta} + \alpha_R + \frac{1}{a}\frac{\partial\bar{v}}{\partial\theta}\right]v'$$

$$+ \frac{\bar{v}}{a}\frac{\partial v'}{\partial\theta} + \bar{w}\frac{\partial v'}{\partial z} - \frac{g}{p}\frac{\partial}{\partial z}(\bar{M}_c v') -$$

$$\frac{g}{p}\frac{\partial}{\partial z}\left(\frac{\mu^\dagger}{H}\frac{\partial v'}{\partial z}\right) + \left[\frac{\partial\bar{v}}{\partial z}\right]w' + \frac{1}{a}\frac{\partial\phi'}{\partial\theta} =$$

$$-\frac{g}{p}\frac{\partial}{\partial z}\left[\bar{M}_c v'_c + M_c'(\bar{v}_c - \bar{v})\right] \qquad (2.2)$$

Hydrostatic approximation:

$$\frac{\partial \phi'}{\partial z} - RT' = 0 \tag{2.3}$$

Continuity equation:

$$\frac{isu'}{a\cos\theta} + \frac{1}{a}\frac{\partial v'}{\partial \theta} - \frac{\tan\theta}{a} v' + \frac{\partial w'}{\partial z} - w' = 0 \tag{2.4}$$

Thermodynamic equation:

$$\left[\frac{1}{a}\frac{\partial \bar{T}}{\partial \theta}\right] v' + \left[\frac{\partial \bar{T}}{\partial z} + \bar{T}\kappa\right] w' +$$

$$\left[-i\sigma + \frac{i\bar{u}s}{a\cos\theta} + \alpha_N + \bar{w}\kappa\right] T' +$$

$$\frac{\bar{v}}{a}\frac{\partial T'}{\partial \theta} + \bar{w}\frac{\partial T'}{\partial z} - \frac{g}{p}\frac{\partial}{\partial z}\left(\frac{\hat{\mu}^{\dagger}}{H}\frac{\partial T'}{\partial z}\right) = \frac{Q'}{C_p} \tag{2.5}$$

The vertical diffusion terms, $\frac{g}{p}\frac{\partial}{\partial z}\left(\frac{\mu^{\dagger}}{H}\frac{\partial u'}{\partial z}\right)$, $\frac{g}{p}\frac{\partial}{\partial z}\left(\frac{\mu^{\dagger}}{H}\frac{\partial v'}{\partial z}\right)$, and $\frac{g}{p}\frac{\partial}{\partial z}\left(\frac{\hat{\mu}^{\dagger}}{H}\frac{\partial T'}{\partial z}\right)$ are necessary for the numerical integration scheme to give nonsingular solutions. Stevens et al. (1977) noted that vanishing of the mass flux M_c at cloud top gives singular solutions of the inviscid equations which can be avoided by including small vertical diffusion terms.

The upper boundary conditions are

$$\frac{\partial u}{\partial z} = \frac{\partial v}{\partial z} = \frac{\partial T}{\partial z} = 0$$

and divergence equal to zero. The lower boundary conditions are

$$\frac{\partial u}{\partial z} = BC \cdot u,$$

$$\frac{\partial v}{\partial z} = BC \cdot v,$$

$$\frac{\partial T}{\partial z} = BC3 \cdot T$$

where

$$BC = \frac{\bar{H}_o \cdot CD \cdot V_o}{\nu_o}$$

$$BC3 = \frac{\bar{H}_o \cdot CD \cdot V_o}{\hat{\nu}_o}$$

and $\bar{H}_o = \frac{RT_o}{g}$, $\nu_o = \nu(z = 0)$, $\hat{\nu}_o = \hat{\nu}(z = 0)$,

and physical vertical velocity equal zero unless otherwise noted. At the model edges, the meridional velocity vanishes.

The model is actually run with $\sin(\theta)$ as the latitudinal coordinate. This places half of the grid points between 30°S and 30°N which is the region we are most interested in studying.

The basic state temperature profile is computed so that the mean zonal wind is in thermal wind balance with the mean temperature distribution. A mean tropical sounding placed at the equator is used as a starting point. The basic state wind fields are arbitrary.

A second order finite difference scheme is used in the vertical and latitudinal directions. The system is then solved in a manner similar to that described in Lindzen and Kuo (1969).

The model is run for several wavenumbers, then the responses are summed up to give the perturbation heating a Gaussian dependence in longitude. The amplitudes are given by the Fourier transform of the heating function. For each wavenumber the amplitude is:

$$\text{Amp} = \frac{\lambda_o}{\sqrt{\pi}} \text{ erf } (\pi/\lambda_o) \begin{cases} \exp \dfrac{(-s^2\lambda_o^2)}{4} & s \neq 0 \\ \dfrac{1}{2} & s = 0 \end{cases} \tag{2.6}$$

where λ_o is the Gaussian scale and s the zonal wavenumber.

3. Comparison with Geisler's Model

Initially, we made two model runs as similar as possible to those discussed in Geisler (1981) in order to assess the similarities and differences between the two models. The first run includes Rayleigh friction and the second run has a cumulus friction term instead of Rayleigh friction.

As Geisler did, we used a heating function that has a vertical dependence that is cubic in pressure. The form of the perturbation heating function is,

$$Q = \exp\left(-(\lambda/\lambda_o)^2\right) \exp\left(-(y/y_o)^2\right) F(p) \tag{3.1}$$

where λ is longitude, $\lambda_o = 40°$, y is sin(latitude), and λ_o is sin(11.5°) = 0.2. The vertical dependence is of the form

$$F(p) = Q_o(p - p_T)(p - p_2)(p - p_b) \tag{3.2}$$

where p_T = 140 mb, p_b = 900 mb, p_2 is chosen to give a maximum heating at 400 mb, and Q_o is chosen to give a maximum precipitation rate of 1 cm/day. (Fig. 3.1)

The mass flux profile is of the form $\frac{\bar{M}_c}{\bar{M}_{co}} = 1 - \exp\frac{-(p - p_T)}{p_D}$ where p_T corresponds to cloud top (140 mb) and p_D is a detrainment scale (100 mb). This form follows that given in Stevens et al. (1977). $g\bar{M}_{co}$ = 2.5 mb/hr as used in Geisler (1981) which corresponds to a zonally averaged rainfall close to the observed mean of 2 m/yr.

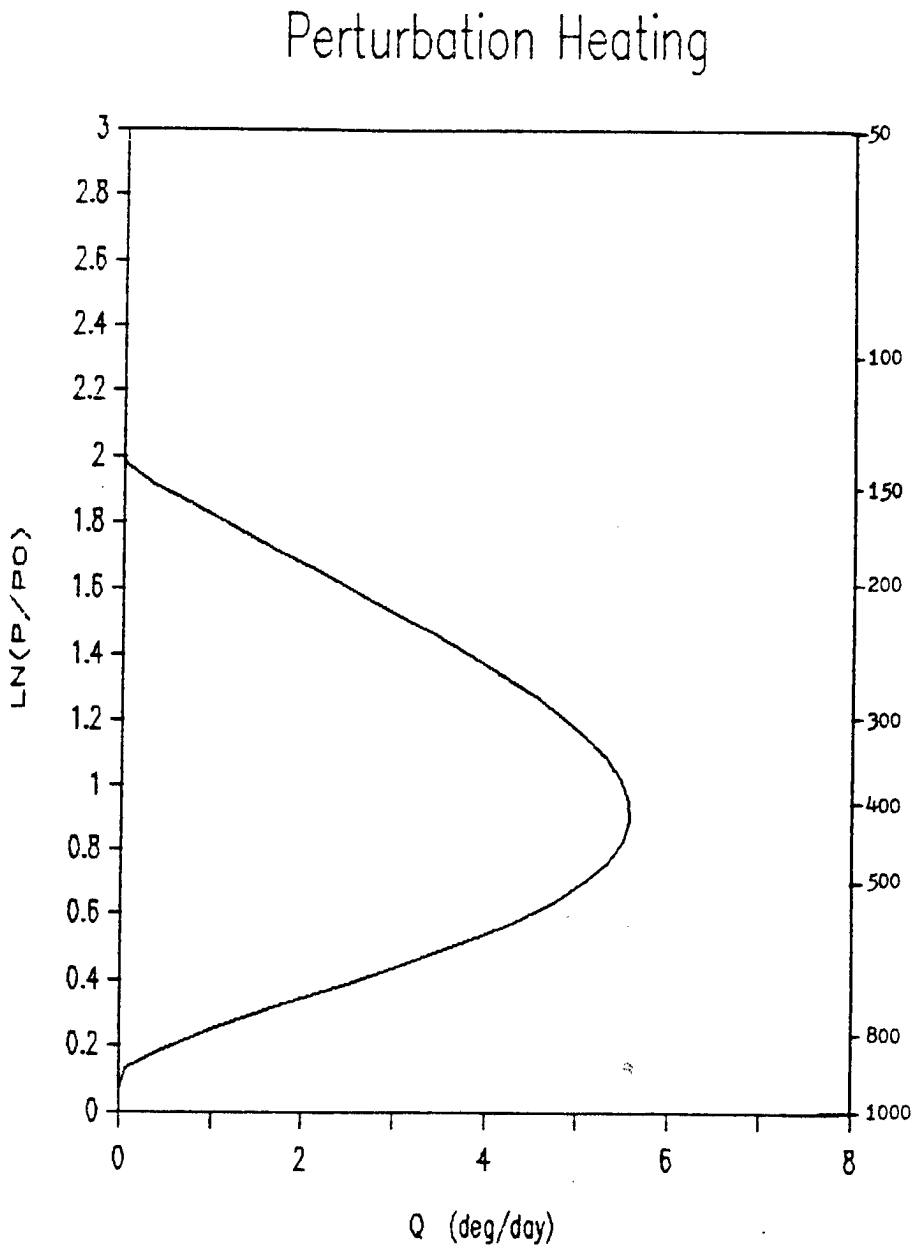

Fig. 3-1. Vertical distribution of the perturbation heating used for comparison with Geisler's (1981) runs. It is normalized to a precipitation rate of 3.65 m/yr.

With the Walker Circulation considered to be the response to the deviation of precipitation from the zonal average, we can then use a perturbation heating that averages to zero around the globe. Following Geisler (1981), we place the base level of the Gaussian in longitude at 1.2 m/year. This is because the zonal average of a Gaussian with an amplitude of 1 cm/day and an e-folding width of 40° is 0.8 m/yr which is then subtracted from the zonal mean of 2 m/yr. This gives the heating field that is shown in Fig. 3.2. In actually running the model, this amounts to neglecting the wavenumber zero response.

The model Geisler used has constant static stability. This would correspond to the mean temperature profile that is given in Fig. 3.3. Note that this profile has no tropopause. The Newtonian cooling coefficient for these comparison runs is α_N^{-1} = 15 days. For the case with no cumulus friction, the Rayleigh friction coefficient is α_R^{-1} = 5 days. The model is run with 41 grid points in the vertical and 25 grid points in the latitudinal direction. Ten wavenumbers are summed using the weighting factors given in (2.6) to obtain the complete wind fields for the Gaussian anomaly.

First we will compare our model results for wavenumber one alone to those presented in Geisler (1981). For these runs the model top was placed at z = 2.56 which corresponds to Geisler's runs with H = 8.8 km. We used the same boundary conditions specified in Geisler's model for these comparison runs, that is, a rigid lid at the top and w = 0 at the bottom.

The phase-amplitude diagram for the perturbation zonal velocity on the equator from our model (Fig. 3.4) is virtually identical to the results shown in Geisler's paper (Fig. 3.5). Our results for the case

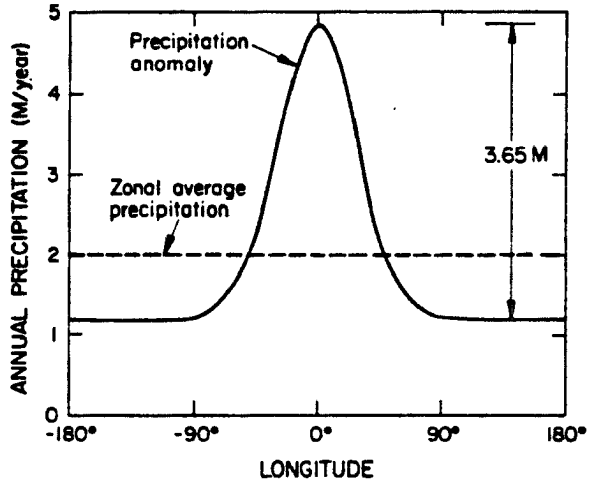

Fig. 3-2. Horizontal distribution of the perturbation heating used for comparison with Geisler's (1981) runs. The solid line is a Gaussian with an e-folding width of 40°. This distribution is partitioned into a zonal average of 2 m/yr plus an anomaly. Figure is taken from Geisler (1981).

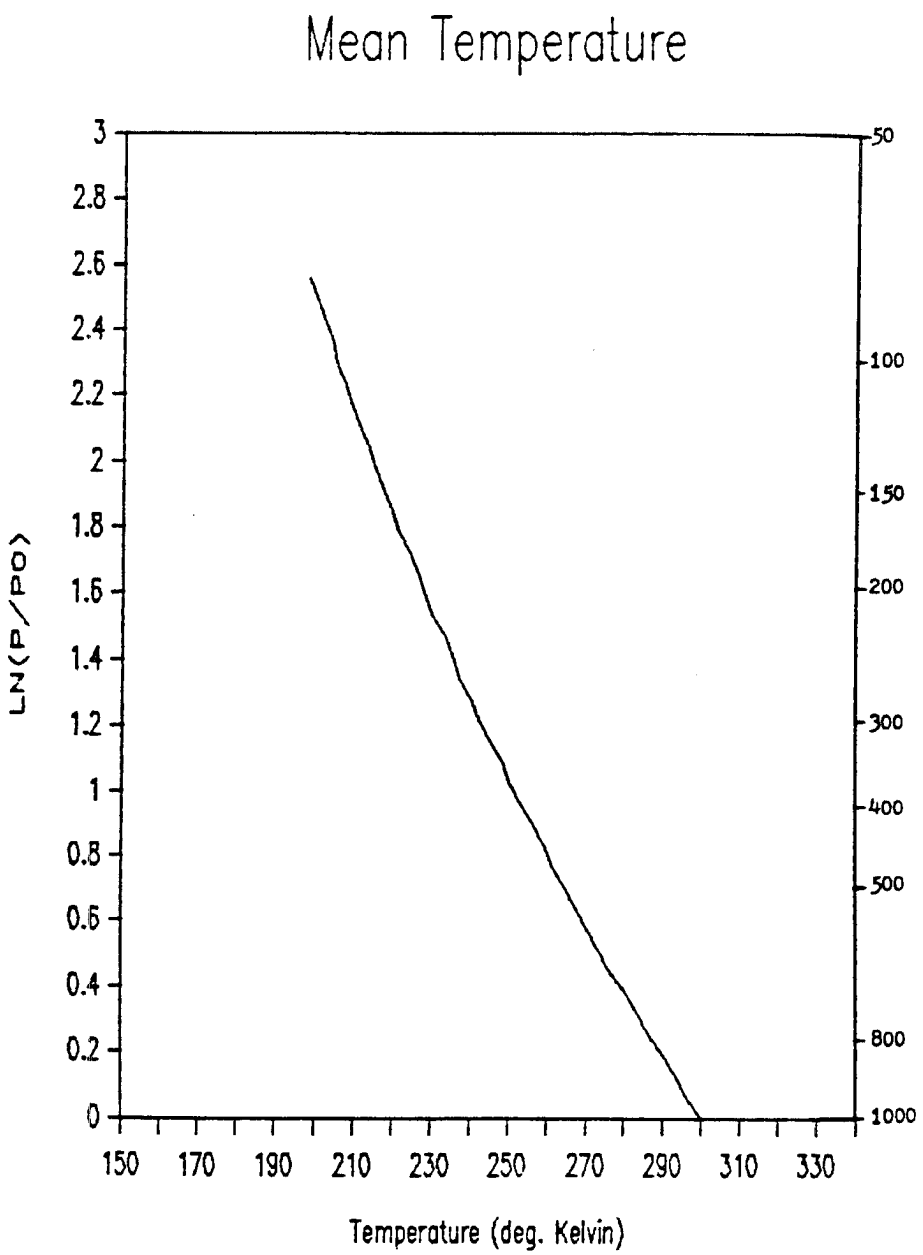

Fig. 3-3. Temperature profile used as the mean tropical sounding for comparison with Geisler's (1981) runs.

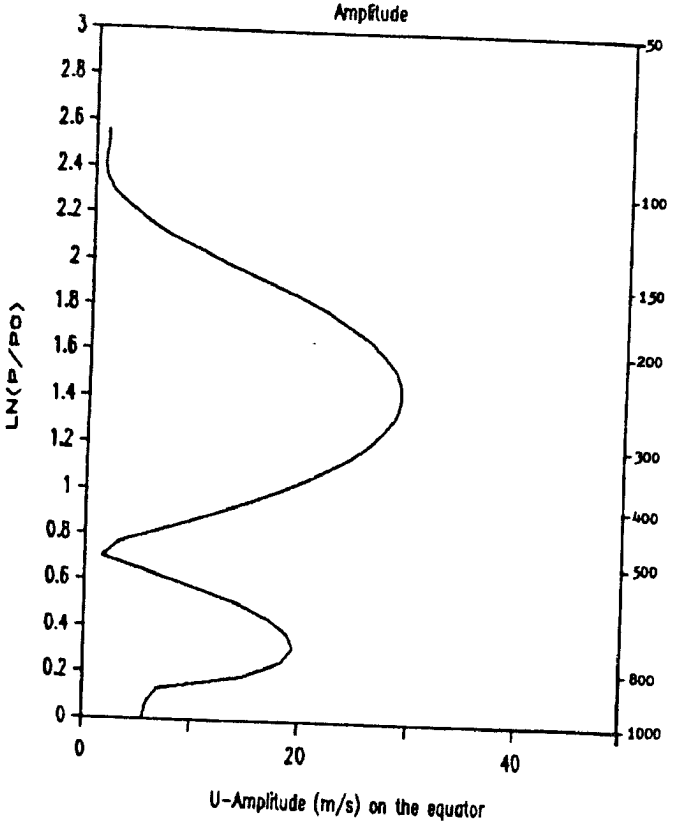

a)

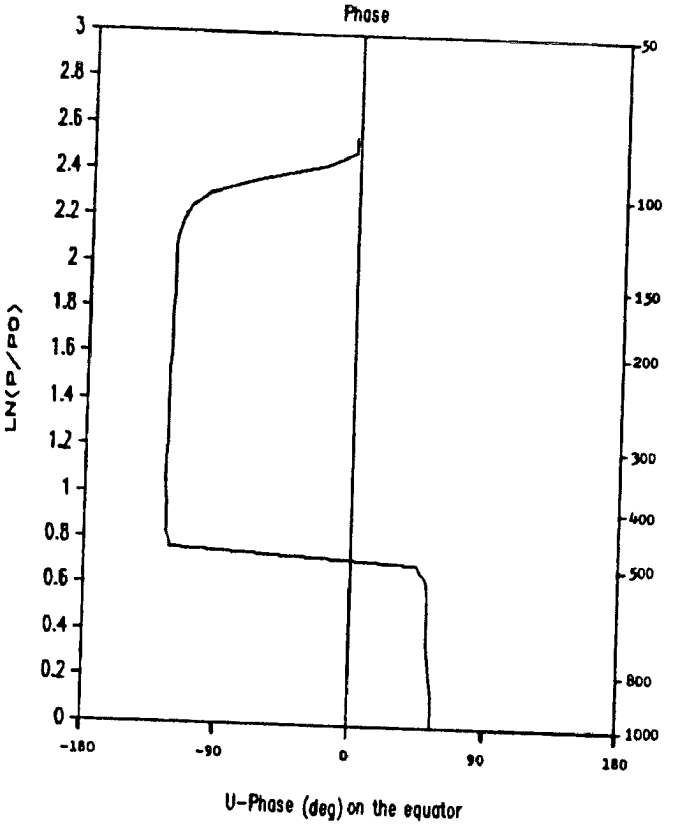

b)

Fig. 3-4. The amplitude (a) and phase (b) of zonal wind on the equator for wavenumber one forcing only. This is for the case of Rayleigh friction having α_R^{-1} = 5 days.

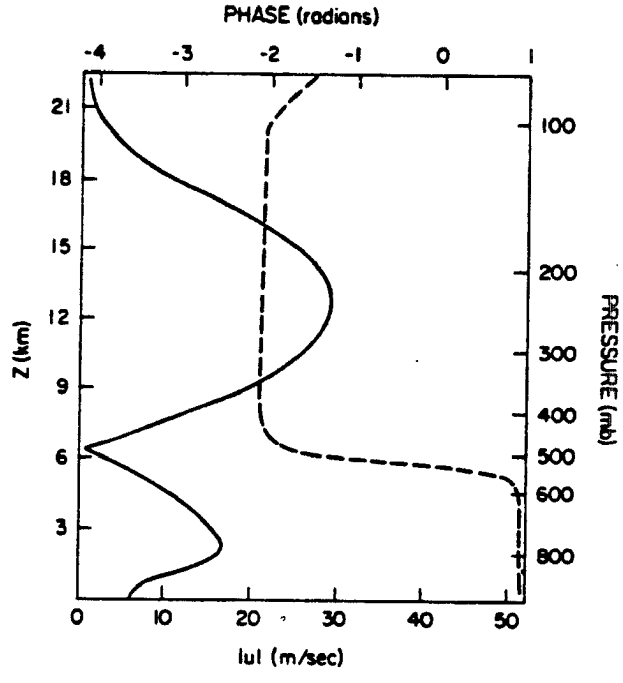

Fig. 3-5. Amplitude (solid line) and phase (dashed line) of zonal wind on the equator for wavenumber one forcing only from Geisler (1981) for his run with Rayleigh friction having $\alpha_R^{-1} = 5$ days.

including cumulus friction (Fig. 3.6) are similar but not identical to Geisler's (Fig. 3.7). The zero wind levels are at approximately the same pressures, however the amplitudes of the upper maximum and lower maximum are slightly larger than those obtained with Geisler's model. This is probably a consequence of the higher vertical resolution in our model, 41 vertical levels as opposed to 16 vertical levels. With the higher number of vertical levels, we are better resolving $\frac{\partial}{\partial z}(\bar{M}_c u'_c)$ in the upper levels where it is a dominant term and $\frac{\partial}{\partial z}(\bar{M}_c u')$ in the lowest levels where it is a very significant term. The amplitudes of the various terms are shown in Figure 3.8.

Although the values for u' on the equator seem to be in good agreement with Geisler's results, when we obtain the solution for the Gaussian anomaly, our results for the run which includes cumulus friction look quite different from Geisler's in both the upper and lower levels.

Geisler's results are shown in Figure 3.9. His figure at 9.75 km would correspond to 330 mb and .75 km would correspond to 918 mb. We have shown results from our model for the closest levels to those given by Geisler.

First we will examine the major differences in the upper level winds. The perturbation velocity winds output from our model run are pictured in Figure 3.10a. The structure of the easterly perturbation winds immediately to the west of the heat source is quite similar to Geisler's case as far as the u field is concerned. However, the region of westerlies to the east of the heat source exhibits a significantly different structure in our results. We see the appearance of a westerly jet at approximately 20° from the equator and 30° to the west of the center of the heat source.

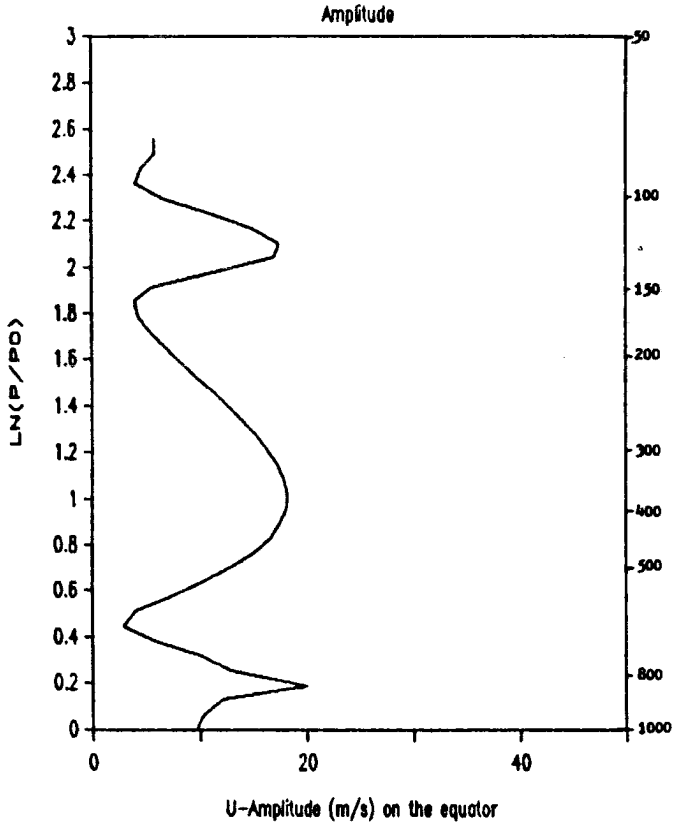

a)

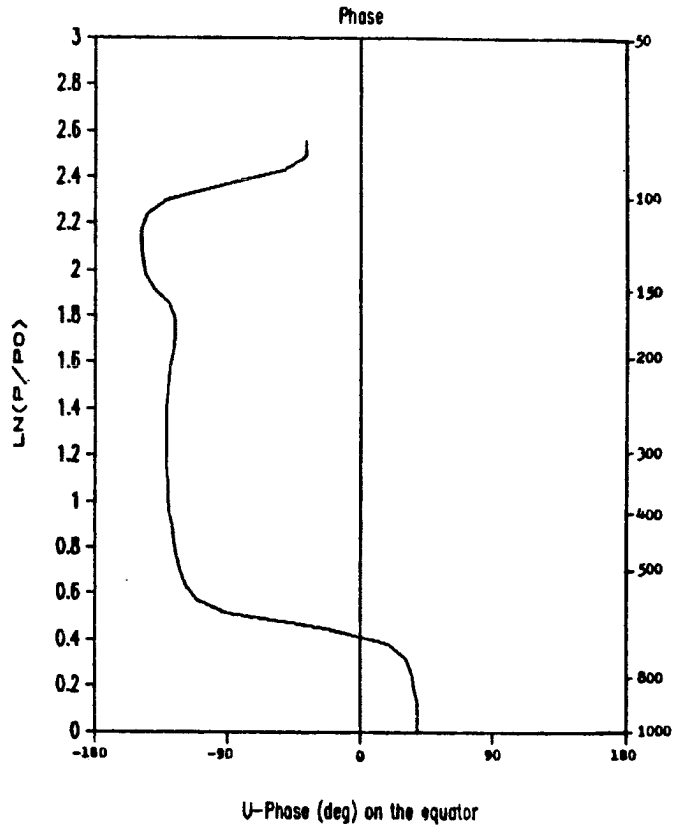

b)

Fig. 3-6. As in Fig. 3.4 except with Rayleigh friction replaced by cumulus friction.

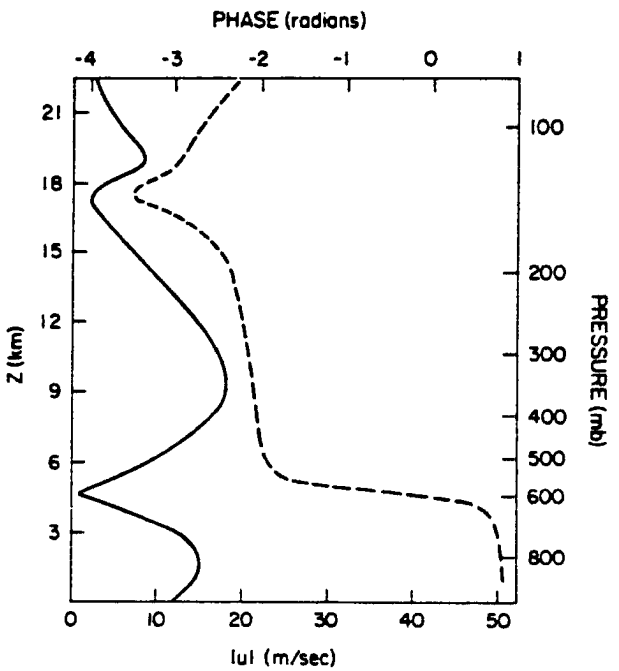

Fig. 3-7. As in Fig. 3.5 except with Rayleigh friction replaced by cumulus friction. Figure taken from Geisler (1981).

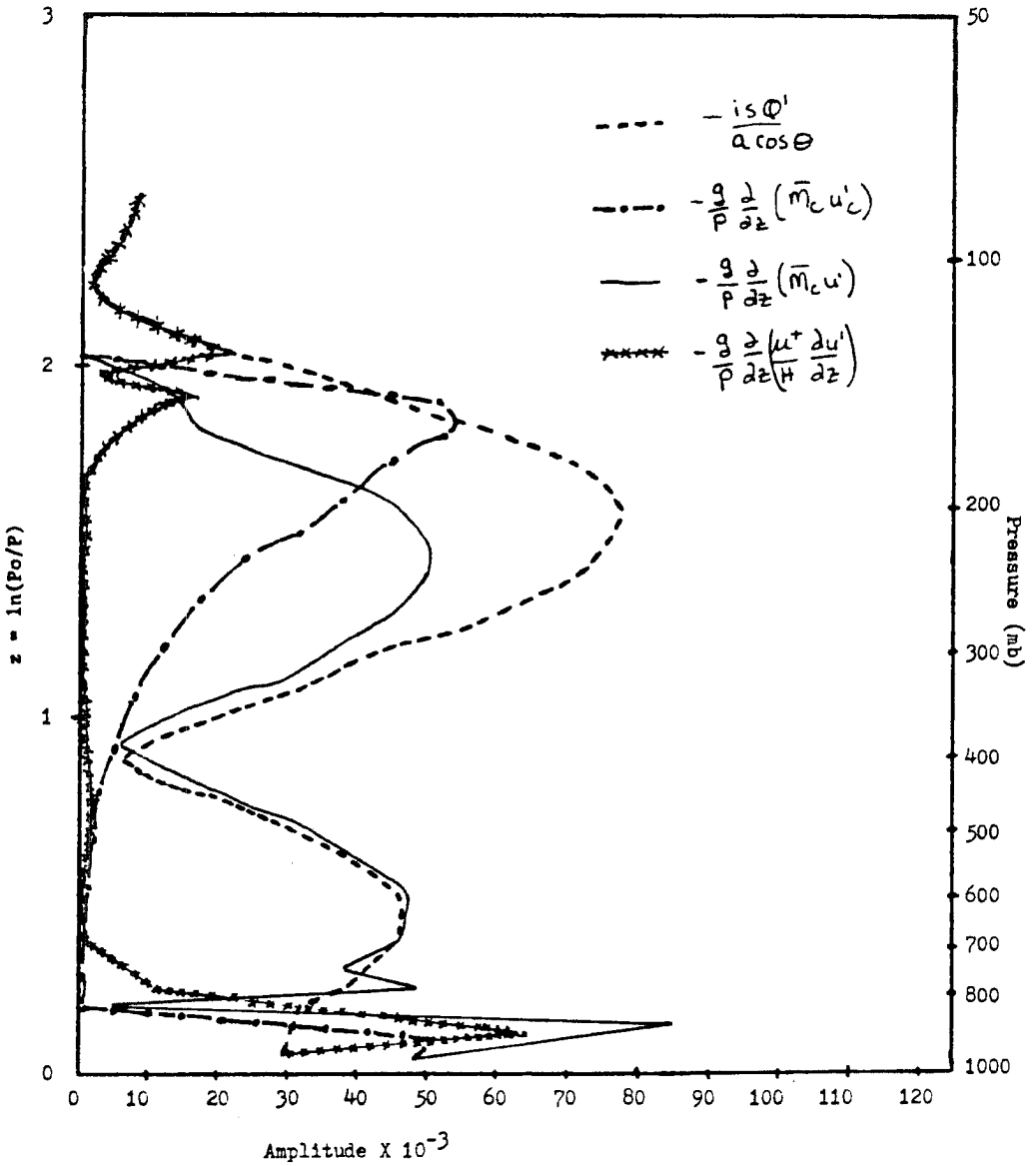

Fig. 3-8. Nondimension amplitude of terms at the equator in the u-momentum equation for wavenumber one only. These are for the case including cumulus friction.

a)

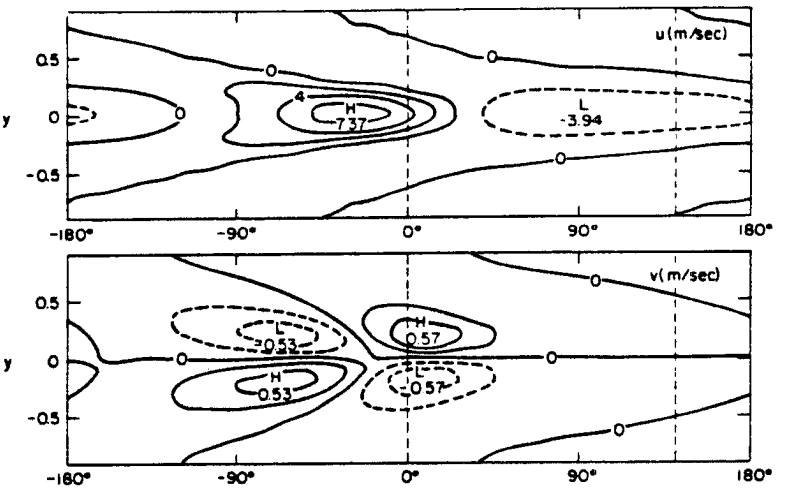

b)

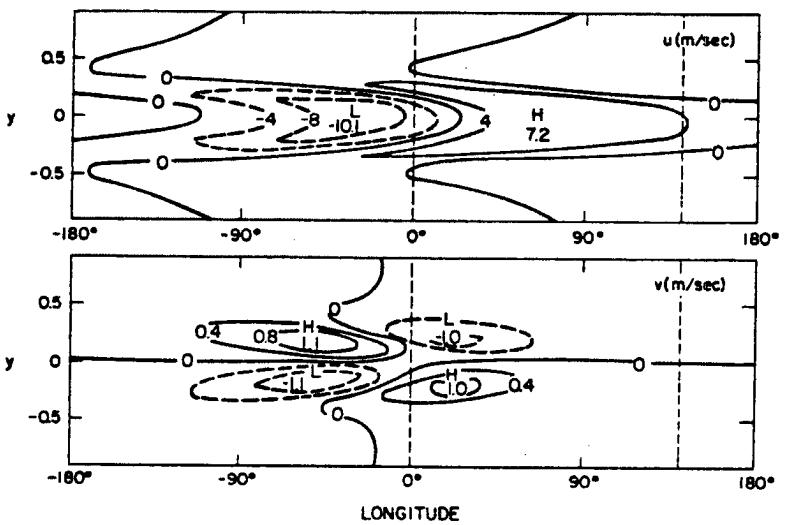

Fig. 3-9. Contours of zonal and meridional velocity at 918 mb (a) and 330 mb (b) as derived by Geisler (1981) for the case including cumulus friction. Dashed lines mark the longitudinal extent of the equatorial pacific.

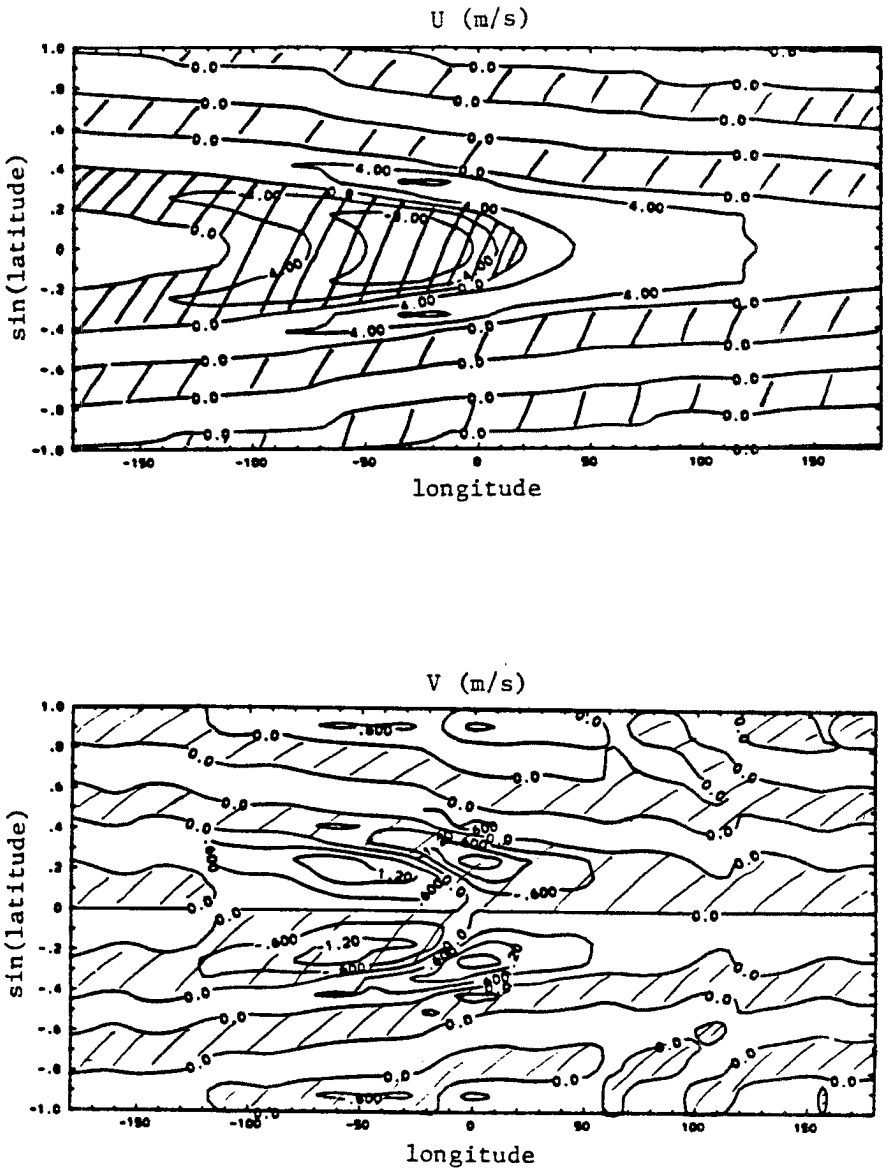

Fig. 3-10a. Contours of zonal (upper panel) and meridional (lower panel) velocity at the level of maximum outflow, 337 mb, for the case including cumulus friction.

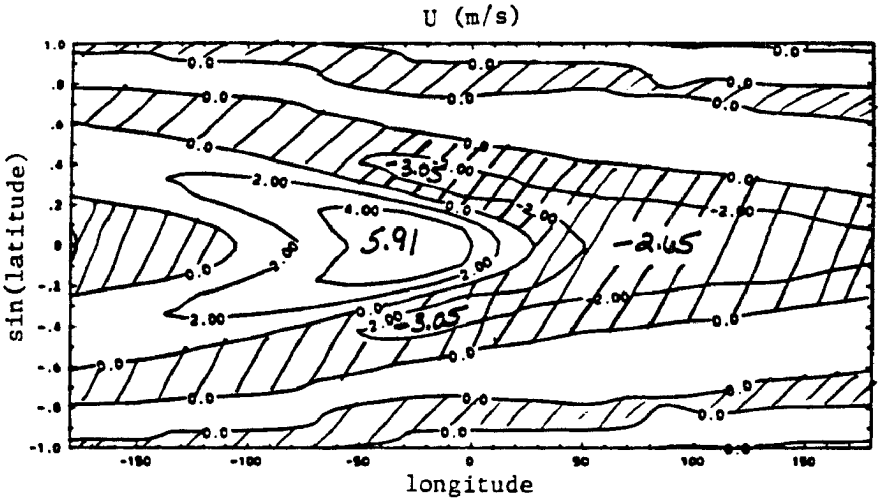

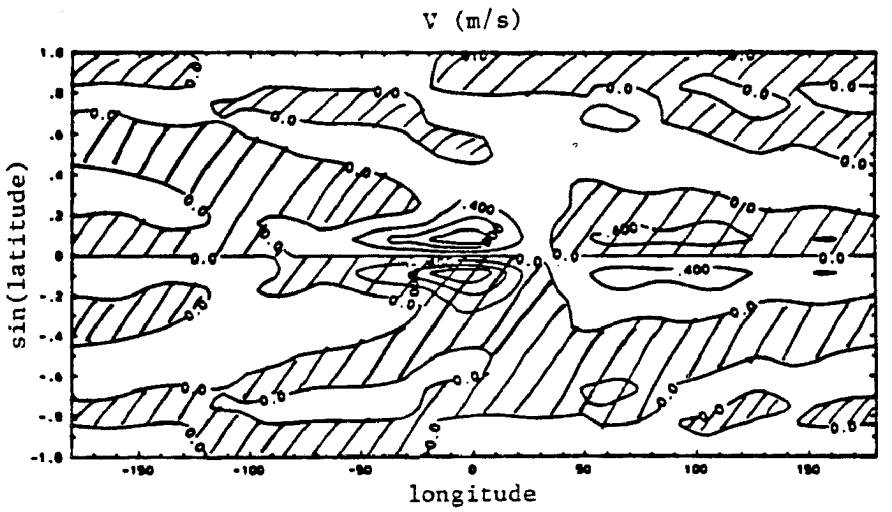

Fig. 3-10b. As in Fig. 3.10a but for the second model level, 938 mb.

In addition, the v field we obtain is somewhat different from that shown in Geisler's paper. To the west of the heat source, the overall pattern is similar although we find a larger magnitude in the circulation that operates in a sense opposite to that of a Hadley cell. The circulation that acts to oppose the Hadley cell has its maximum about 10° east of the center of the heating in our run, but in Geisler's case the maximum occurs about 30° east of the center of the heating. We also find that to the east of the heat source, the circulation that acts to enhance the Hadley cell is stronger than for Geisler's run.

If we compare the two models' results in the lower levels, again we see differences. Our perturbation u field (Fig. 3.10b) is similar to Geisler's west of the heating, but much different east of the heating. Again, our maximum is off the equator in the response east of the heating while Geisler's is not. Our v field response that acts to oppose the Hadley cell has its maximimum very close to the center of the heating as does Geisler's. However, our v field response that acts to enhance the Hadley cell covers a broader longitudinal region than does Geisler's. It also has its maximum east of the heating rather than west of the heating as occurs in Geilser's run. These differences in the lower levels are probably due to the viscosity profile we are using. For our run, the diffusion terms are of the form $\frac{g}{p}\frac{\partial}{\partial z}\left(\frac{\mu^{\dagger}}{H}\frac{\partial V}{\partial z}\right)$, where $\frac{\mu^{\dagger}}{H}$ is a function of height. In the lowest 100 millibars of the model this is a dominant term and is probably contributing to the differences in the lower levels. For our run we use a larger viscosity below cloud base to simulate a boundary layer. In other runs we will discuss in later sections, a viscosity profile was used that did not include a higher value of viscosity near the surface and for these cases, the

maximum in the v field in the lowest levels occurs near 60 degrees west of the heating as is the case in Geisler's run. For the run Geisler did, he used a diffusion term of the form $\frac{\partial}{\partial z}$ ($K \frac{\partial V}{\partial z}$) where $K = 5 \times 10^4$ $\frac{cm^2}{s}$, not a function of height. However, this is not a dominant term near 300 mb and does not explain the differences in the u field there.

Because we found these differences between the two models, we tried a third model to see if it would agree with our results. John Anderson (1984) has developed a prognostic model to study the 40-50 day oscillation that is very similar to ours as far as the equations are concerned, but is solved using completely different techniques. To obtain a steady state solution, we ran his model to equilibrium. His model is also linear, is formulated on a finite beta-plane, and is spectral in both horizontal directions. His model has the same cumulus friction parameterization as previously discussed, and was forced with the same cubic heating profile. Different mean temperature and viscosity profiles were used. The resulting perturbation u field at the closest level in John Anderson's model that corresponds to the level being discussed is shown in Figure 3.11. This model also produces westerly jets of a similar magnitude between 15° and 20° off the equator. This result gives us confidence that the cumulus friction parameterization is correctly done in our model.

Because of this agreement between two independent models, we suspect a possible coding error in Geisler's implementation of cumulus friction. We intend to pursue this question further in consultation with Professor Geisler.

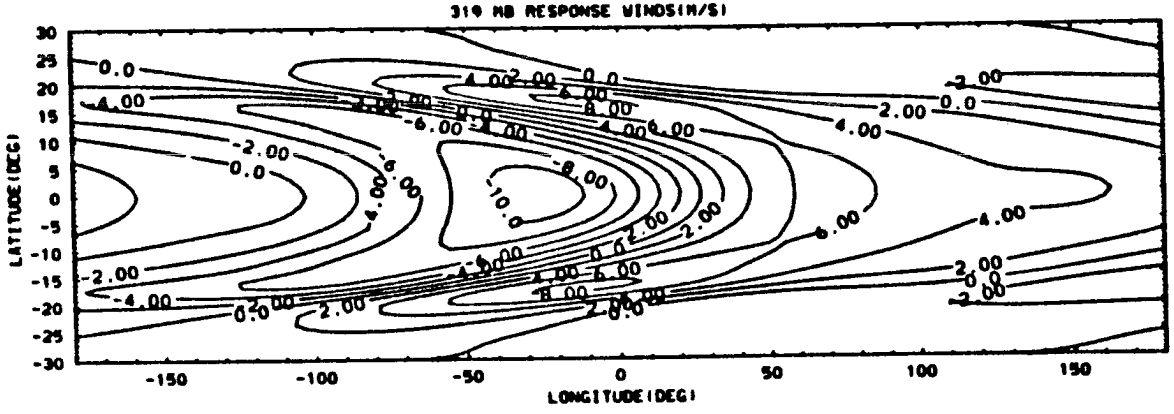

Fig. 3-11. Contours of zonal velocity at 319 mb computed using John Anderson's model.

4. Effects of changing stability and adding a mean cumulus mass flux

One step that can be taken to approach a more realistic basic state on which to simulate a Walker Circulation is to use a realistic temperature profile. The temperature profile used for the runs discussed in the previous section did not have a tropopause, however cloud top did not go to the top of the model, but cut off at 140 mb. For the runs we will discuss in this section, a mean tropical temperature was obtained from the U.S. Standard Atmosphere Supplement (1966). This profile is shown in Figure 4.1. The tropopause is located at 100 mb and the heating (Fig. 4.2) and mass flux profile both extend from 900 mb to tropopause height. The heating is of the same horizontal structure as used in Geisler (1981). The vertical dependence is as given in equation 3.2, with p_T = 100 mb, p_b = 900 mb, and Q_o again chosen to give a precipitation rate of 1 cm/day.

For the runs that did not include $\bar{M}_c$, the structure of the response below 250 mb (Fig. 4.3) is very similar to the response using Geisler's mean temperature profile (Fig. 3.4). Because the heating extends higher for the case with the tropopause, we see a larger response in the upper troposphere. The results summed up for wavenumbers one to ten are shown in Figures 4.4 and 4.5. At comparable levels, the response for the two cases near 300 mb are nearly the same. Essentially, the change in mean stability does not affect the response for the case where there is no mean cumulus mass flux.

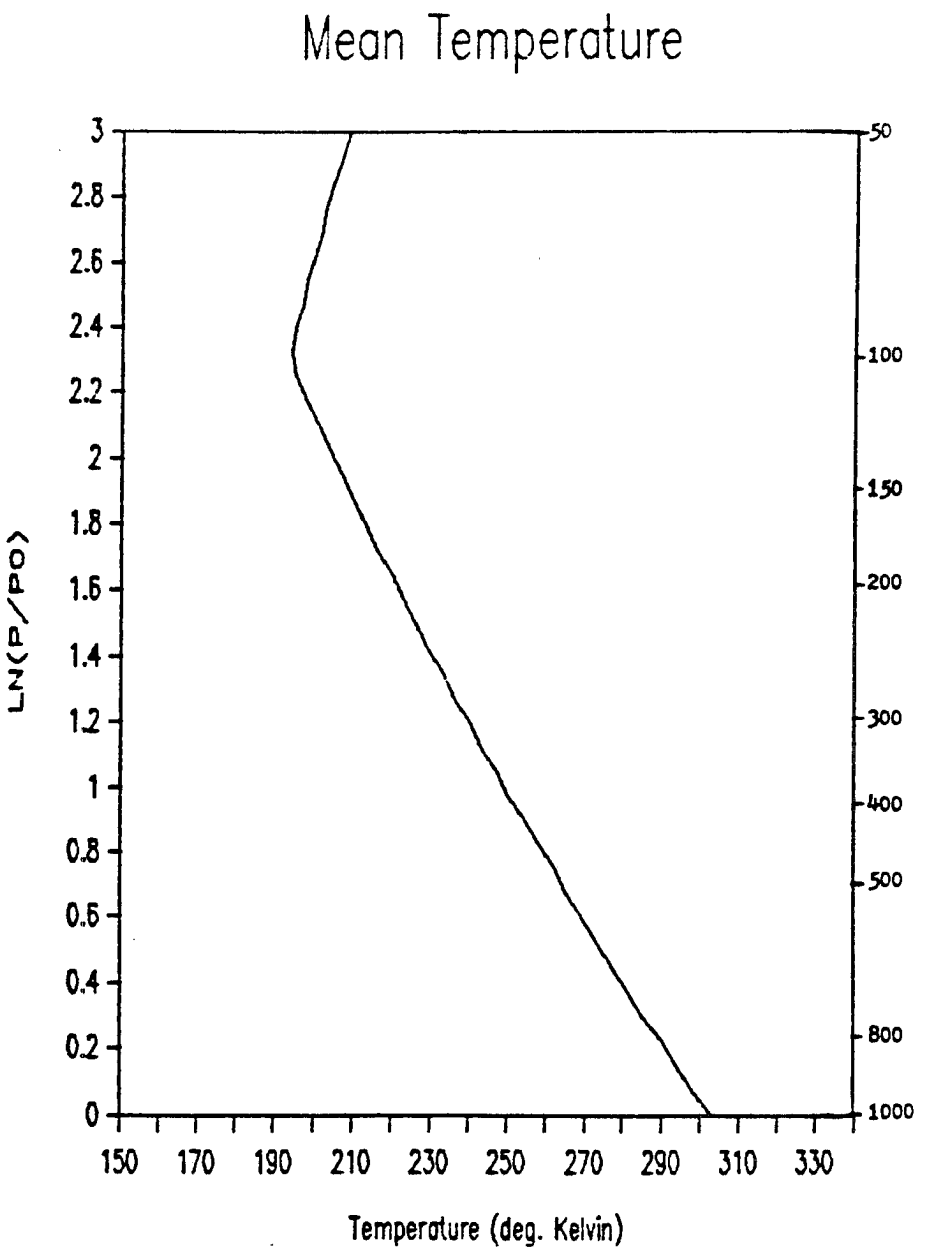

Fig. 4-1. Temperature profile used as the mean tropical sounding for cases which include a tropopause.

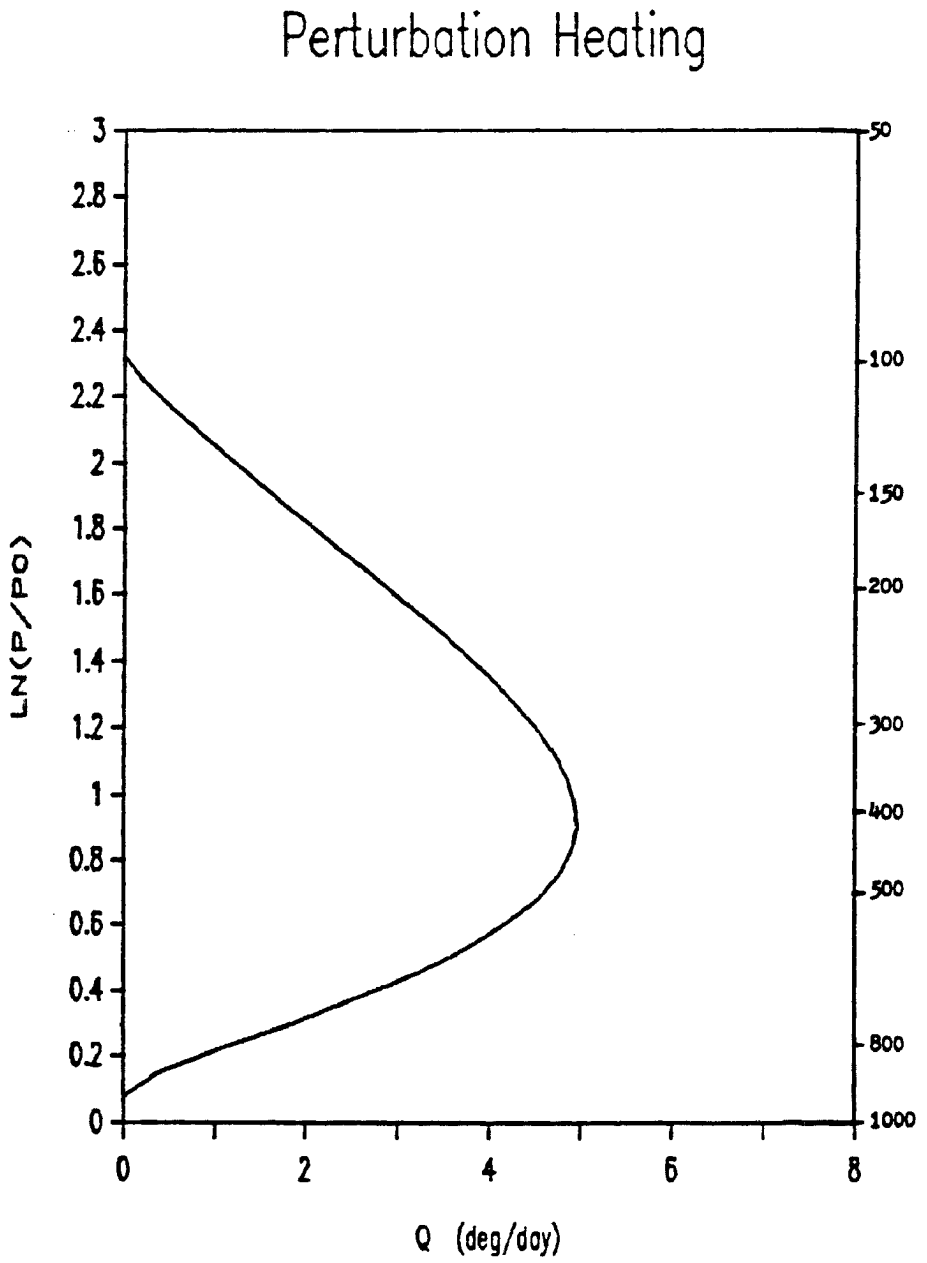

Fig. 4-2. Vertical distribution of the perturbation heating for cases which include a tropopause normalized to a precipitation rate of 3.65 m/yr.

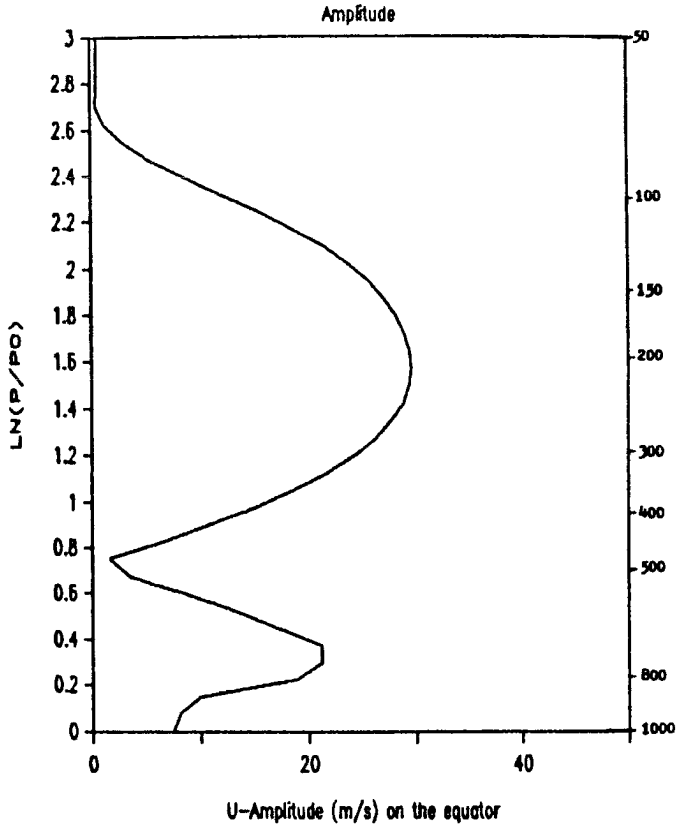

a)

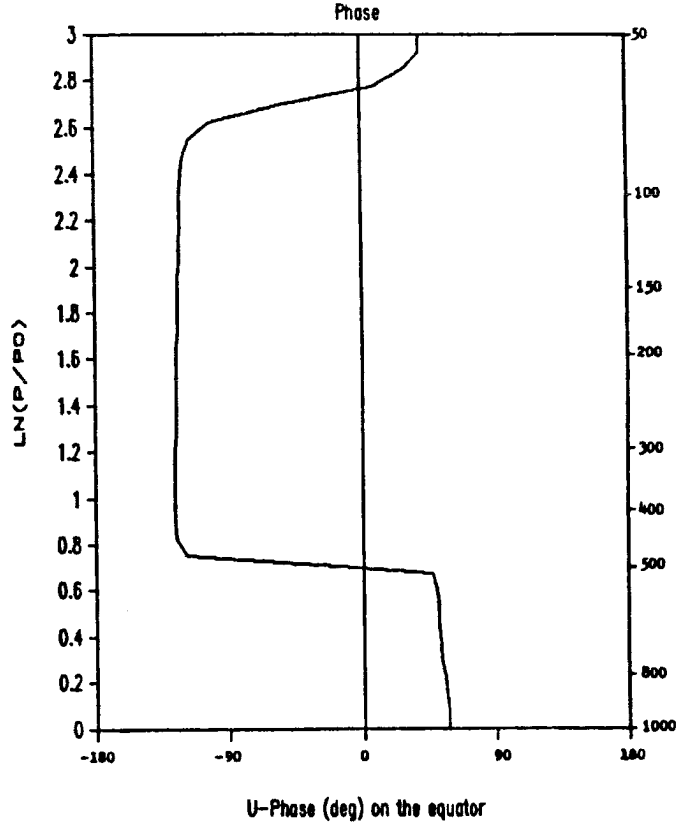

b)

Fig. 4-3. The amplitude (a) and phase (b) of zonal wind on the equator for wavenumber one forcing only. This is for the case with a mean temperature profile which includes a tropopause and with Rayleigh friction having α_R^{-1} = 5 days.

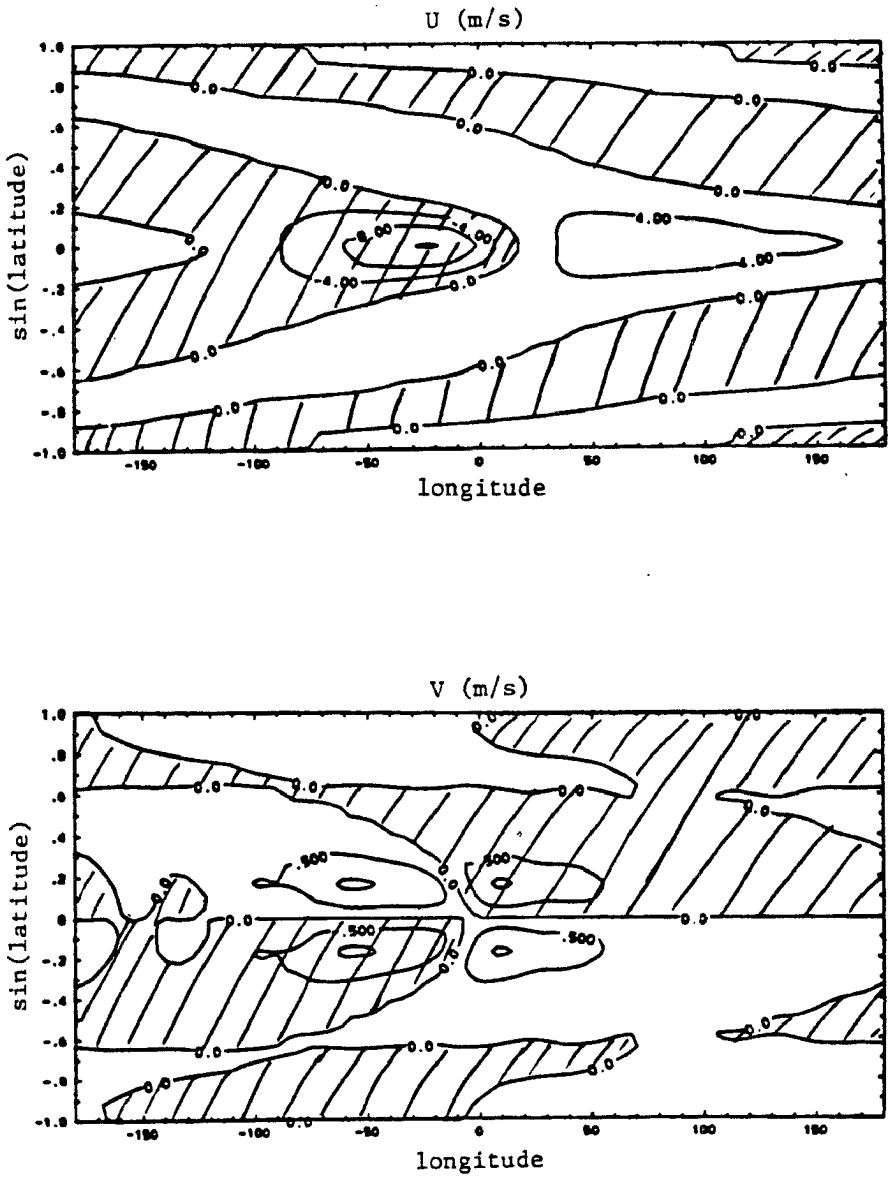

Fig. 4-4. Contours of zonal (upper panel) and meridional (lower panel) velocity near the level of maximum outflow, at 337 mb, for the case using the mean temperature profile without a tropopause and with Rayleigh friction having $\alpha_R^{-1} = 5$ days.

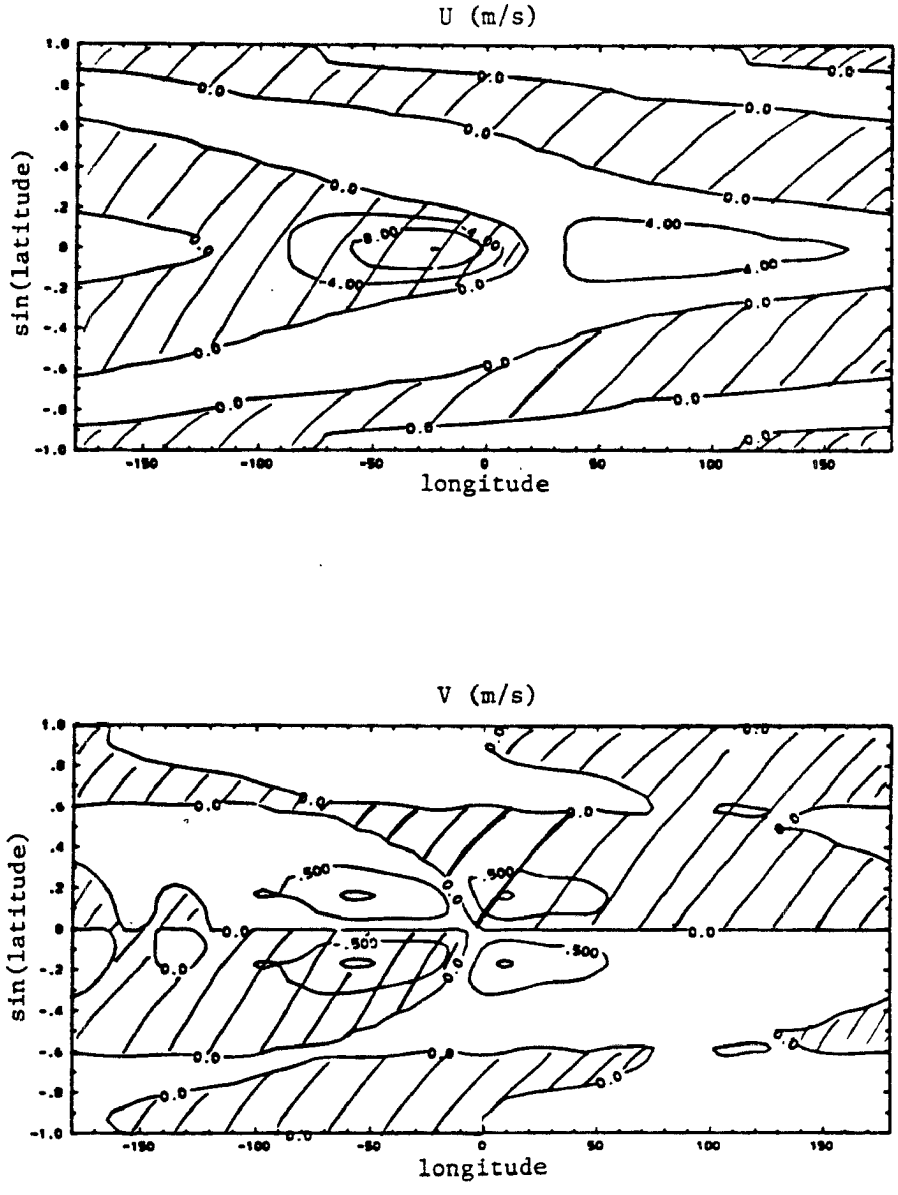

Fig. 4-5. Contours of zonal (upper panel) and meridional (lower panel) velocity near the level of maximum outflow, at 325 mb, for the case using the mean temperature profile with a tropopause and with Rayleigh friction having $\alpha_R^{-1} = 5$ days.

However, for the case which includes a cumulus mass flux, there is a much more fundamental difference between the responses using different stabilities. Again the perturbation u response on the equator below 200 mb for the case with a tropopause (Fig. 4.6) is very similar to the response using Geisler's stability (Fig. 3.6). However, the case run with no tropopause shows a third maximum in amplitude above the top of the heating and $\bar{M}_c$ profiles at 140 mb. The maximum amplitude occurs at 120 mb. This maximum does not appear in the case with a tropopause in the mean temperature profile. This is not a consequence of the heating being placed below the tropopause, but is rather due to the $\bar{M}_c$ profile ending below the minimum temperature. In other runs we have done including a temperature profile with a tropopause, when the $\bar{M}_c$ ends below the tropopause, a third maximum occurs in the upper troposphere above the momentum detrainment layer because cumulus drag is locally absent. However, if the mass flux profile ends at or above the tropopause, that maximum does not occur.

To examine how the inclusion of cumulus friction in the model equations affects the response for the case with a motionless basic state, we will compare the two runs previously discussed (Figs. 4.3 and 4.6) that use a mean temperature profile which includes a tropopause. One basic difference is that the maximum amplitude of the perturbation u field is significantly larger for the case with no $\bar{M}_c$. This is an understandable result given that the cumulus mass flux is essentially a dissipation term.

Another significant difference is that the level of zero wind is about 160 mb higher for the case with no $\bar{M}_c$. This can also be seen in diagrams of mass flux on the equator, which in a crude sense can give a

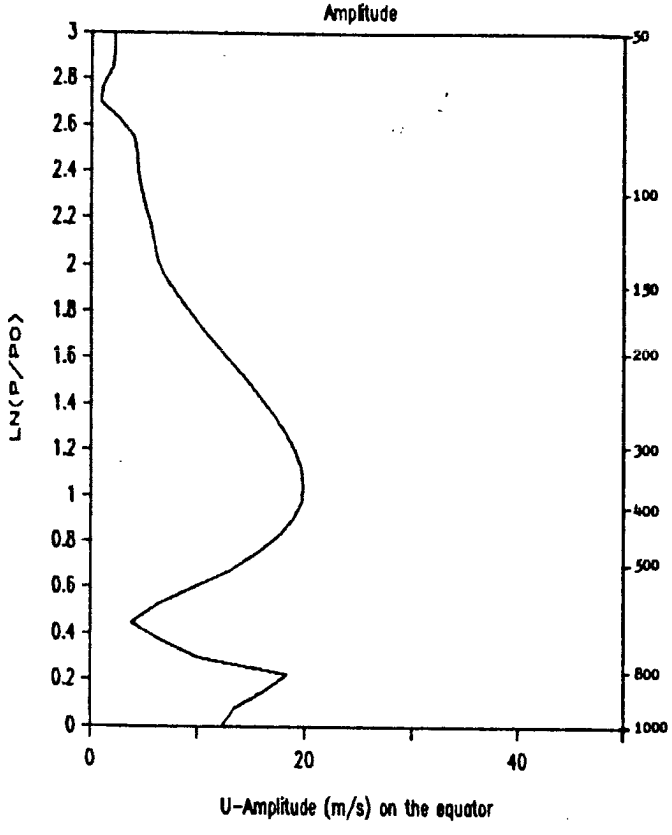

a)

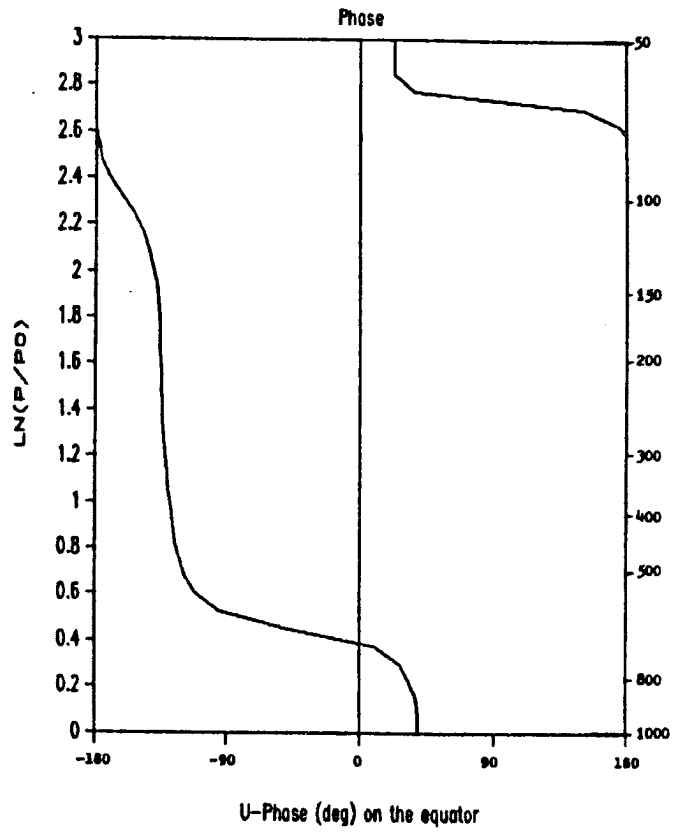

b)

Fig. 4-6. As in Fig. 4.3 except with Rayleigh friction replaced by cumulus friction.

direction of flow (Newell et al., 1974). Figure 4.7 shows mass flux diagrams derived from our model results on the equator. These show that the inclusion of $\bar{M}_c$ tends to narrow the horizontal extent of the circulation to the west of the heating and both widen and weaken the circulation to the east of the heat source. The vertical extent of the circulation is also reduced by including a mean cumulus mass flux with a motionless basic state.

A third consequence of adding a mean $\bar{M}_c$ to the basic state is to change the structure of the perturbation u and v fields. The resulting fields at 325 mb, the level of maximum outflow, are shown in Figures 4.5 and 4.8. The maximum in the westerly response is offset from the equator for the case that includes $\bar{M}_c$ and the response on the equator is damped. We also see a larger easterly response off the equator. In addition, the response in the v field is stronger for the case with $\bar{M}_c$. The circulation to the east of the heating which acts in a sense opposite to a Hadley cell is twice as strong as the response with no $\bar{M}_c$. The response to the west of the center of the heating, which adds to a mean Hadley cell, is also stronger than without $\bar{M}_c$.

Thus we see that including $\bar{M}_c$ produces a significantly different response than when $\bar{M}_c$ is not included. This is quite unlike the results obtained when the runs using different stabilities were compared. The change from using a constant static stability to using a mean temperature profile which includes a tropopause has virtually no effect on our runs which do not incorporate cumulus friction. However, when cumulus friction is included, we do find a difference in response between the two stability cases. This difference is largely confined to the upper levels. If the mean cumulus mass flux ends below the tropopause, we

a)

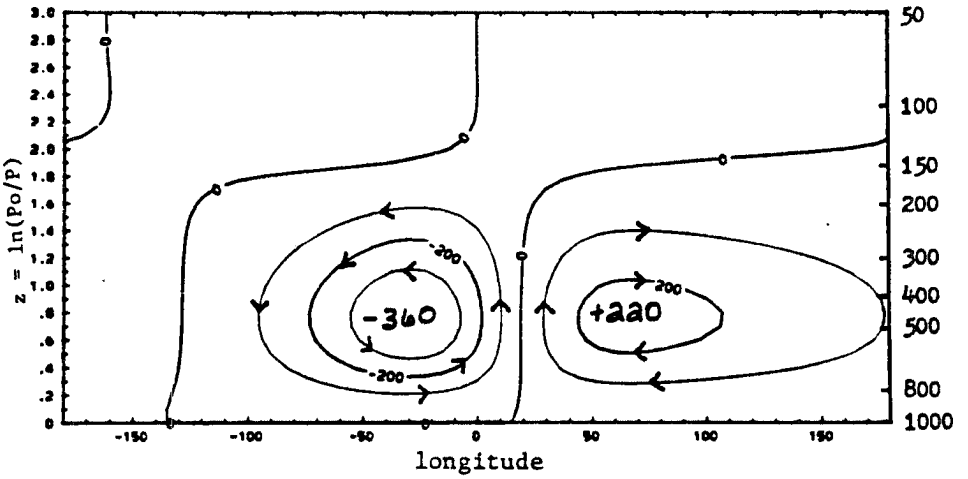

b)

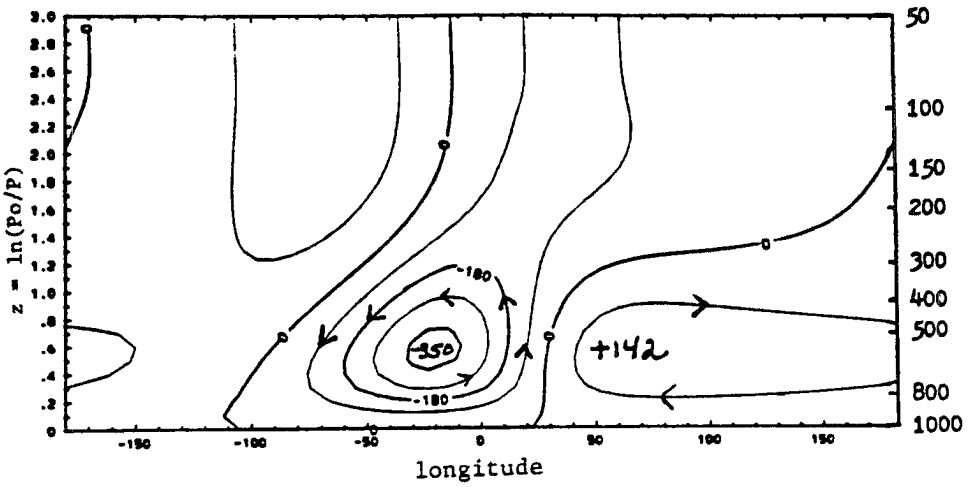

Fig. 4-7. Contours of zonal mass flux (units of 10E11 gm/s) in a 10° wide strip centered on the equator derived from the model results for the runs including a tropopause, without cumulus friction (a), and with cumulus friction (b).

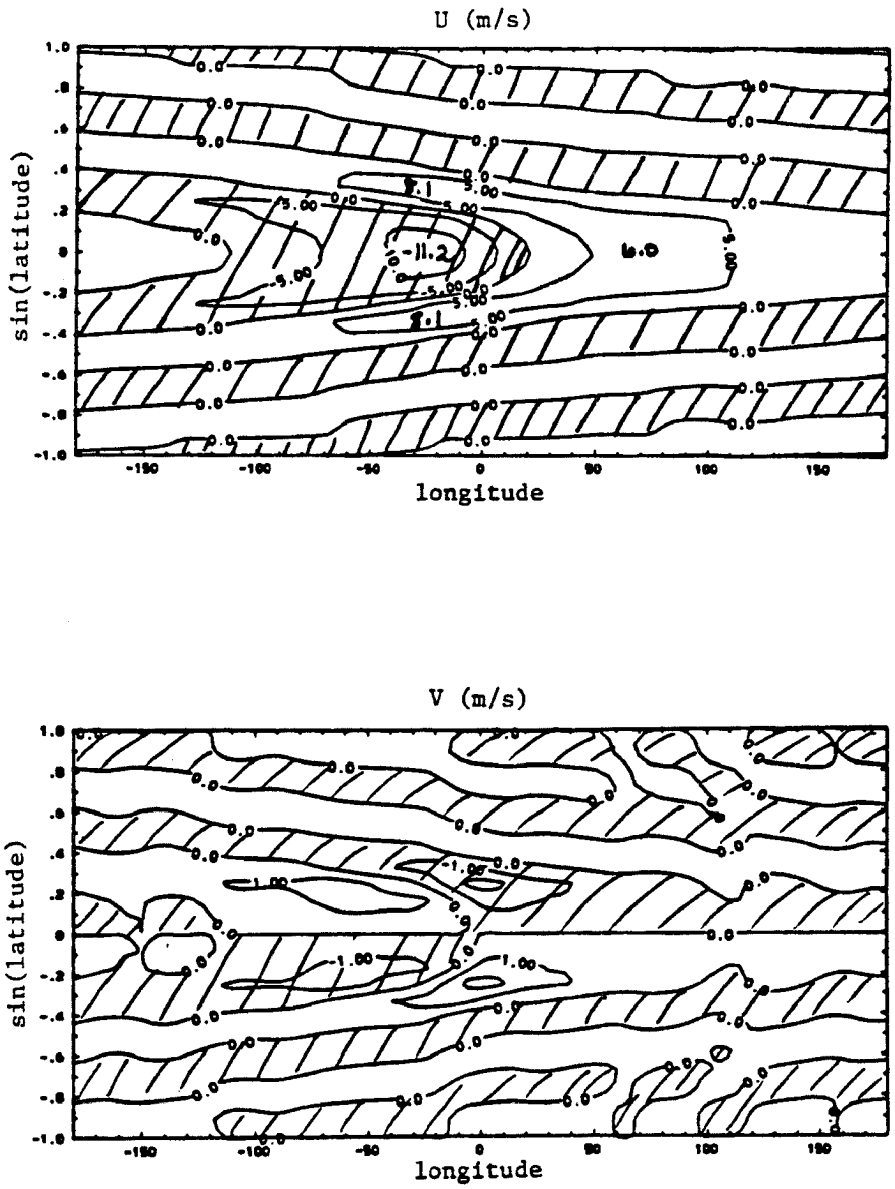

Fig. 4-8. As in Fig. 4.5 except with Rayleigh friction replaced by cumulus friction.

find an additional maximum in the u field response above the momentum detrainment layer. This does not occur if $\bar{M}_c$ ends at the tropopause. Use of a constant static stability throughout the model produces the same result, again because of the lack of an extremely stable layer above the mass flux layer. This, however, has little effect on the region we are concerned with in studying the Walker Circulation. That is because the constant stability used is a fairly accurate representation of that of the realistic temperature profile below the tropopause (Fig. 4.9).

Including $\bar{M}_c$ does make a significant difference on the circulation we are interested in studying. There is a lowering of the level of zero wind and a weakening of the zonal winds on the equator when $\bar{M}_c$ is included. We also find that the maximum u response occurs away from the heating center when $\bar{M}_c$ is included. This type of result would not be found if the only dissipation included is Rayleigh friction which is constant everywhere in the domain as was the case in Gill (1980). However, it is questionable how valid it is to include a mean mass flux without also including a mean basic state. In the next section we will examine what the effects of including a mean basic state are.

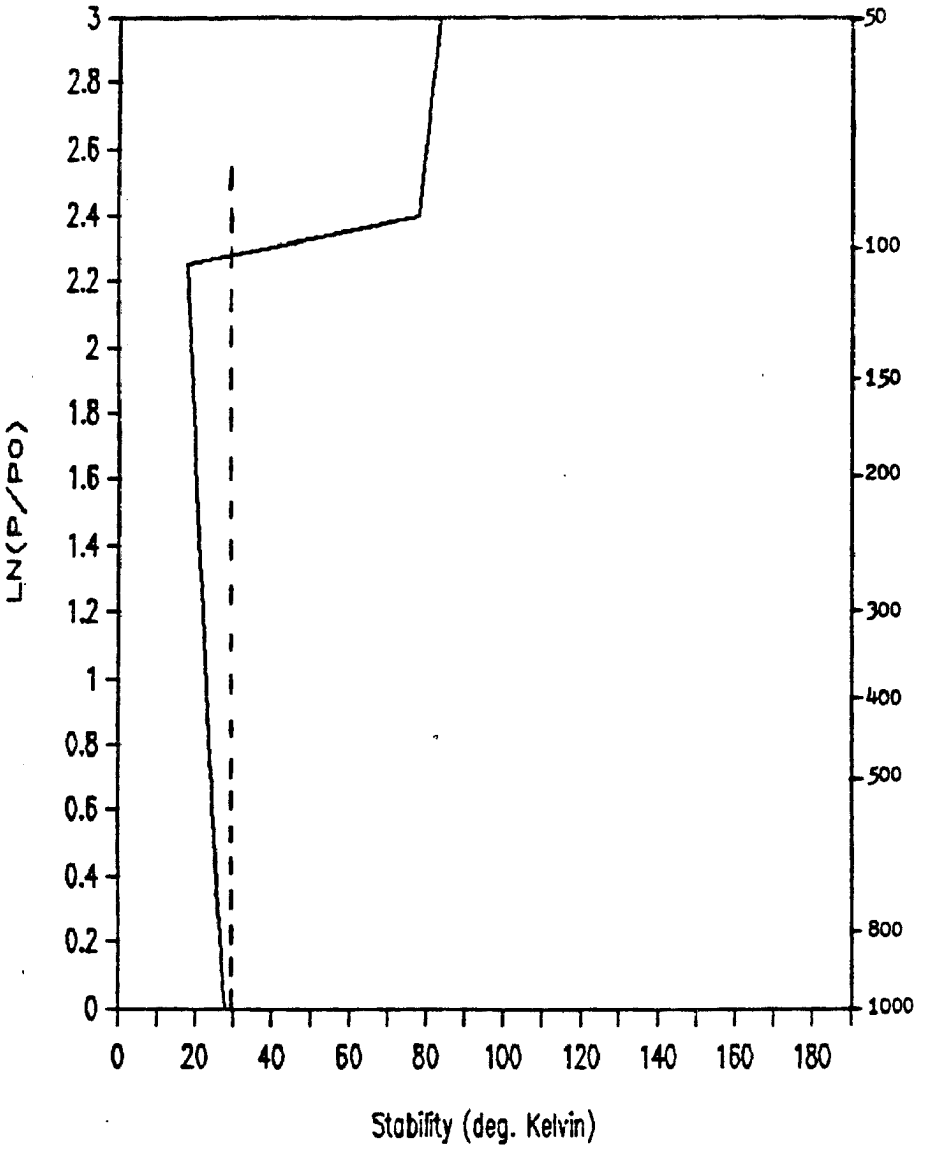

Fig. 4-9. Stability profile ($\frac{\partial T}{\partial z} + \kappa \bar{T}$) used for the case which includes a tropopause (solid line) and for the case of constant stability (dashed line).

5. Effects of including a nonzero basic state

5.1 Description of model parameters

In order to assess the effects of different mean basic states, several runs were made ranging from a motionless basis state to a complete Hadley cell with a mean zonal wind. All of the runs discussed in this section do not include wavenumber zero. Summations to get complete perturbation wind fields are done with wavenumbers one through ten using the amplitudes given in (2.6). Wavenumbers larger than ten were not included because the response is negligible for the broad heating used. Actually, for wavenumber ten the response is five orders of magnitude less than that of wavenumber one for the Gaussian distribution we are using. The main features of the response can be seen using only wavenumbers one through three.

The perturbation heating (Fig. 5.1) has a longitudinal e-folding width of 40° and a latitudinal e-folding width of 9°. It is of the form

$$Q = \exp(-(\lambda/\lambda_0)^2)\ \exp(-(\theta/\theta_0)^2)F(p)$$

where F(p) is as given in equation 3.2 with p_T = 100 mb, p_b = 900 mb, and Q_0 is chosen to give a maximum precipitation of 2 m/yr. The $\bar{M}_c$ (Fig. 5.2) used also has an e-folding width of 9° and the M_c' distribution corresponds to that of the perturbation heating. Both $\bar{M}_c$ and M_c' are of the form given in equation 3.3, with gM_{co}' = 2.3 mb/hr and $g\bar{M}_{co}$ = 3 mb/hr. The rising branch of the mean Hadley cell coincides with the

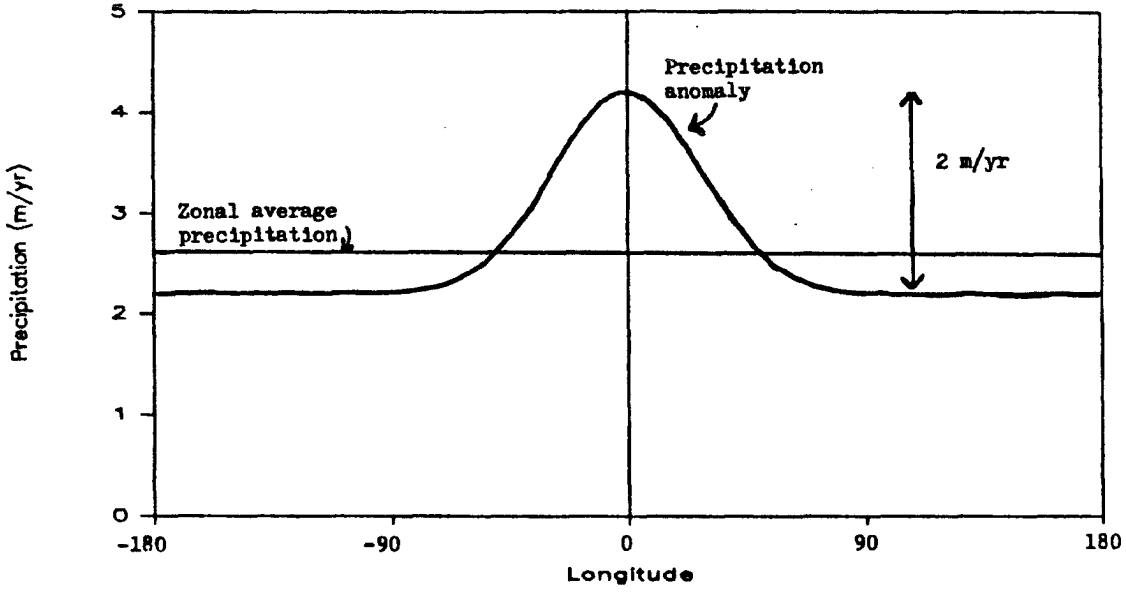

Fig. 5-1a. Horizontal distribution of the heating used as model input. The anomaly is a Gaussian with an e-folding width of 40° and amplitude of 2 m/yr. The zonal average is taken to be 2.6 m/yr.

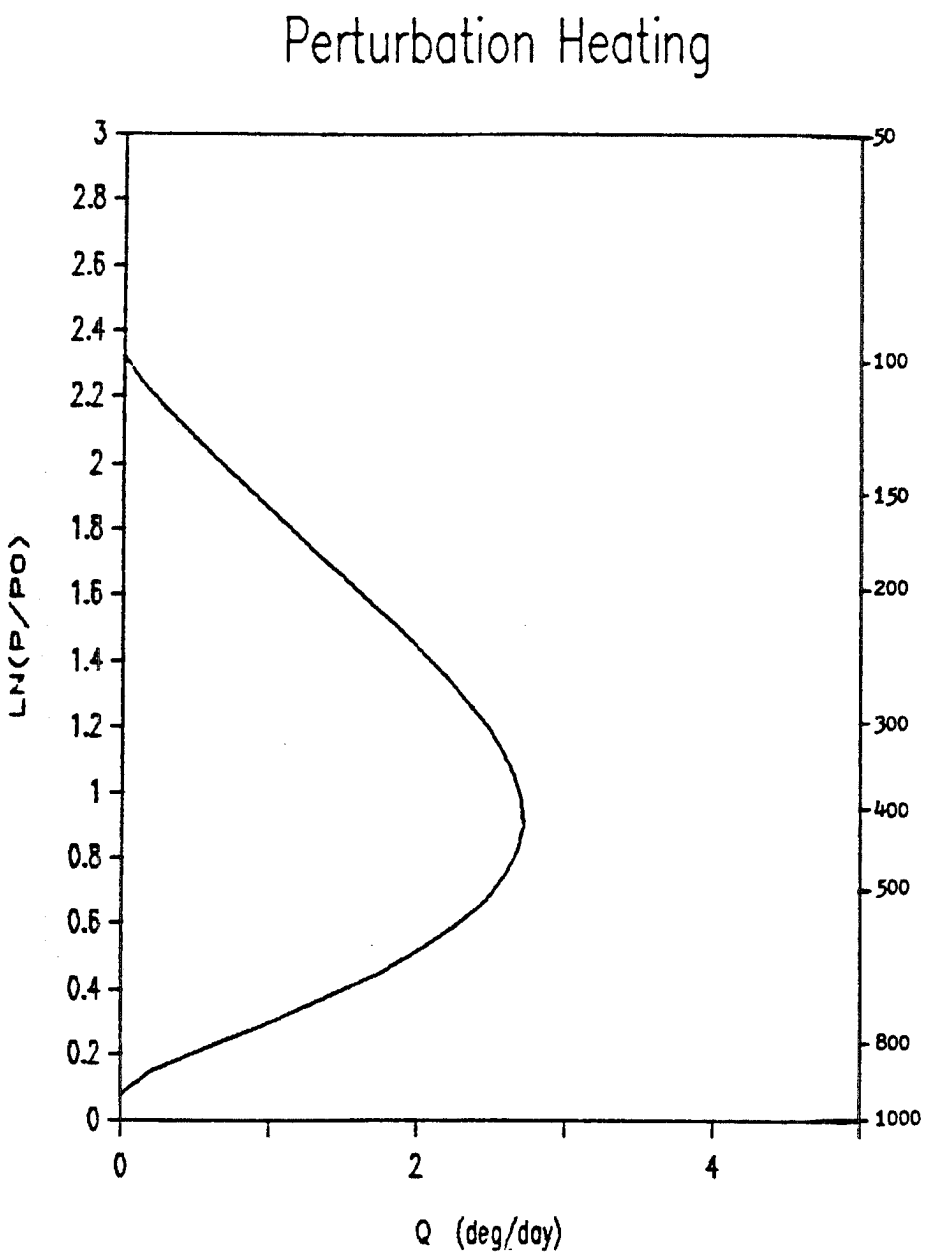

Fig. 5-1b. Vertical distribution of the perturbation heating normalized to a precipitation rate of 2 m/yr.

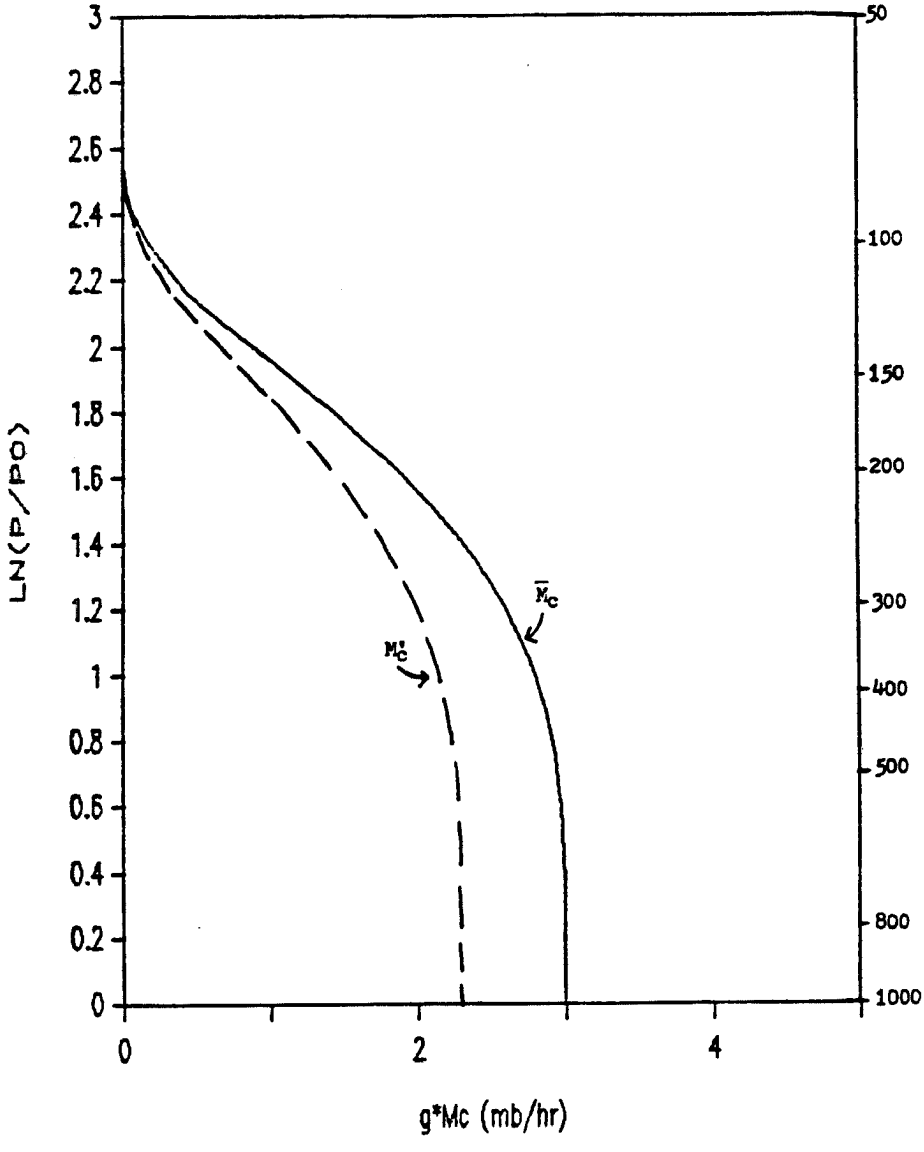

Fig. 5-2. Vertical distributions of the mean (solid line) and perturbation (dashed line) cumulus mass flux.

distribution of $\bar{M}_c$. A mean precipitation rate is assumed to be 2.6 m/yr at the center of the heating. This is larger than a typical zonal tropical average of approximately 2 m/yr. However this is not a bad assumption when one considers that the center of the Hadley cell in the physical world tends to move around and distribute the rainfall over an area to achieve a 2 m/yr average, while a model Hadley cell is stationary. The actual average in the rising branch of the physical Hadley cell is probably larger than 2 m/yr.

The perturbation heating used produces a precipitation rate with an amplitude of 2 m/yr. So that it is possible to neglect the wavenumber zero response, the average of the perturbation heating must be equal to zero. The actual zonal average of a Gaussian with amplitude 2 m/yr and e-folding width of 40° is about .4 m/yr. The base of the perturbation heating is then placed at 2.2 m/yr. The maximum precipitation at the center of the heating is then 4.2 m/yr which is a reasonable precipitation rate for the Indonesian region.

The diffusion terms are of the form $\frac{g}{p}\frac{\partial}{\partial z}\left(\frac{\mu^{\dagger}\partial V}{H\ \partial z}\right)$ where $\mu = \rho\nu$ and $\nu = 1\ \frac{m^2}{s}$ throughout the model. For any run with a motionless basic state, the M_c' term does not enter into the calculation because it always occurs multiplied by the mean wind.

Two series of model runs were done to look at the sensitivity of the response to different basic states. The first was with the perturbation heating centered on the equator, and the second with the heating centered on 9° north. Each series of runs consists of one with a motionless basic which includes $\bar{M}_c$, one with a mean northern hemisphere winter zonal wind, one with a mean northern hemisphere summer zonal wind, and one with a mean zonal wind and a mean Hadley cell. These are summarized in Table 5.1.

Table 5.1. Model runs

Run	Basic State	Heating Center	Dissipation
1a	rest	equator	$\alpha_R^{-1} = \alpha_N^{-1} = 20$ days, $\bar{M}_c$
1b	winter zonal wind	equator	$\alpha_R^{-1} = \alpha_N^{-1} = 20$ days, $\bar{M}_c$, M_c'
1c	summer zonal wind	equator	$\alpha_R^{-1} = \alpha_N^{-1} = 20$ days, $\bar{M}_c$, M_c'
1d	winter zonal wind equatorial Hadley cell	equator	$\alpha_R^{-1} = \alpha_N^{-1} = 20$ days, $\bar{M}_c$, M_c'
2a	rest	9°N	$\alpha_R^{-1} = \alpha_N^{-1} = 20$ days, $\bar{M}_c$
2b	winter zonal wind	9°N	$\alpha_R^{-1} = \alpha_N^{-1} = 20$ days, $\bar{M}_c$, M_c'
2c	summer zonal wind	9°N	$\alpha_R^{-1} = \alpha_N^{-1} = 20$ days, $\bar{M}_c$, M_c'
2d	summer zonal wind 9°N Hadley cell	9°N	$\alpha_R^{-1} = \alpha_N^{-1} = 20$ days, $\bar{M}_c$, M_c'

The data for the mean zonal winds were the European Center for Medium Range Weather Forecasting (ECMWF) level III b FGGE analysis obtained from NCAR. The winter average (Fig. 5.3) consists of FGGE data averaged over the Pacific (100°E to 100°W) from Dec. 1, 1978 to Mar. 6, 1979. The summer average (Fig. 5.4) is over the same area using data from May 26, 1979 to Sep. 6, 1979. The summer average has a deep layer of easterlies in the equatorial region while the winter average has weak westerlies above the easterlies. A polar night jet is also present in the southern hemisphere in the summer average which does not appear in the winter average. The data had to be interpolated to our model grid using a cubic spline routine. The mean Hadley cells, one centered around the equator and one centered around 9° N were obtained by prescribing an analytical stream function Ψ, where $v = \frac{1}{\cos\theta}\frac{\partial\Psi}{\partial p}$ and $w = -\frac{1}{a}\frac{\partial\Psi}{\partial\theta}$. Our derived Hadley cell for the winter case (Fig. 5.5) is

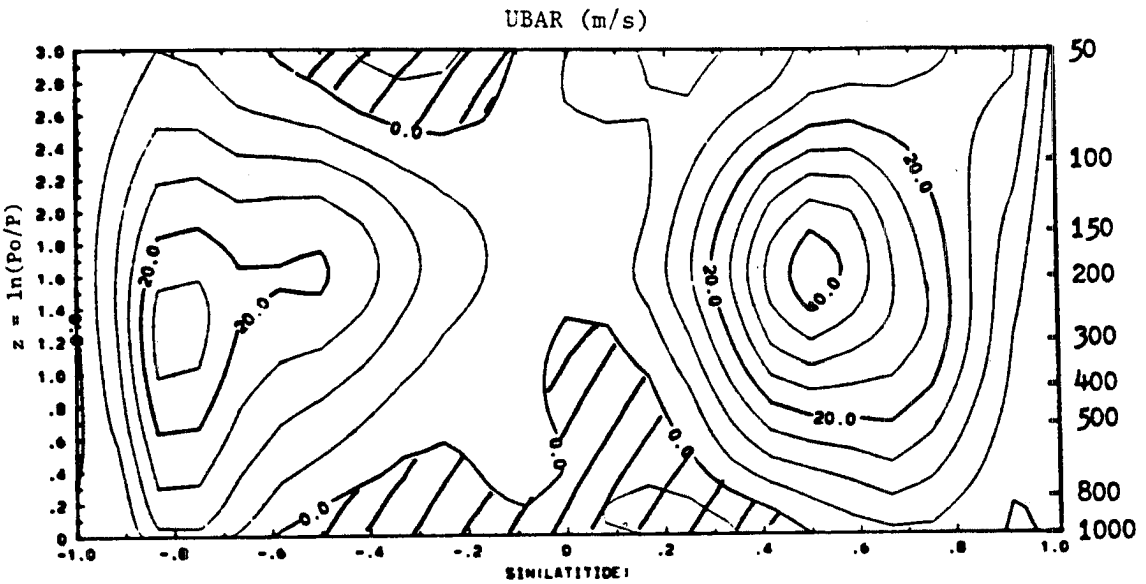

Fig. 5-3. Contour plot of the mean zonal winds used for the winter case. Winds were averaged over the Pacific from Dec. 1, 1978 through Mar. 6, 1979, then interpolated to the model grid.

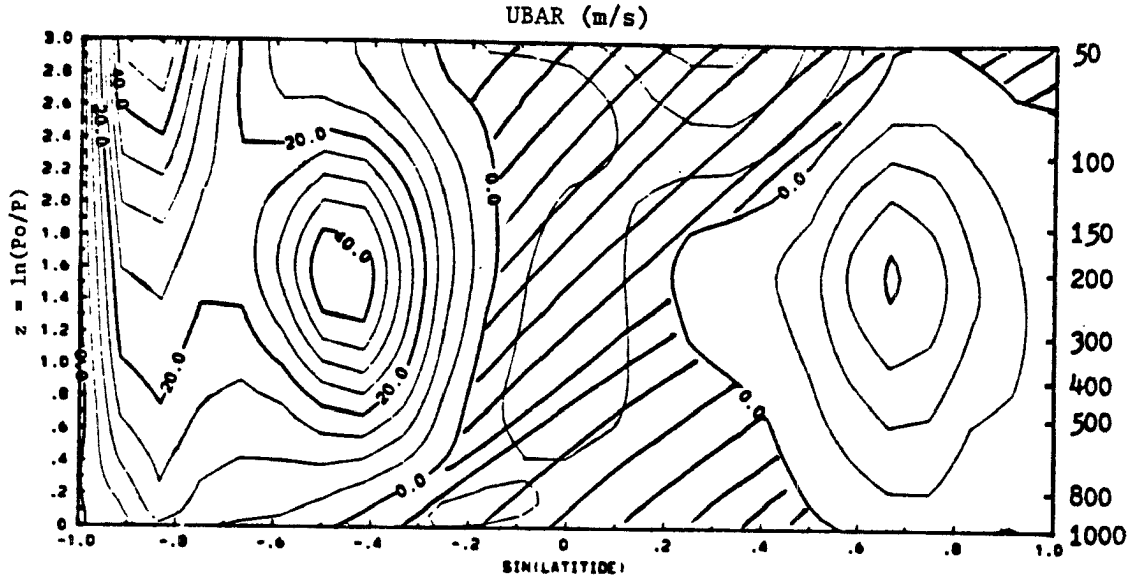

Fig. 5-4. Contour plot of the mean zonal winds used for the summer case. Winds were averaged over the Pacific from May 26, 1979 through Sept. 6, 1979.

a)

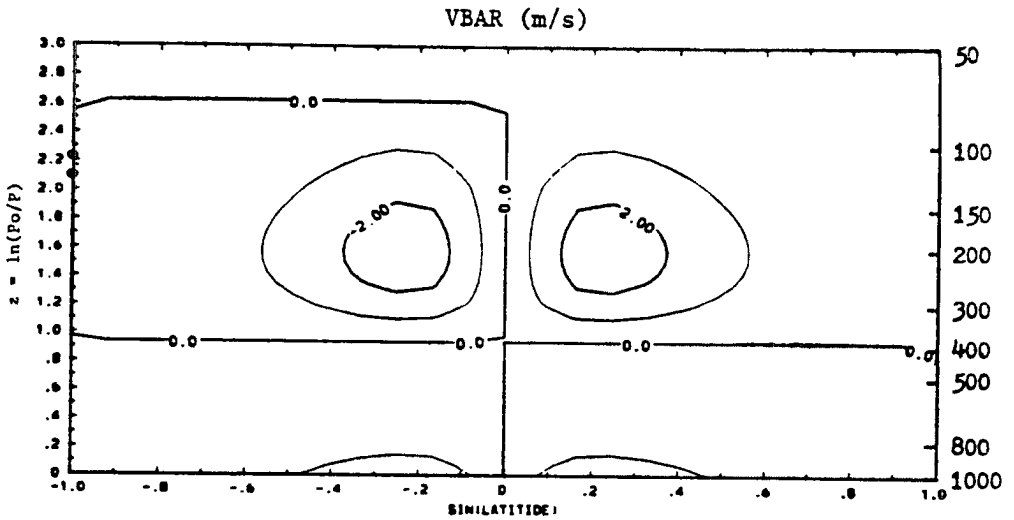

b)

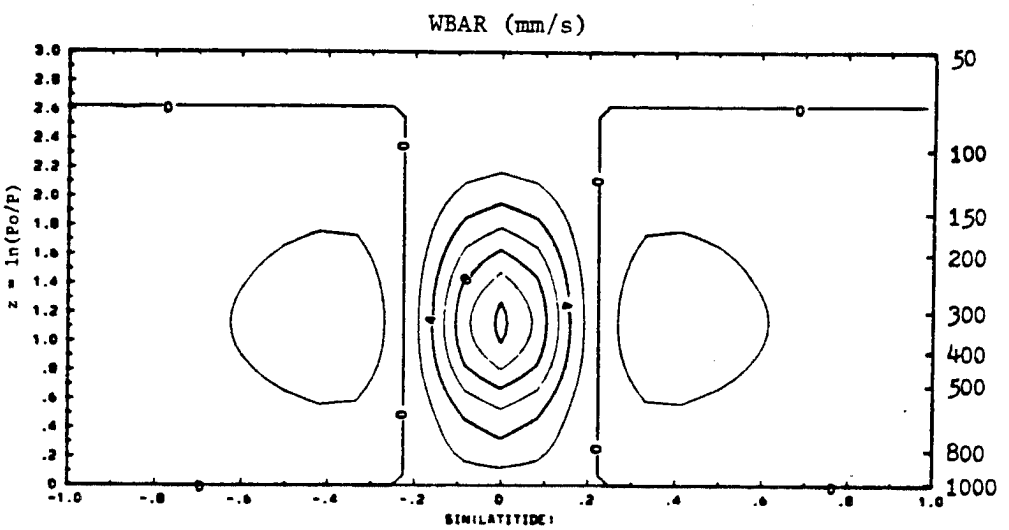

Fig. 5-5. Derived Hadley cell centered on the equator, meridional velocity (a) and vertical velocity (b).

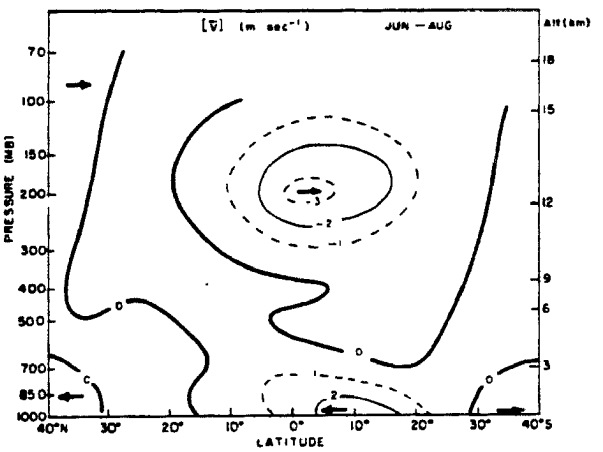

Fig. 5-5c. Winter average meridional velocity field taken from Newell et al. (1972).

symmetric around the equator while the observed circulation from Newell et al. (1972) is clearly very asymmetric; however, ours coincides adequately as far as the winter hemisphere is concerned and the magnitudes of the wind speeds are close to the observed winds. Again, for the case centered at 9° N (Fig. 5.6), details are not identical between the derived Hadley cell and the observed, but the overall character is similar. These prescribed mean Hadley cells should provide some insight into what the effects of including such a mean circulation are in spite of the fact that they do not exactly duplicate observations.

The Rayleigh friction and Newtonian cooling both have magnitudes of α^{-1} = 20 days. The boundary conditions used are those given in Chapter 2, with physical vertical velocity equal to zero at the bottom and divergence equal zero at the top.

5.2 Discussion of runs with heating centered on the equator

The base run for this heating, run 1a, includes $\bar{M}_c$ but has a motionless basic state. The phase and amplitude for the wavenumber one response (Fig. 5.7) show the level of zero wind and the corresponding 180° phase shift for this run occur at about z = .4 or 670 mb. The response for the run that includes a winter average zonal wind, run 1b, shows that the level of zero wind changes very little from the base run (Fig. 5.8). There is a slight difference in the very upper model levels, but it is of small amplitude and not very significant. Right at the equator, the mean winter wind is weak, so the similar results between the two runs is not surprising. However, the run using a mean summer zonal wind, run 1c, is significantly different from the base run (Fig. 5.9). For this case on the equator, the mean zonal winds are

a)

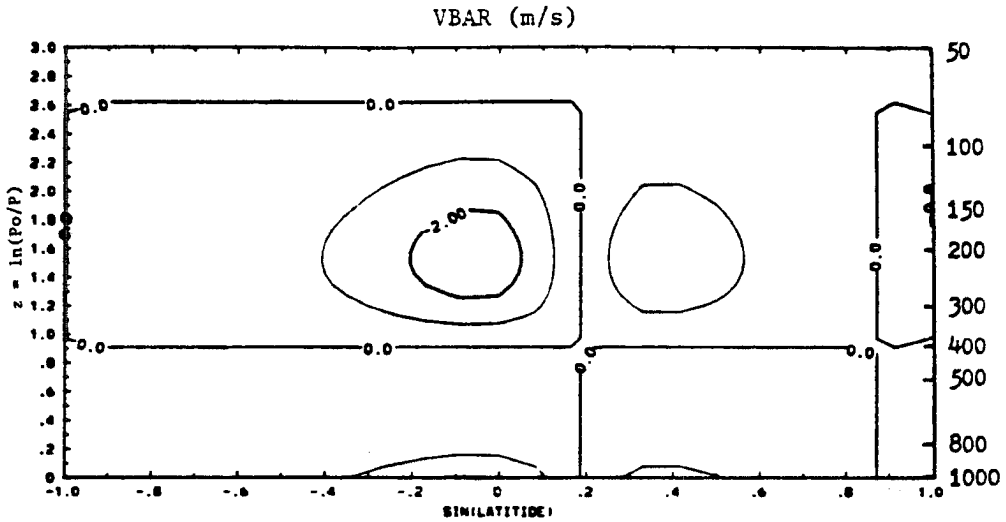

b)

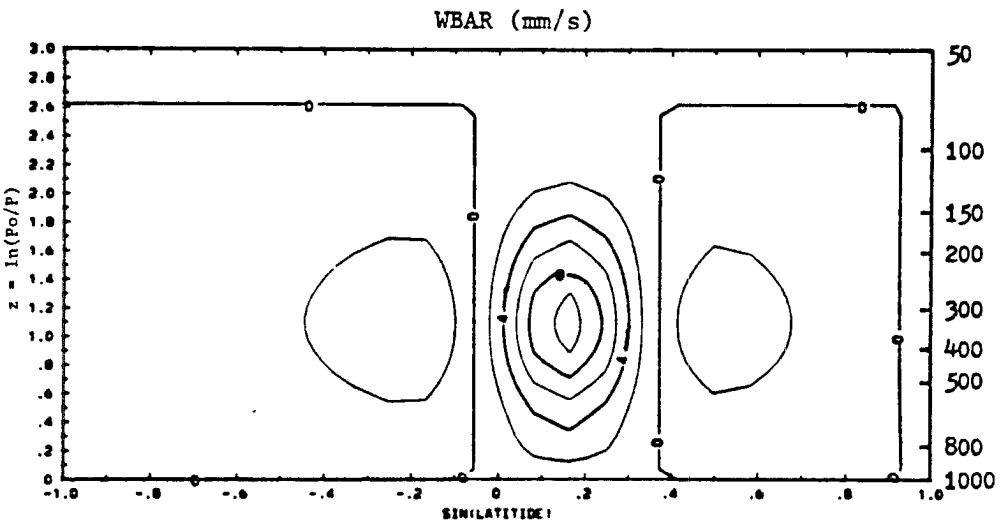

Fig. 5-6. Derived Hadley cell centered at 9°N, meridional velocity (a) and vertical velocity (b).

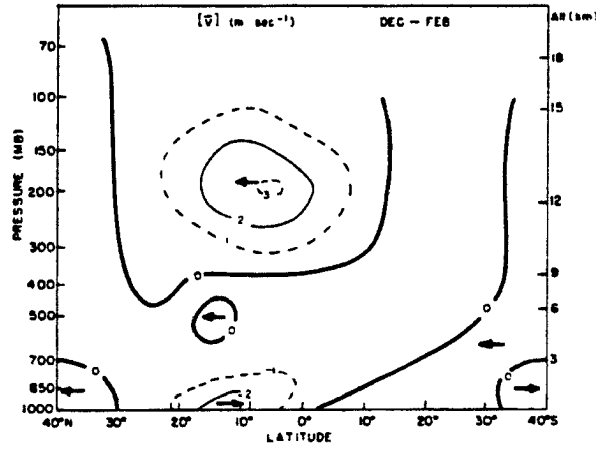

Fig. 5-6c. Summer average meridional velocity field taken from Newell et al. (1972).

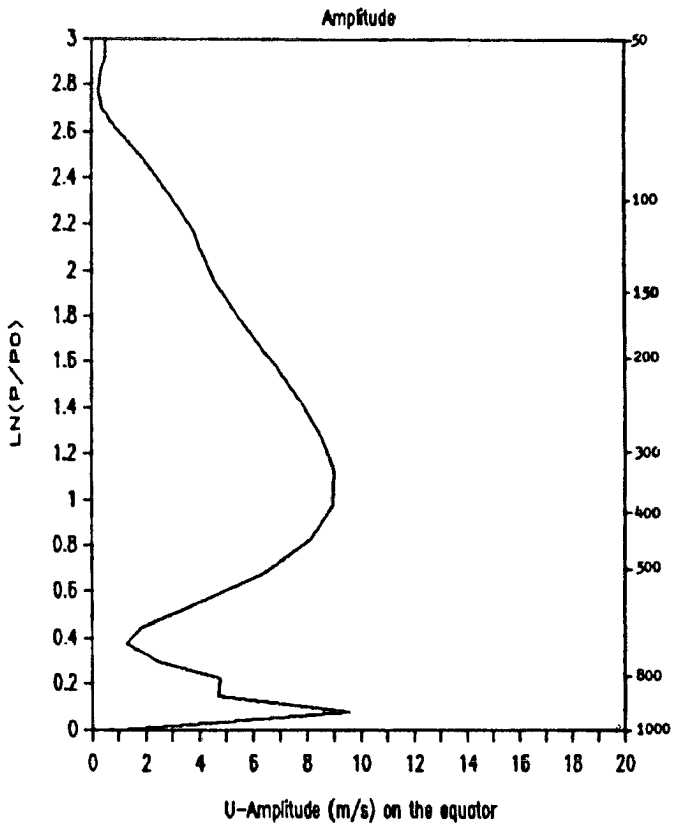

a)

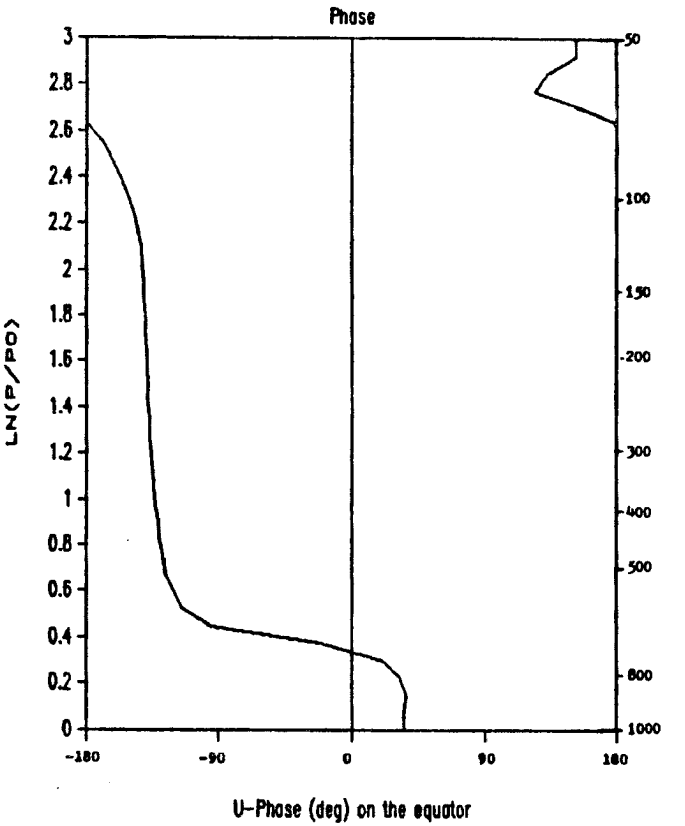

b)

Fig. 5-7. Amplitude (a) and phase (b) of zonal wind on the equator for wavenumber one forcing only for the case with a motionless basic state including cumulus friction.

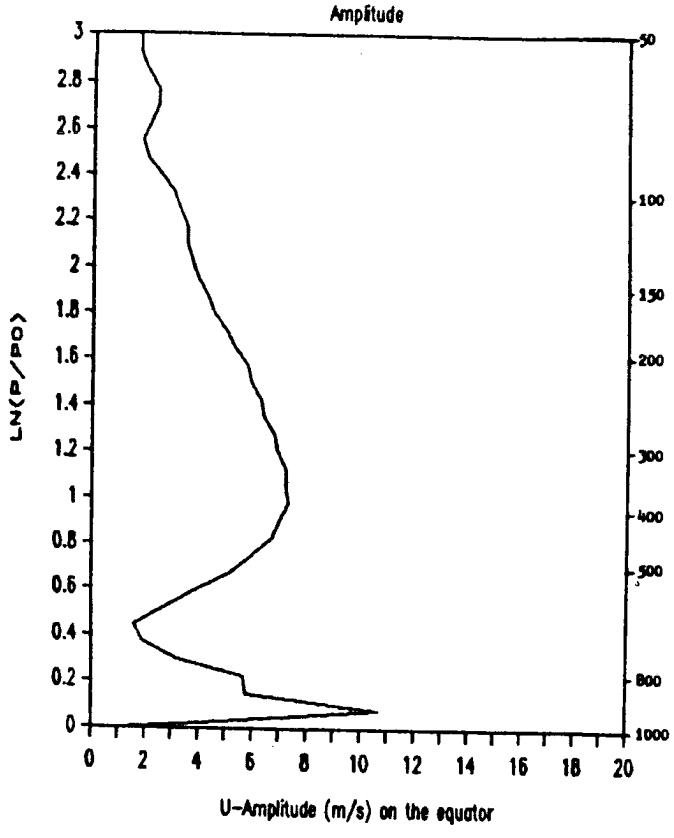

a)

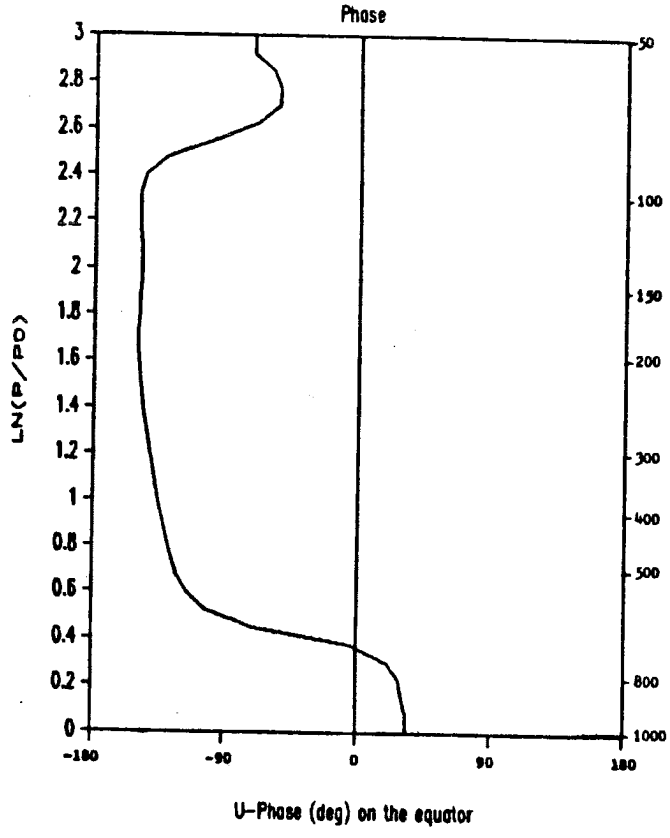

b)

Fig. 5-8. As in Fig. 5.7 except with a basic state consisting of a mean winter zonal wind.

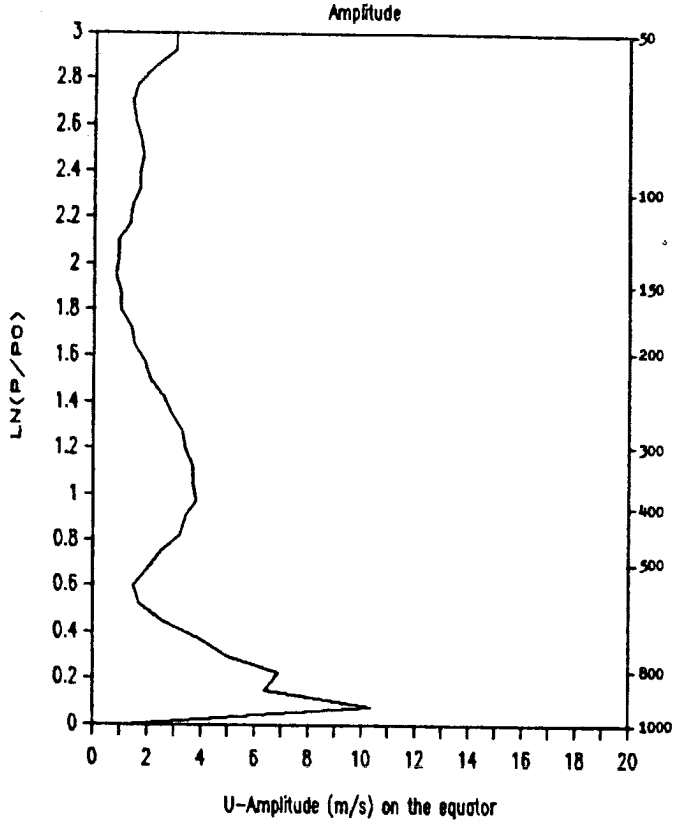

a)

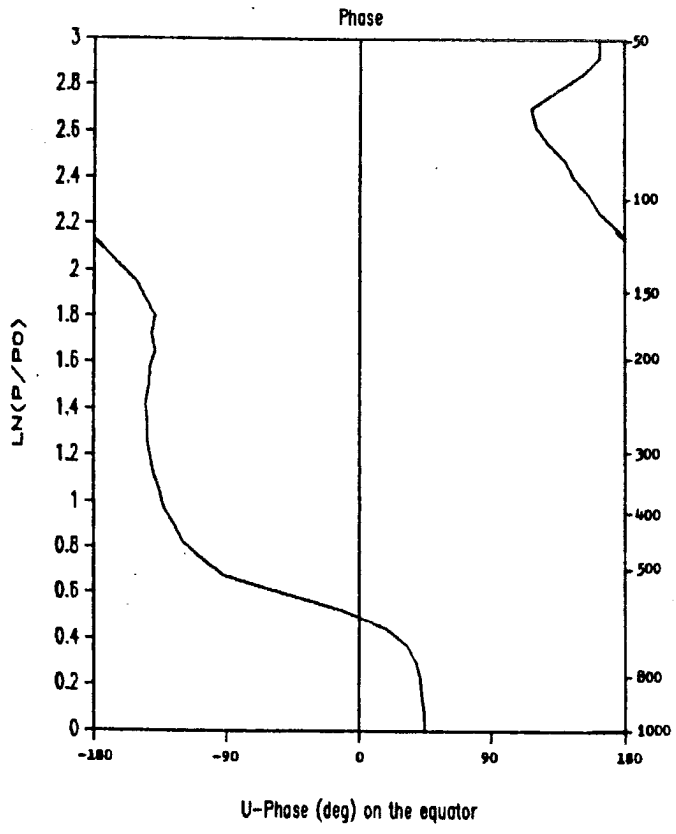

b)

Fig. 5-9. As in 5.7 except with a basic state consisting of a mean summer zonal wind.

easterly and fairly steady at 5 m/s throughout a considerable depth of the troposphere. The response for this case has a similar amplitude below 700 mb, but the zero wind level is higher. It occurs near 550 mb. The winds above that level are significantly weaker than for either the base run or the mean winter zonal flow run. The wavenumber one response for the run which includes a complete basic state with a derived Hadley cell centered on the equator and a mean winter zonal wind, run 1d, is quite different from the previous runs (Fig. 5.10). The level of zero wind is higher as was previously postulated. It occurs for this case between z = .65 and z = .7, or near 500 mb. The amplitude in the lowest levels is larger than for the other three cases, and the amplitude above the zero wind line is similar to that for the mean winter zonal wind case as is the phase.

An examination of the terms in the u momentum equation reveals that the terms with the largest magnitudes near the equator are the following: $\frac{v}{a}\frac{\partial u'}{\partial \theta}$, $\bar{w}\frac{\partial u'}{\partial z}$, $-\frac{g}{p}\frac{\partial}{\partial z}(\bar{M}_c u')$ and $\frac{is\phi'}{a\cos\theta}$. The magnitude of the term $\bar{w}\frac{\partial u'}{\partial z}$ is slightly smaller than that of the term $-\frac{g}{p}\frac{\partial}{\partial z}(\bar{M}_c u')$; however, it is of the opposite sign. Thus the inclusion of a mean vertical velocity field acts to diminish the effect of the cumulus friction.

The differences in response using the different basic states are better revealed upon examining the summation of wavenumbers one through ten. Perturbation u and v fields at several levels are shown in Figures 5.11 through 5.14. The most obvious effect of including a mean state is that a significant response is seen in extratropical latitudes where without a mean state the response is confined to the tropics. This is even more apparent in the geopotential field (Fig. 5.15), where a large mid-latitude response is seen in the winter hemisphere. Webster (1982)

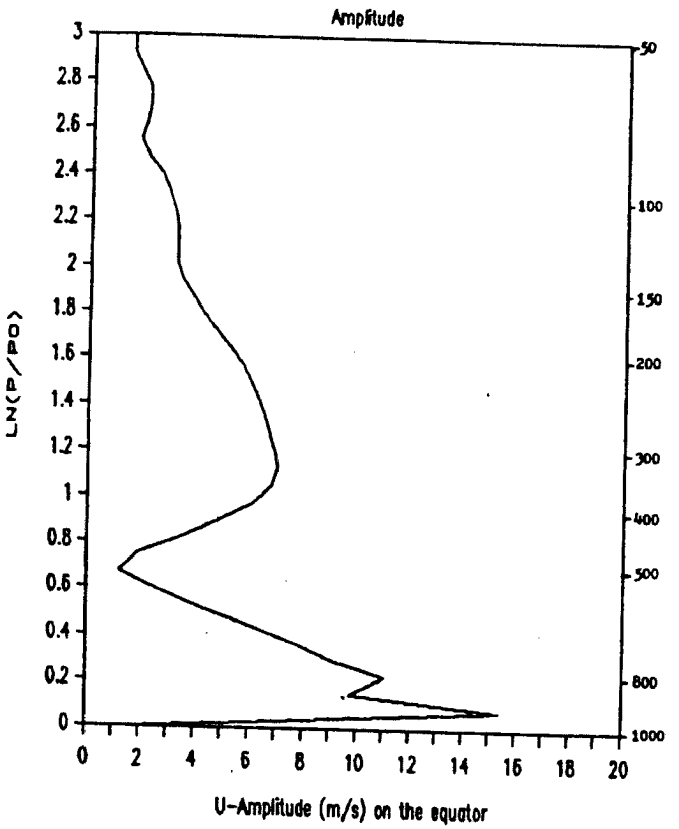

a)

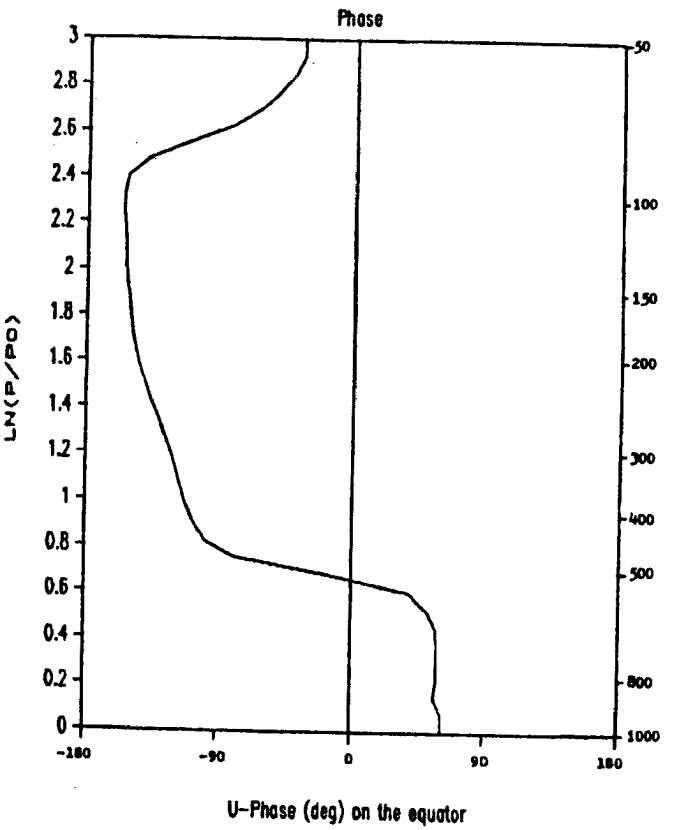

b)

Fig. 5-10. As in Fig. 5.7 except with a basic state consisting of mean winter zonal wind and a Hadley cell centered on the equator.

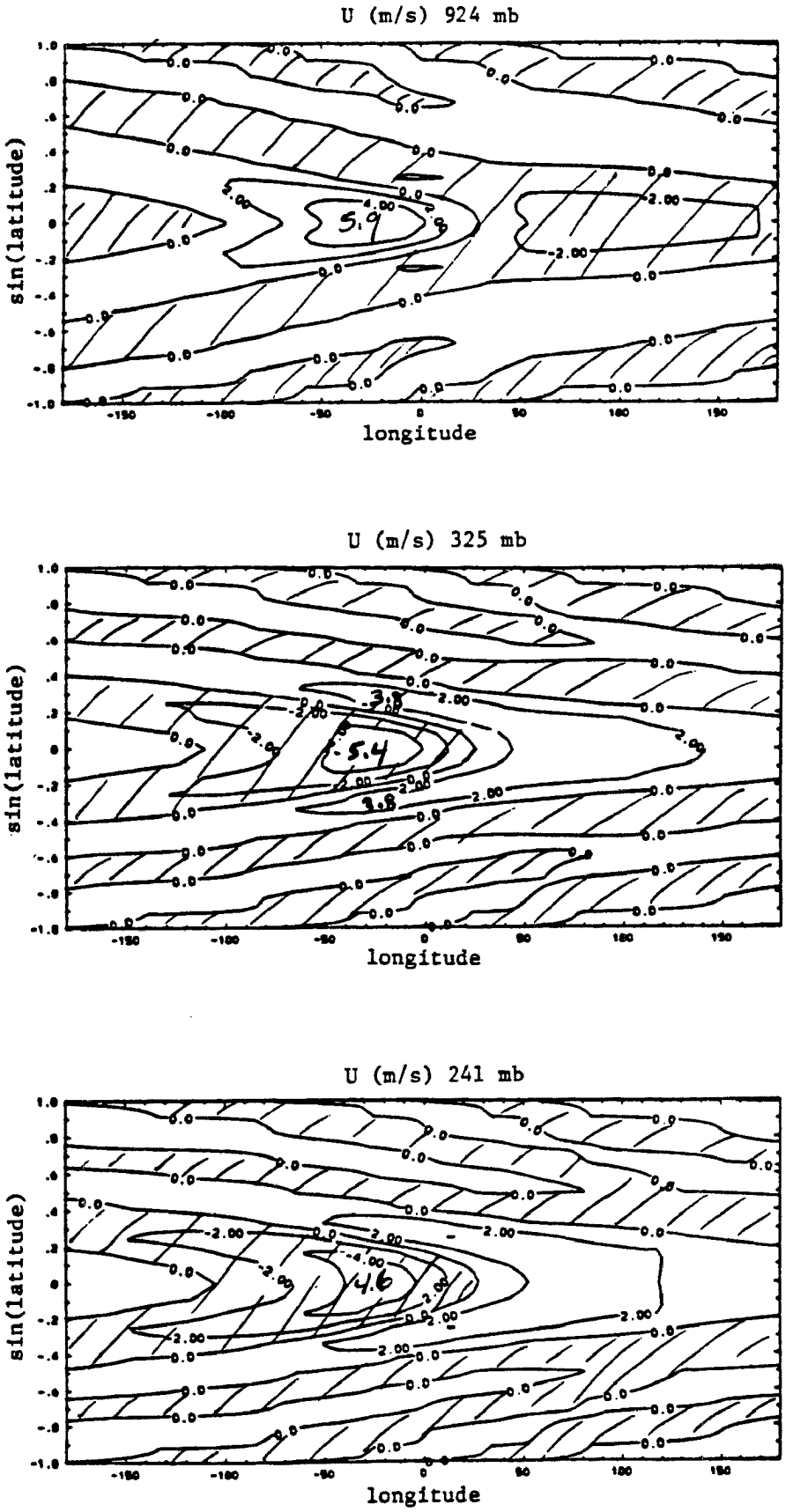

Fig. 5-11a. Perturbation u field for the run with a motionless basic state including cumulus friction. The heating is centered on the equator.

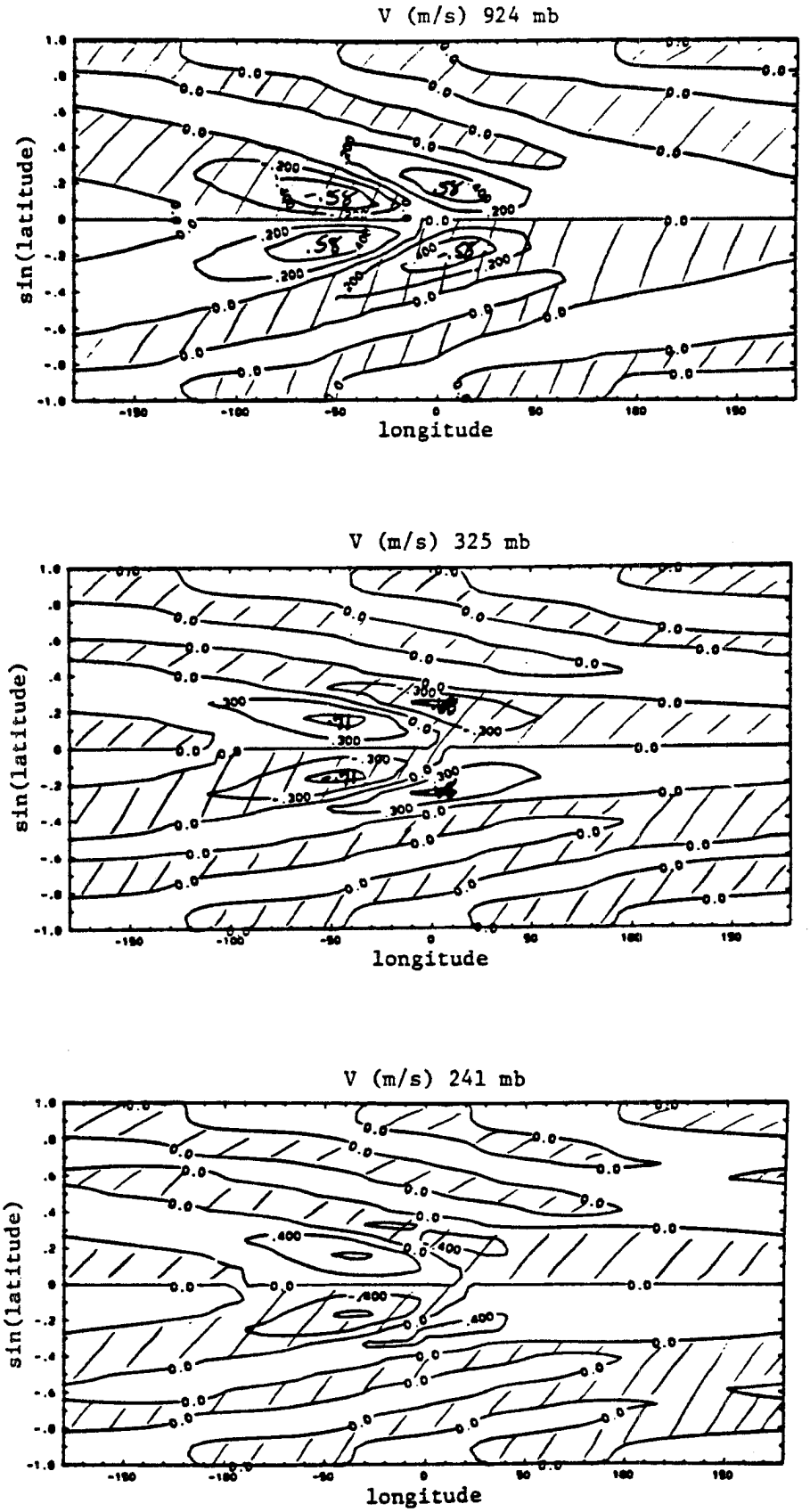

Fig. 5-11b. Perturbation v field for the run with a motionless basic state including cumulus friction. The heating is centered on the equator.

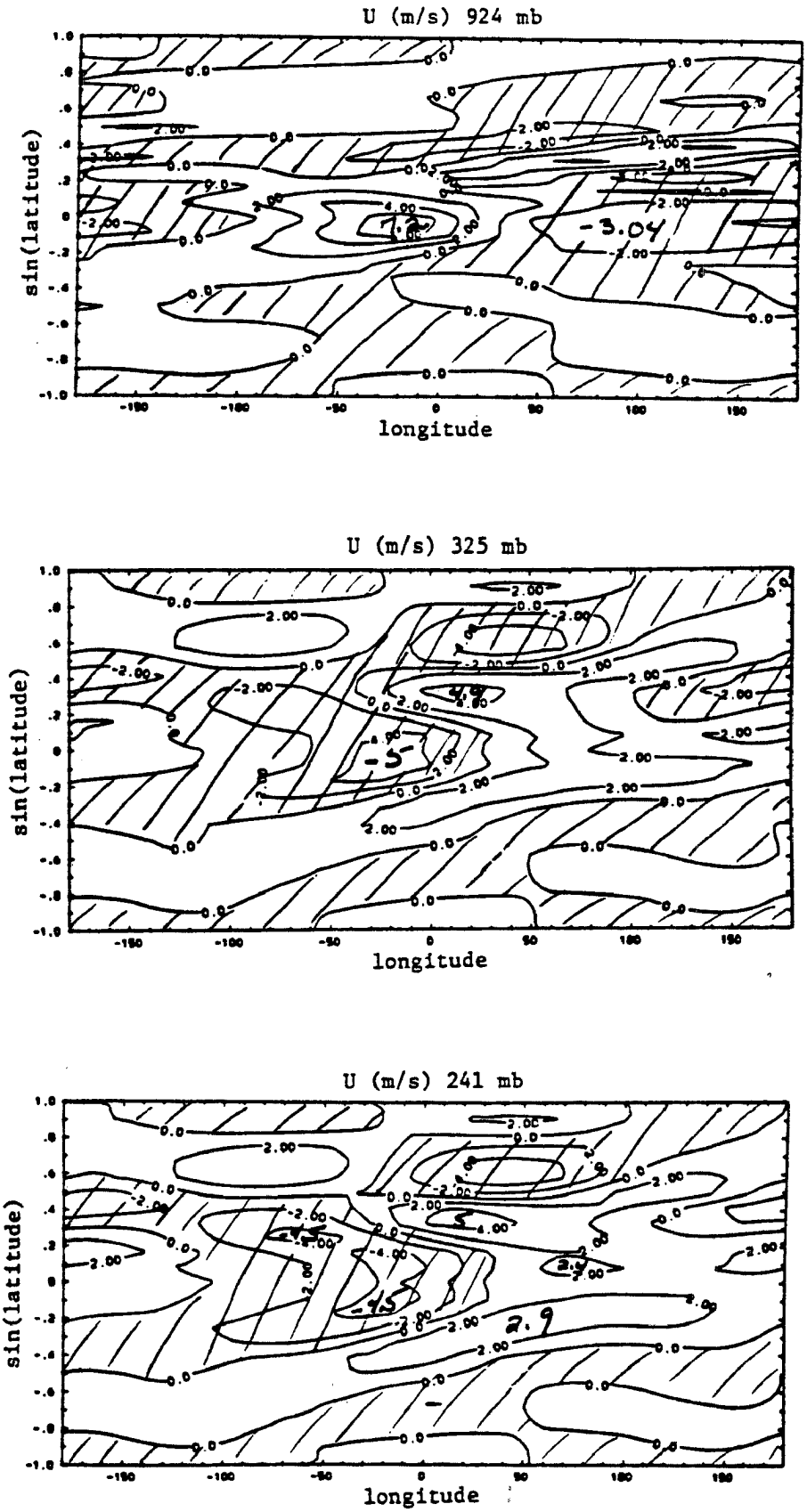

Fig. 5-12a. As in Fig. 5.11a except with a basic state consisting of a mean winter zonal wind.

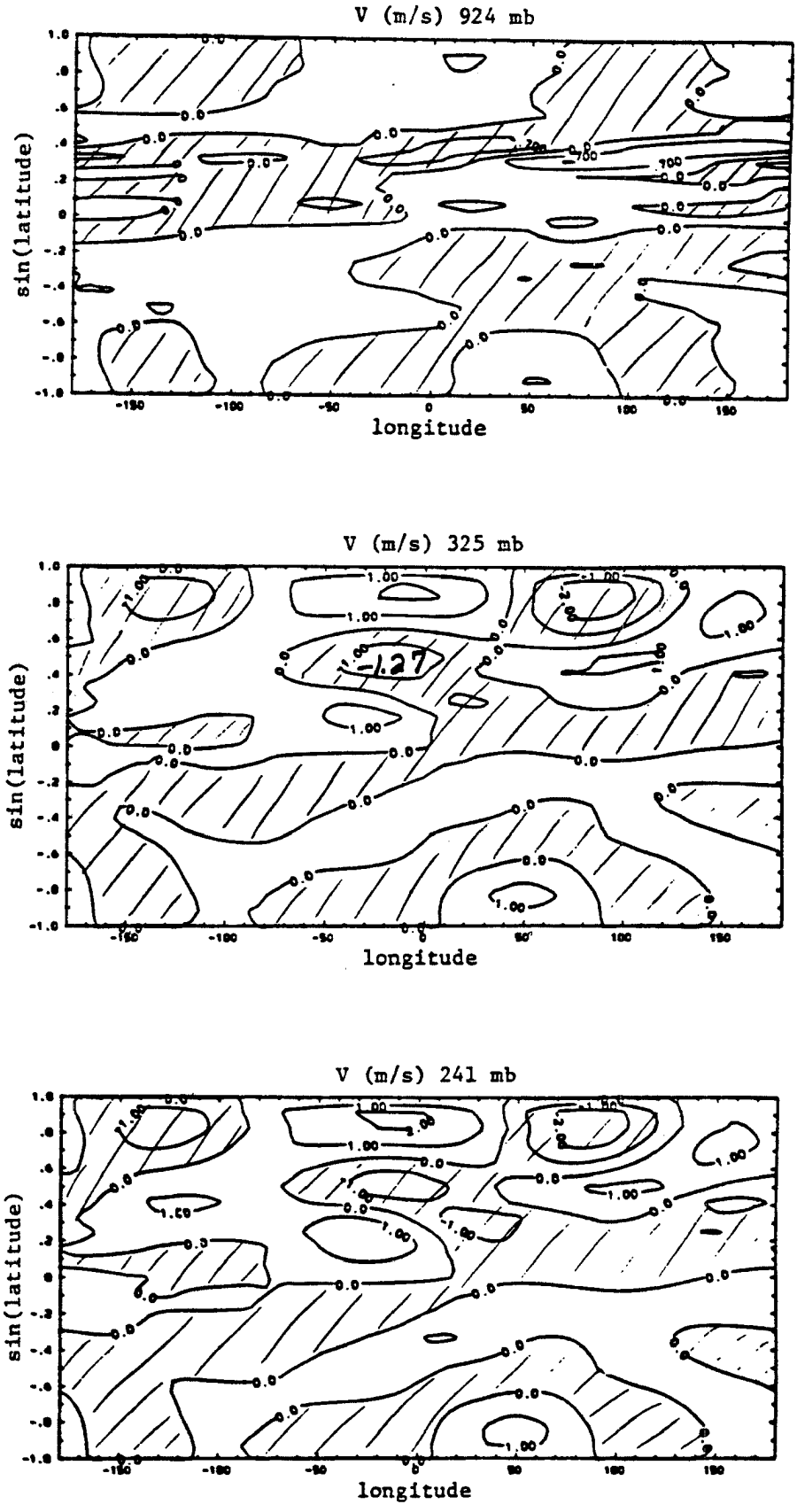

Fig. 5-12b. As in Fig. 5.11b except with a basic state consisting of a mean winter zonal wind.

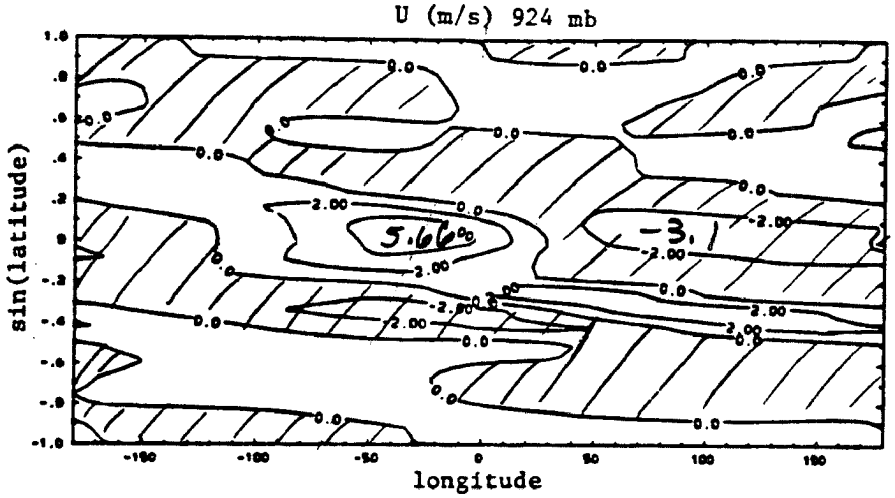

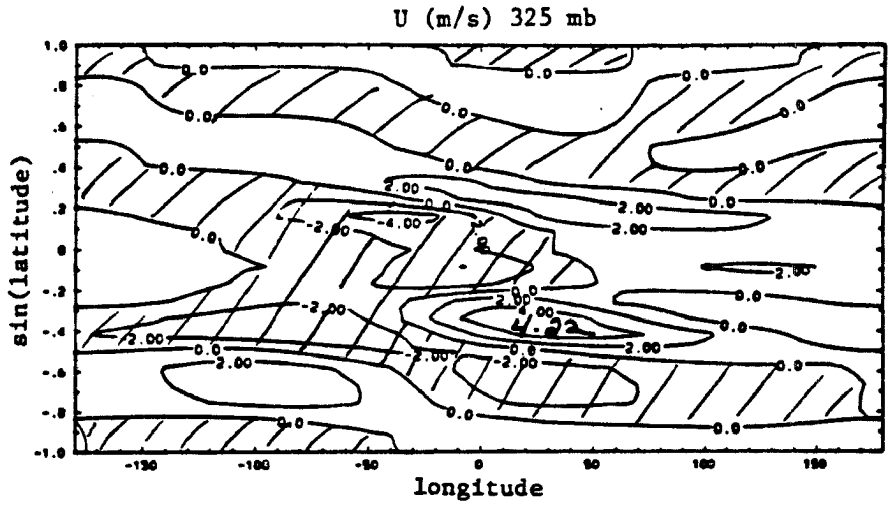

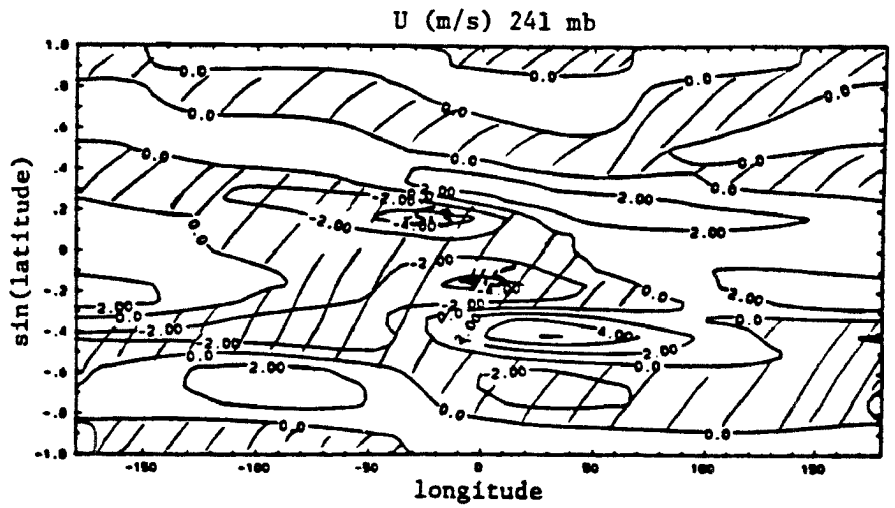

Fig. 5-13a. As in Fig. 5.11a except with a basic state consisting of a mean summer zonal wind.

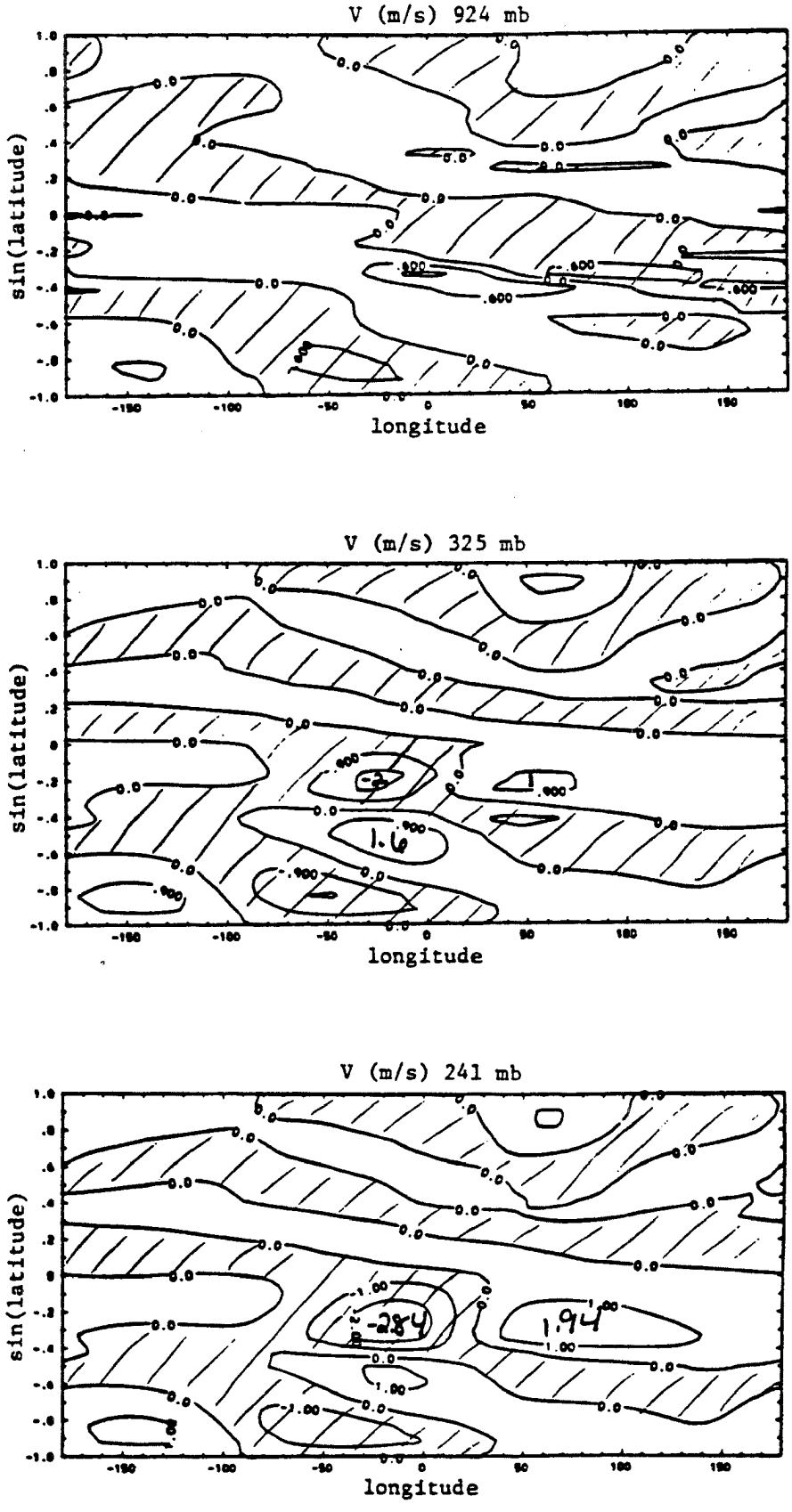

Fig. 5-13b. As in Fig. 5.11b except with a basic state consisting of a mean summer zonal wind.

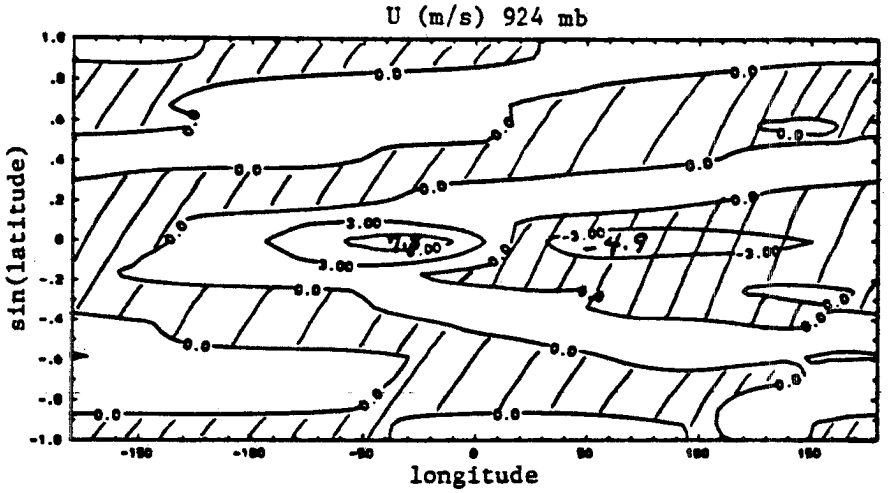

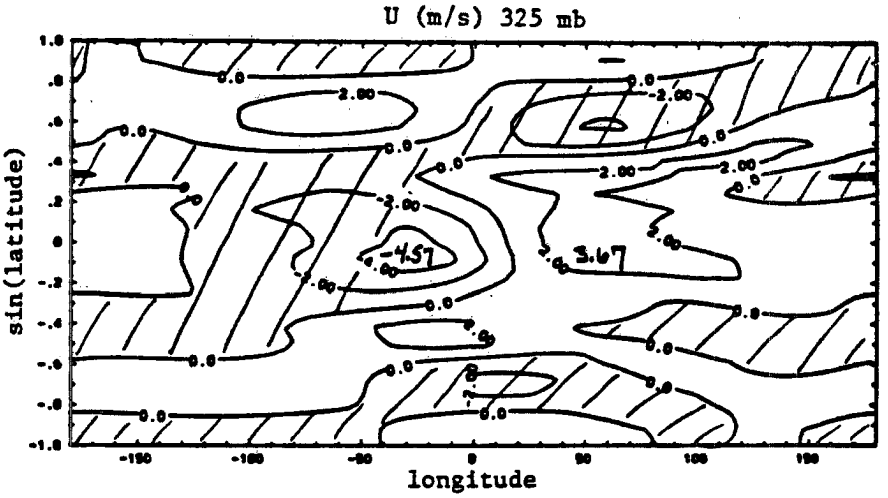

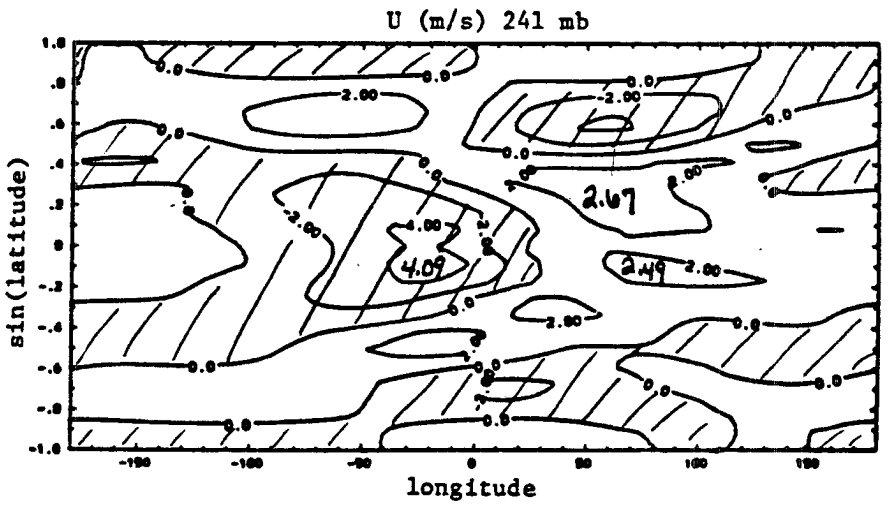

Fig. 5-14a. As in Fig. 5.11a except with a basic state consisting of a mean winter zonal wind and a Hadley cell centered on the equator.

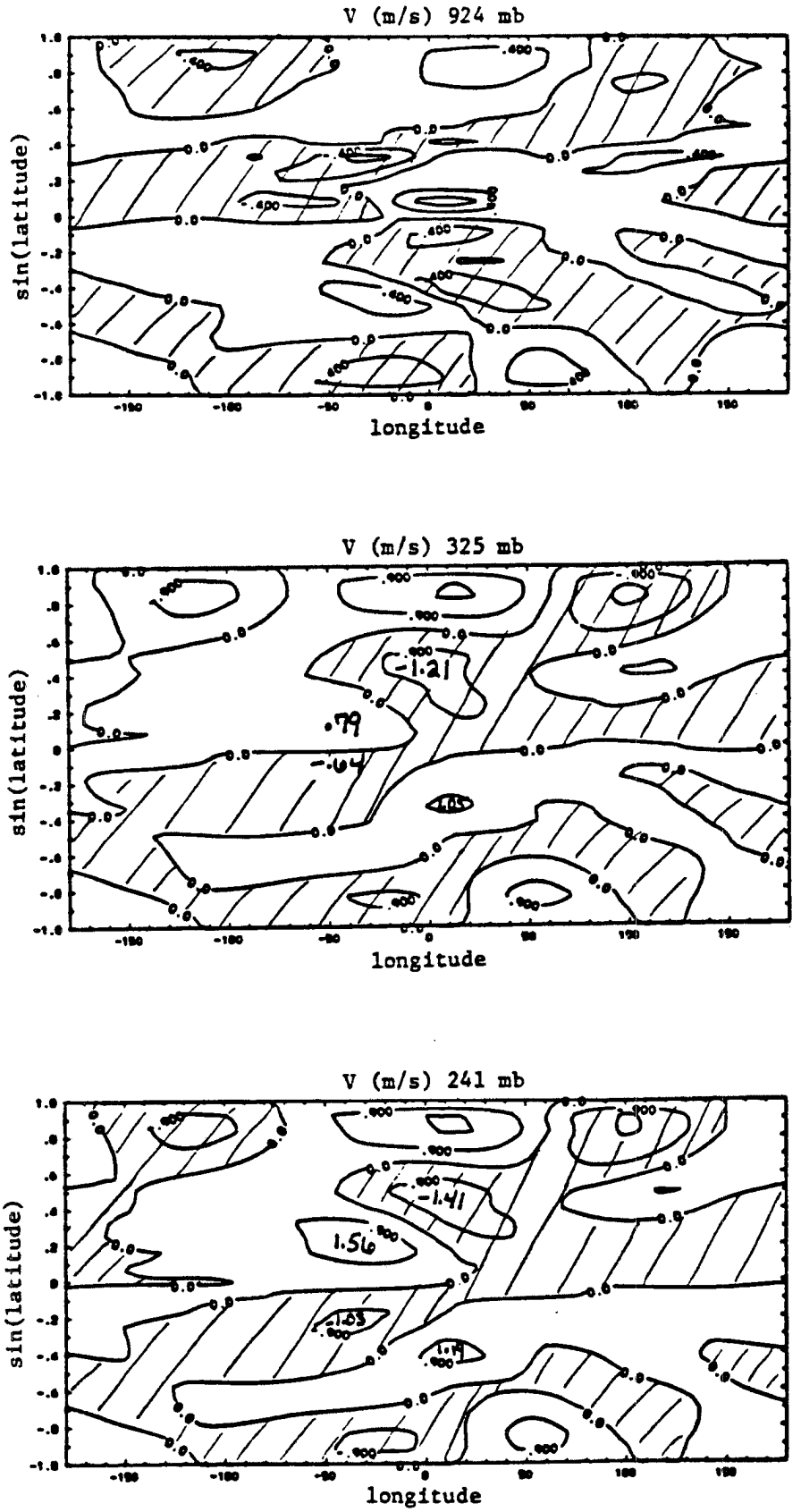

Fig. 5-14b. As in Fig. 5.11b except with a basic state consisting of a mean winter zonal wind and a Hadley cell centered on the equator.

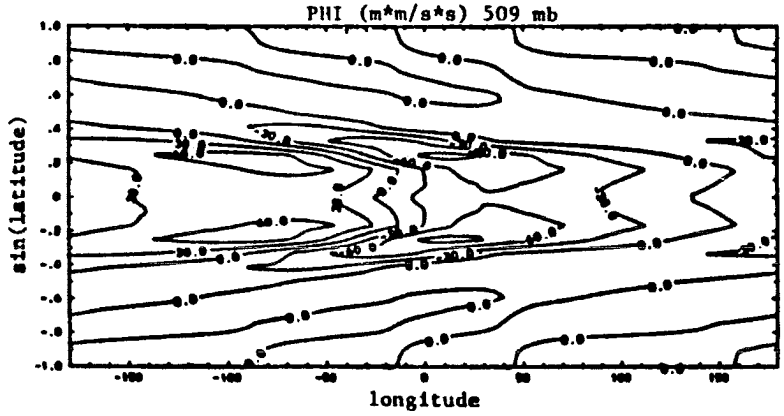

a)

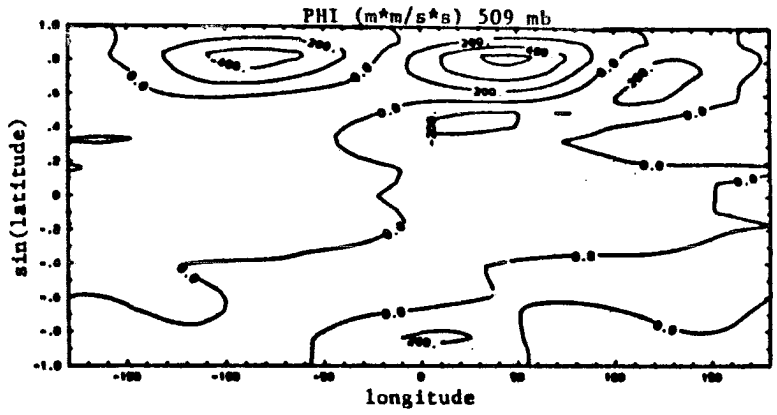

b)

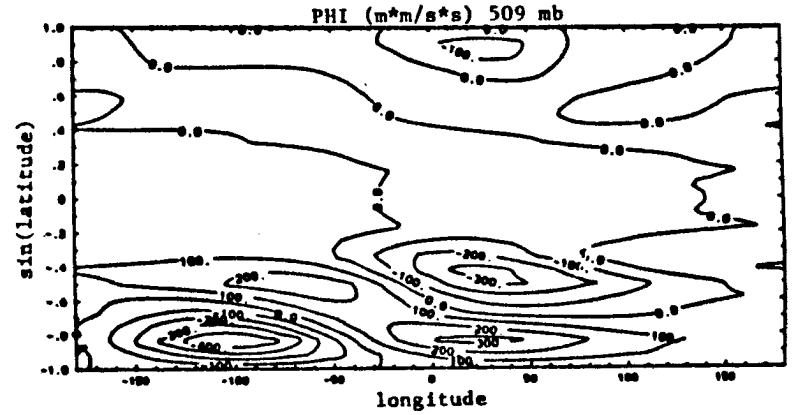

c)

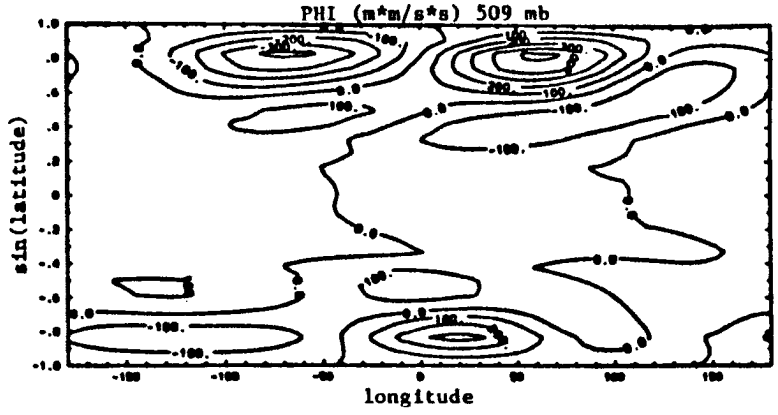

d)

Fig. 5-15. Perturbation geopotential at 509 mb for heating centered on the equator for a motionless basic state (a), a mean winter zonal wind basic state (b), a mean summer zonal wind basic state (c), a mean winter zonal wind and Hadley cell basic state.

and Lau and Lim (1982) both found results similar to this also using linear models. These two studies found that an anomaly embedded entirely in mean easterly winds will tend to produce an equatorially trapped response. We find that this is also true for an anomaly with no mean wind as did Gill (1980). However, if a heating anomaly lies either completely or partially within the weak equatorial westerlies, Rossby modes which can propagate poleward may be forced (Webster, 1982). The westerlies in which the anomaly occurs must be weak enough to allow what Webster terms a significant local response so that the remote response at higher latitudes may occur. If the mean winds are too strong, the heating is effectively dispersed over too great an area to produce a large local response. The reason that one should expect to see this teleconnection type response better in the winter hemisphere is that the mean westerlies extend further equatorward. Thus, more of the anomaly exists in weak westerlies in the winter hemisphere. Lindzen et al. (1982) also found an enhanced response to a tropical forcing when they used a mean wind consisting of unbroken westerlies across the tropical upper troposphere.

The heating used for the runs in this study effectively extends from 20° S to 20° N (Fig. 5.16). The mean wind fields we are using would therefore allow some of the anomaly to lie in the weak westerlies, so the extratropical response in the wind and geopotential fields is seen.

In order to assess the effect of including a mean circulation on the model Walker Circulation, mass fluxes (Fig. 5.17) and the u field (Fig. 5.18) on the equator were examined. Including a mean winter zonal wind slightly weakened the circulation to the east of the heating in the

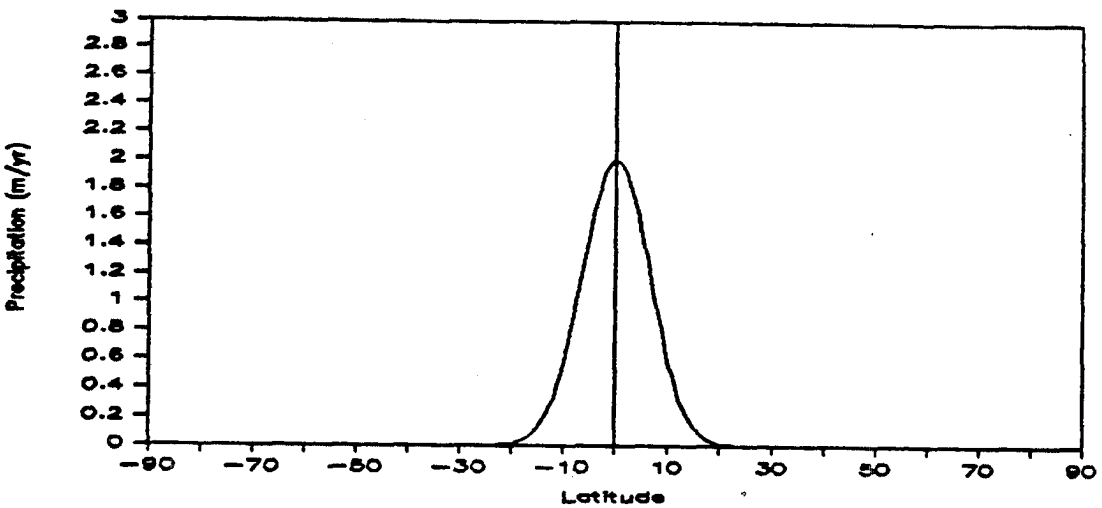

Fig. 5-16. Latitudinal structure of the perturbation heating. The anomaly is a Gaussian with a latitudinal e-folding width of 9° and amplitude of 2 m/yr.

a)

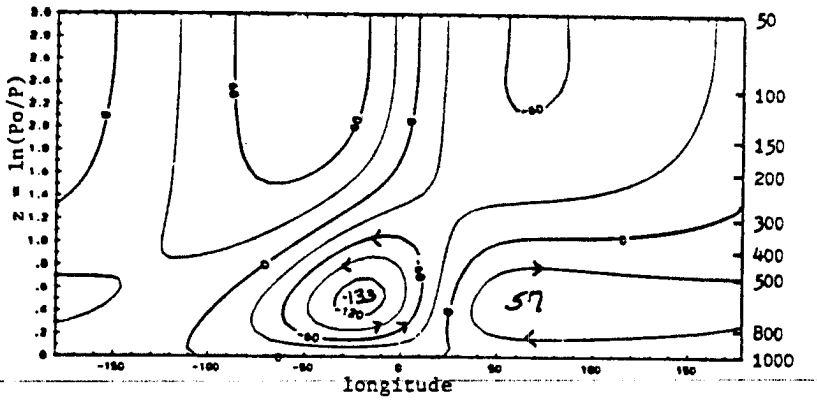

b)

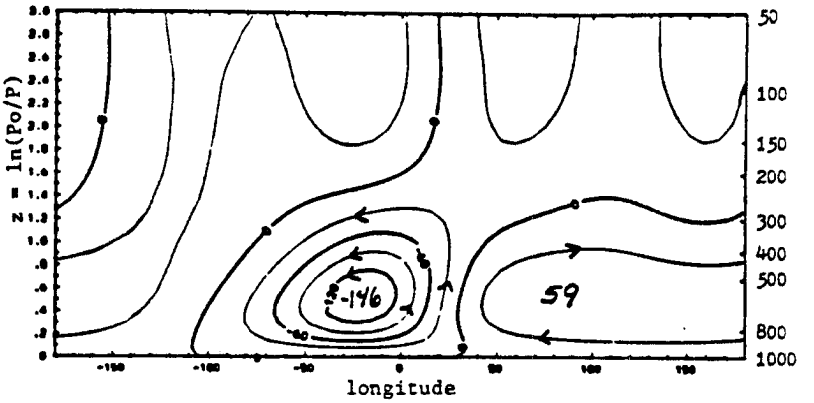

c)

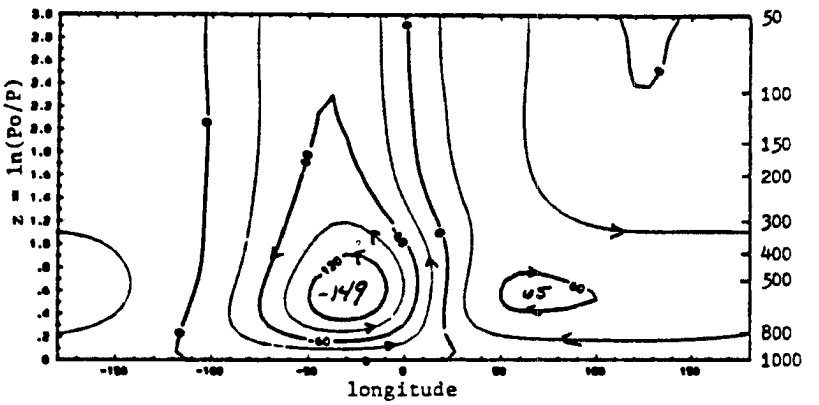

d)

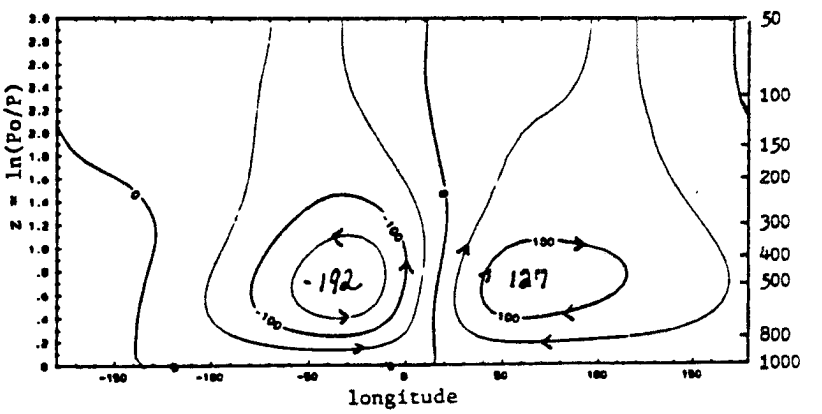

Fig. 5-17. Contours of mass flux (units of 10E11 gm/s) overturning in a strip 10° wide centered on the equator for a motionless basic state (a), a mean winter zonal wind basic state (b), a mean summer zonal wind basic state (c), a mean winter zonal wind and Hadley cell basic state

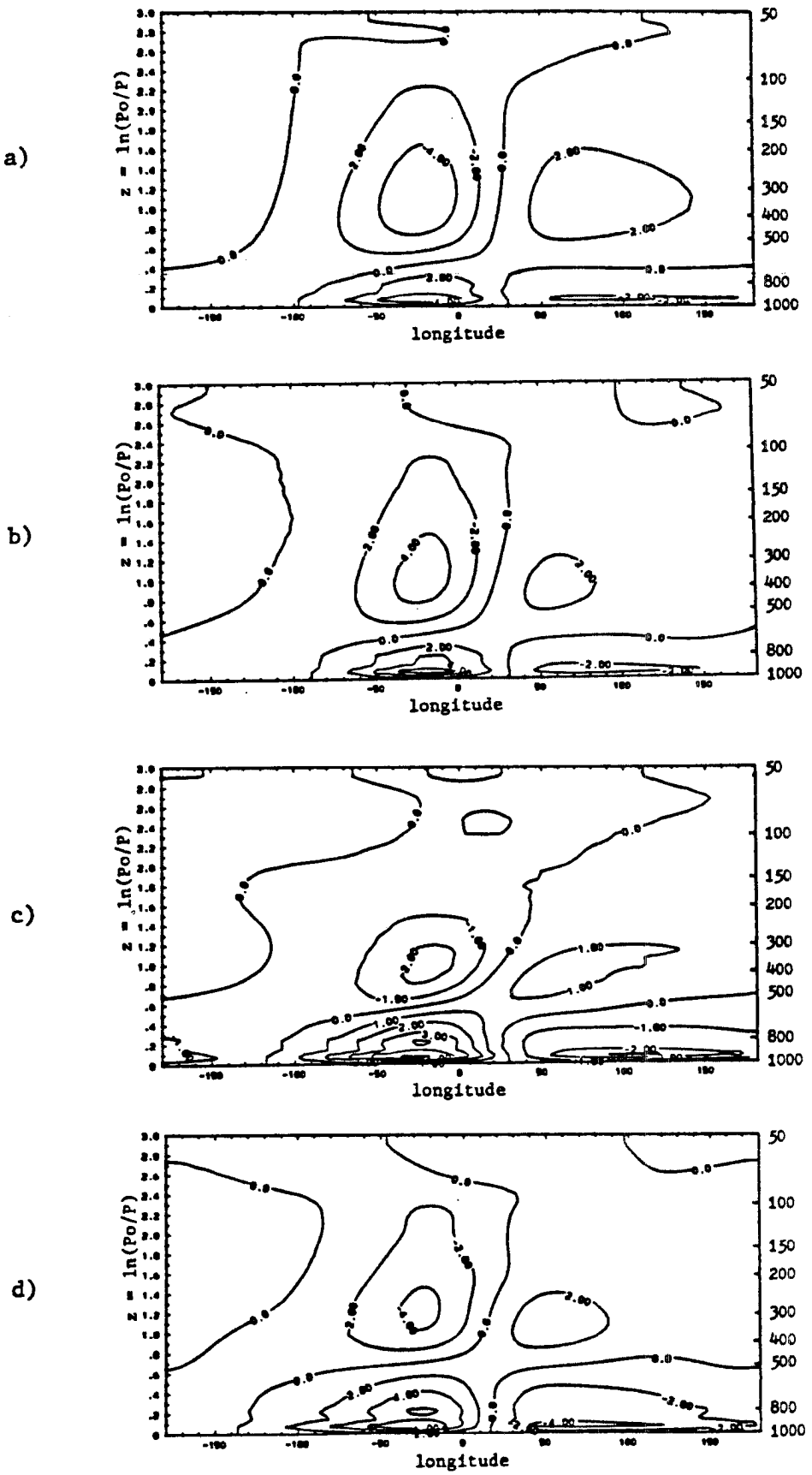

Fig. 5-18. Perturbation u field for the cases described in Fig. 5.17.

upper levels. Including the mean summer zonal wind which consisted entirely of easterlies on the equator greatly weakened the circulation in the upper levels, but the zonal wind convergence in the lower levels increased. This extra convergence in the lower levels is compensated for by a greatly increased meridional velocity to the south in upper levels. Including a mean Hadley cell along with the winter basic state brings about a rise in the zero wind level, and slightly weakens the upper westward flow. However, the lower level circulation is somewhat increased. This appears to be compensated for by a weakening in the lower levels of the meridional circulation that operates in the same sense as the Hadley cell. There is little change in the magnitude of the poleward flow of the upper levels, but there is a small increase in the area that the poleward flow covers. In addition, the intensity of the eastern branch of the Walker Circulation is increased relative to the westward branch.

The mass fluxes derived from model results show that either having the heating embedded in mean easterlies or including a mean Hadley cell tends to eliminate the tilt of the circulation seen for the other two cases. This makes the mass flux appear more like that derived from observations (Fig. 1.1). In addition, the circulation to the east of the heating is strengthened relative to the response west of the heating for the case including a mean Hadley cell. This also appears more like the observations; however our model circulation east of the heating is still weaker relative to that to the west than is the case for the observed mass flux.

5.3 Discussion of runs with heating centered at 9° N

The heating for these runs is also a Gaussian with an e-folding width of 9° in the latitudinal direction and 40° in the longitudinal direction. It is of the form

$$Q = \exp\left[-\left(\frac{\lambda}{\lambda_0}\right)^2\right]\exp\left[-\left(\frac{\theta-\theta'}{\theta_0}\right)^2\right]F(p)$$

where $\theta' = 9°$, and F(p) is given in equation 3.2 with $p_T = 100$ mb and $p_b = 900$ mb. The base run again includes $\bar{M}_c$ but has a zero basic state. Mc' has the same latitudinal and longitudinal distribution as the heating field, and $\bar{M}_c$ is also centered on 9° N and is Gaussian in latitude with an e-folding width of 9°.

Four runs were made with this heating, these are summarized in Table 5.1. Run 2a is with a resting basic state, run 2b is with a mean winter zonal wind, run 2c is with a mean summer zonal wind, and run 2d is with the summer zonal wind field and a mean Hadley cell centered at 9° N.

The wavenumber one response at the heating center for the resting basic state run, run 2a, shows the level of zero wind occurs at approximately z = .45 or 640 mb (Fig. 5.19). This is slightly higher than for run 1a with the heating centered on the equator. When the mean summer zonal wind is used, run 2c, the level of zero wind is about the same, and the overall response at 9° N is very similar (Fig. 5.20). Including a mean Hadley cell with the summer mean zonal wind, run 2d, significantly changes the response (Fig. 5.21). The level of zero wind is lifted to near 500 mb as was the case for the heating centered on the equator. In addition, the amplitude of the zonal wind response is increased with the peak near 240 mb which is almost twice that of the

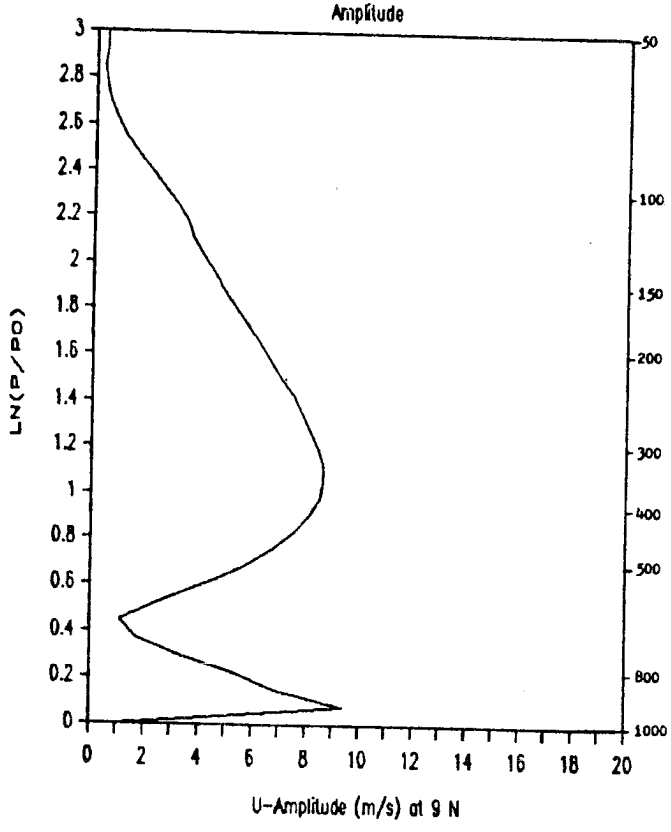

a)

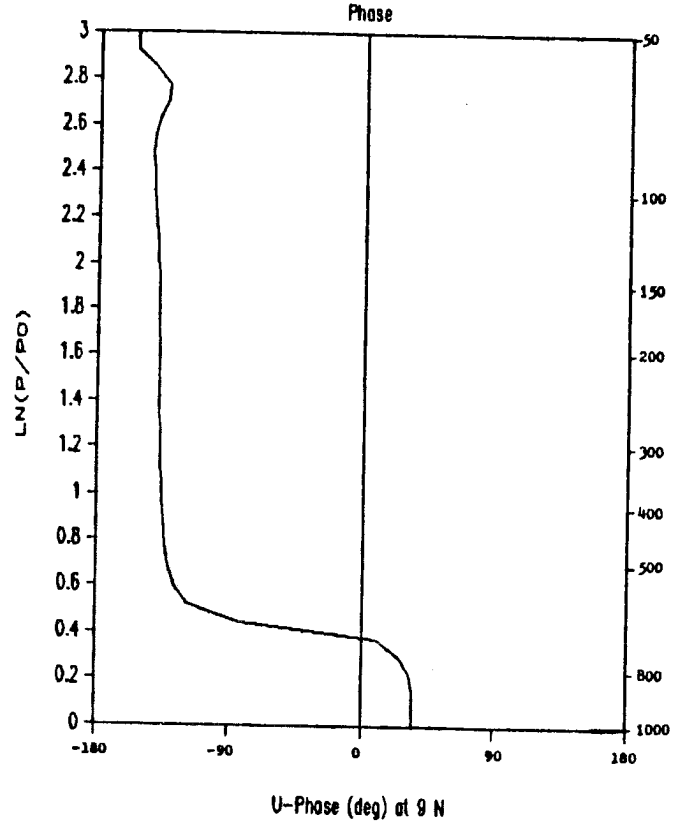

b)

Fig. 5-19. Amplitude (a) and phase (b) of zonal wind at 9°N for wavenumber one forcing only for the the run with a motionless basic state including cumulus friction. The heating is centered at 9°N.

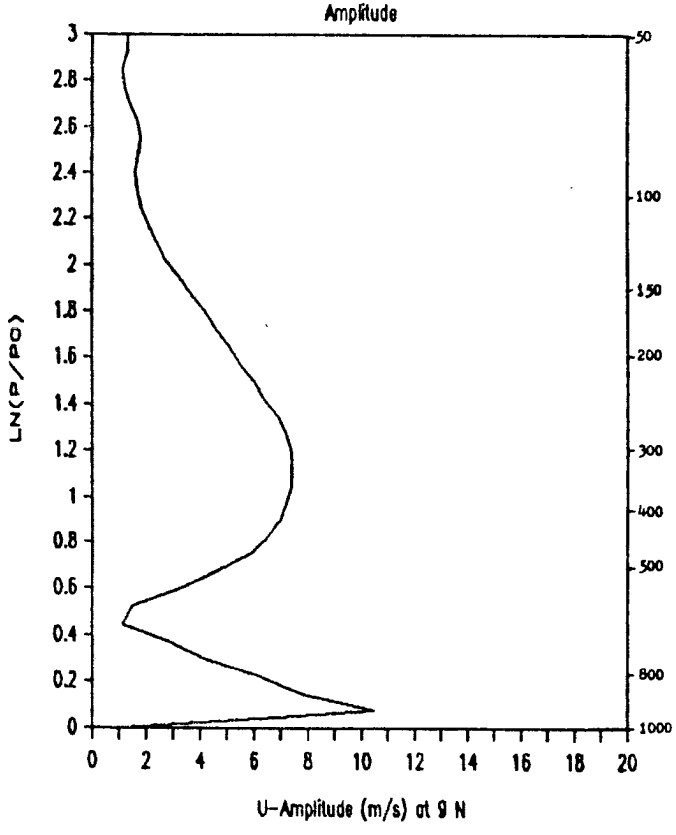

a)

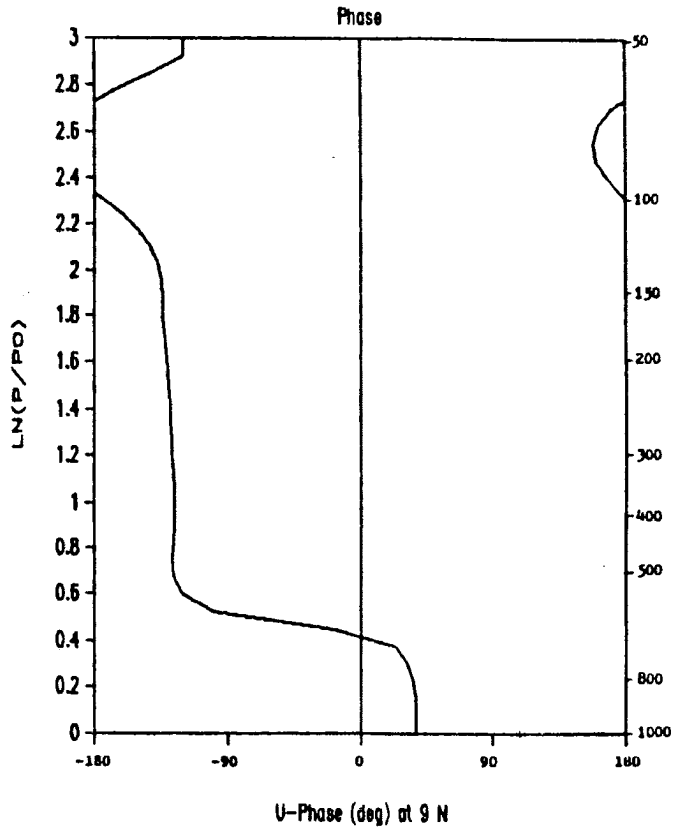

b)

Fig. 5-20. As in Fig. 5.19 except with a basic state consisting of a mean summer zonal wind.

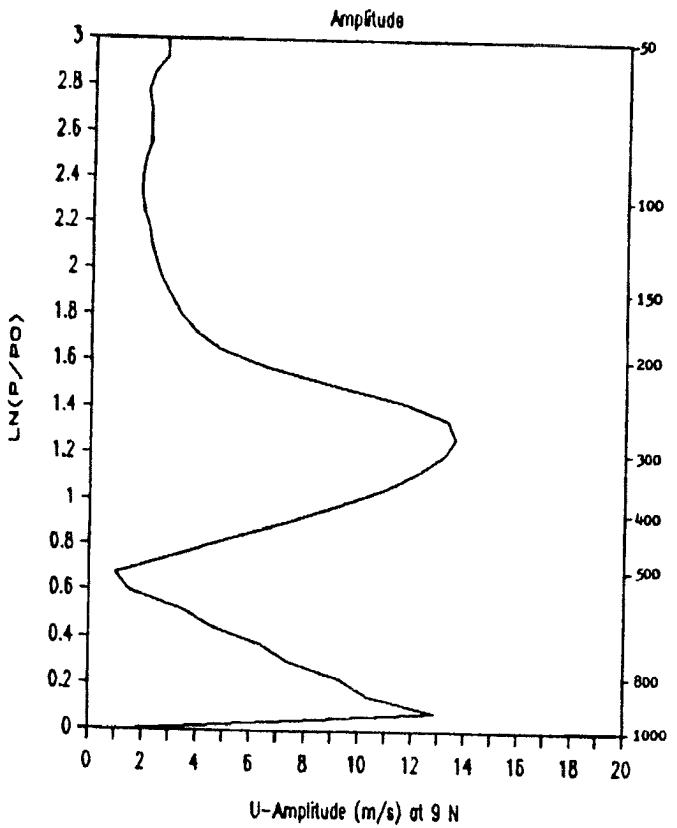

a)

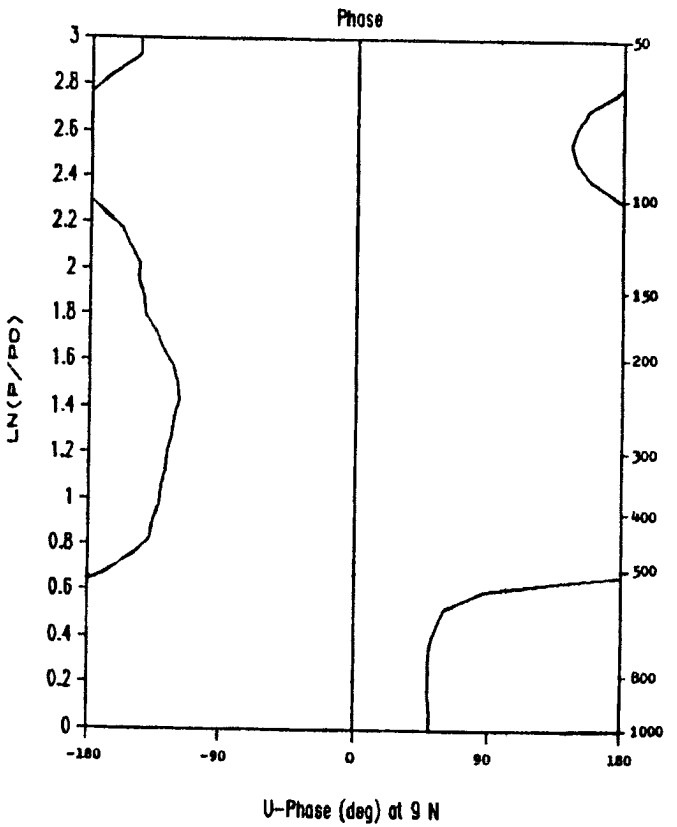

b)

Fig. 5-21. As in Fig. 5.19 except with a basic state consisting of a mean summer zonal wind and a Hadley cell centered at 9°N.

case with no Hadley cell. In addition to the terms with the largest magnitudes discussed for the case with the heating on the equator, the $-fv'$ term is also significant at 9°N. Again, the term $\bar{w}\frac{\partial u'}{\partial z}$ has slightly smaller magnitude that the term $-\frac{g}{p}\frac{\partial}{\partial z}(\bar{M}_c u')$, but is of the opposite sign. Including a mean Hadley cell then diminishes the effect of the cumulus friction.

The summations of wavenumbers one through ten reveal several unexpected results. The first is that even though the heating is centered in the northern hemisphere, a significant response is seen in the southern hemisphere. For run 1a, with the heating centered on the equator (Fig. 5.11), the maximum response in the perturbation u field to the west of the heating occurs right on the equator. However, for the 9° N heating, run 2a, that maximum is seen south of the heating center and in the upper troposphere it is south of the equator (Fig. 5.22). The maxima to the west are no longer vertically stacked as was the case for the equatorial heating, but tilt southward with increasing height. The westerly jets near 300 mb are still present, and slightly stronger. At 325 mb, the response is greatest in the southern hemisphere. This is most likely due to the cumulus friction term, which damps the response in the vicinity of the heating. For a case that was run with no cumulus friction and no basic state, maximum responses are found to occur very close to the heating and the total response is mostly in the northern hemisphere but south of 30° N. The perturbation v field has its largest magnitude in northern hemisphere and the complementery circulation in the southern hemisphere is not as strong as for the equatorial heating. The circulation that acts in the sense opposite to that of a Hadley cell tilts southward with height and is stronger relative to the v response

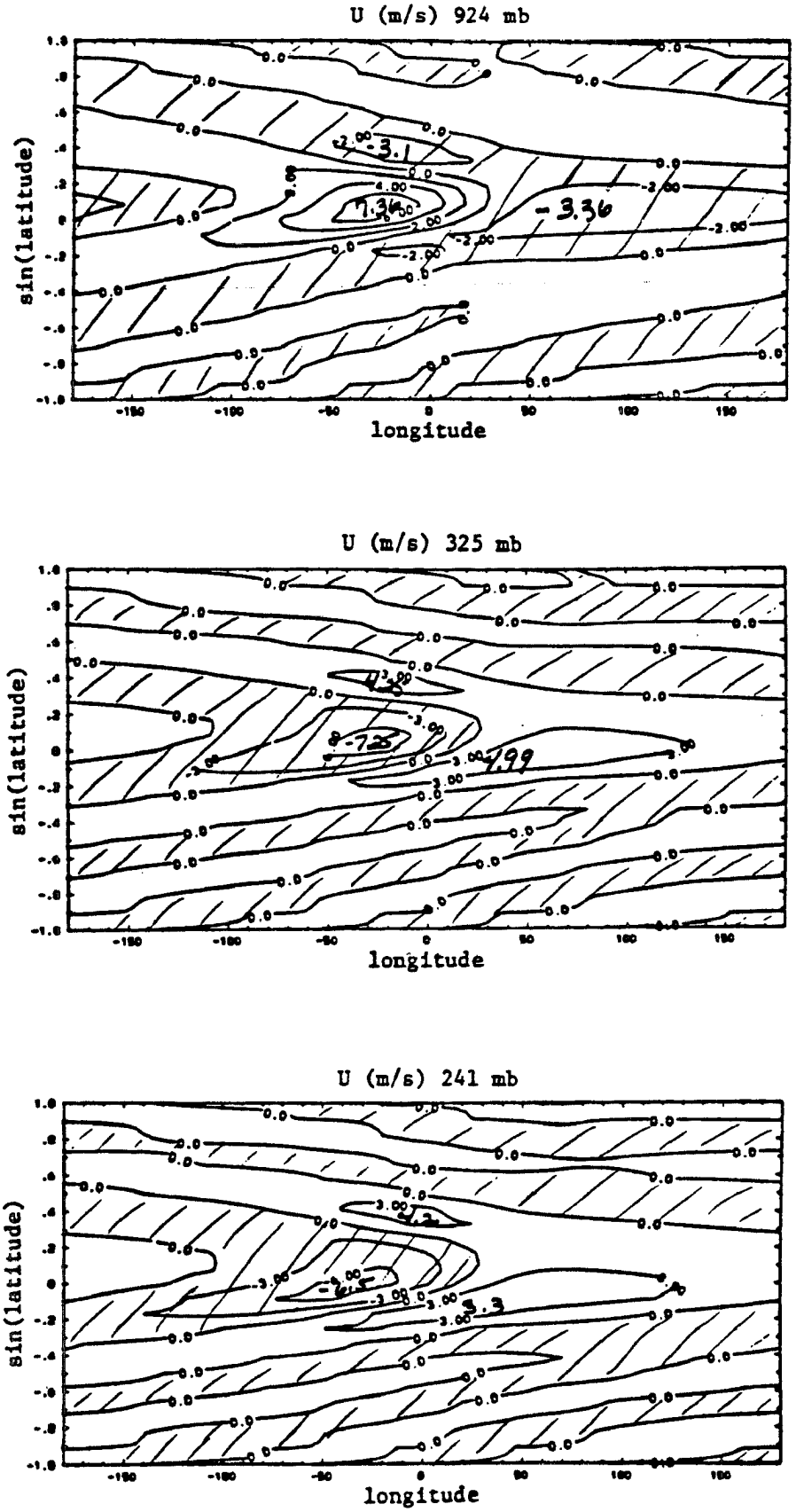

Fig. 5-22a. Perturbation u field for the run with a motionless basic state including cumulus friction. The heating is centered at 9°N.

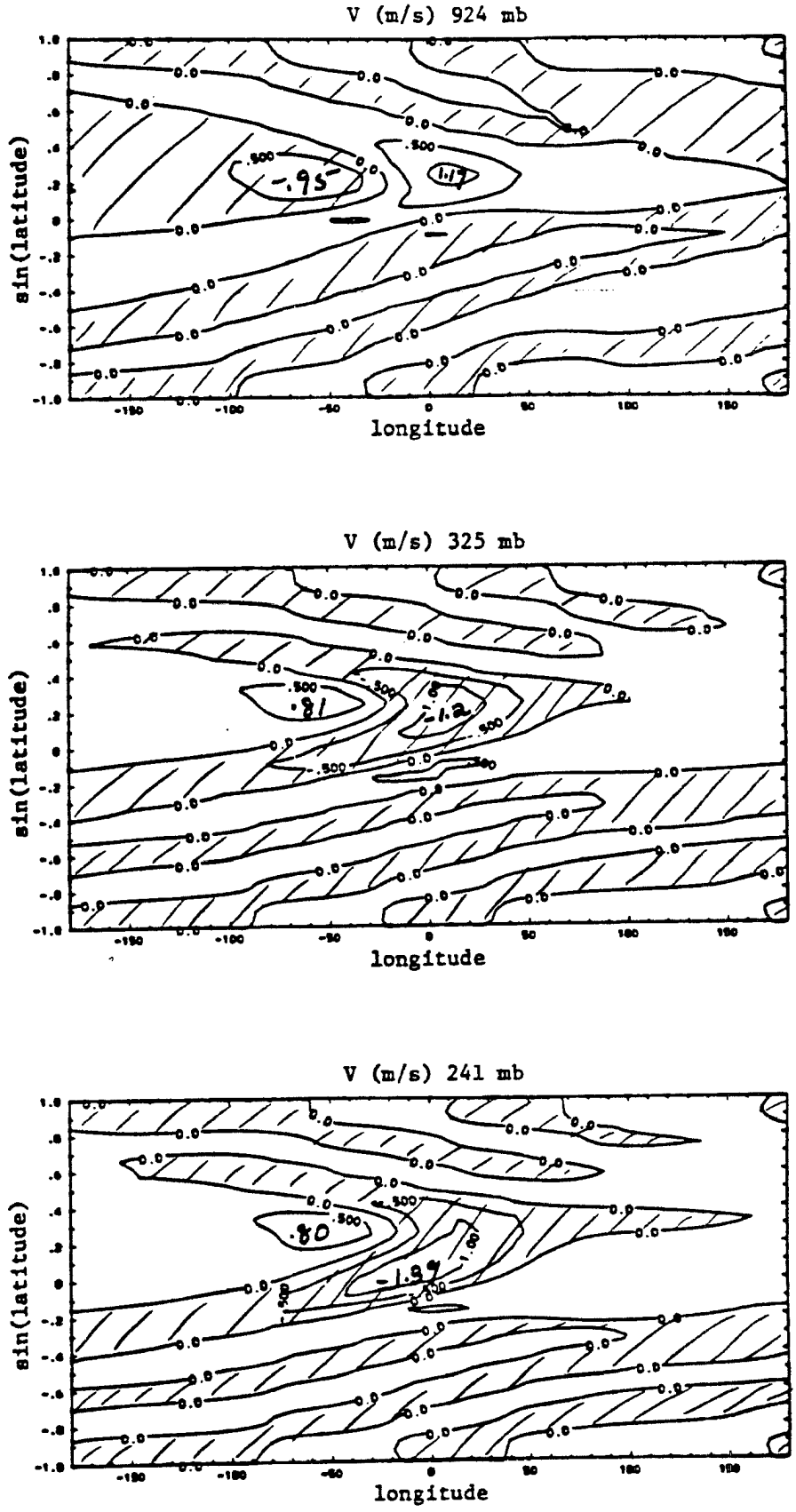

Fig. 5-22b. Perturbation v field for the run with a motionless basic state including cumulus friction. The heating is centered at 9°N.

west of the heating that for the equatorial heating case. Thus, we would expect to see an even weaker northern hemisphere Hadley cell over the eastern Pacific when the heating is off the equator.

When the winter average mean zonal wind is included, run 2b, again the most significant difference is the appearance of a large amplitude response in the higher latitudes of the northern hemisphere (Fig. 5.23). It is even larger than for the equatorial heating with the same basic state, most likely because for this case a larger portion of the perturbation heating lies in weak westerlies.

When the summer average mean zonal wind is used for the basic state, run 2c, the major perturbation u response is in the southern hemisphere as was the case for the equatorial heating (Fig. 5.24). However, we do not see the significant response in the higher latitudes. This is probably due to the fact that most of the heating lies in mean easterly winds. For the equatorial heating, run 1c, the major response in the v fields occurs in the southern hemisphere. However, when the heating is moved to 9° N, run 2c, there is a similar magnitude v response in the northern hemisphere. Another difference between the run with the heating at 9° N and that on the equator is that the magnitude of the meridional circulation east of the heating is greater relative to that west of the heating for the off-equator heating.

Including a mean Hadley cell centered at 9° N with the summer zonal wind, run 2d, acts to increase the u response near the heating in the northern hemisphere (Fig. 5.25). A larger magnitude extratropical response in the southern hemisphere also appears as a result of including a mean Hadley cell. In addition, the intensity of the u response to the east of the heating is increased relative to the circulation to the

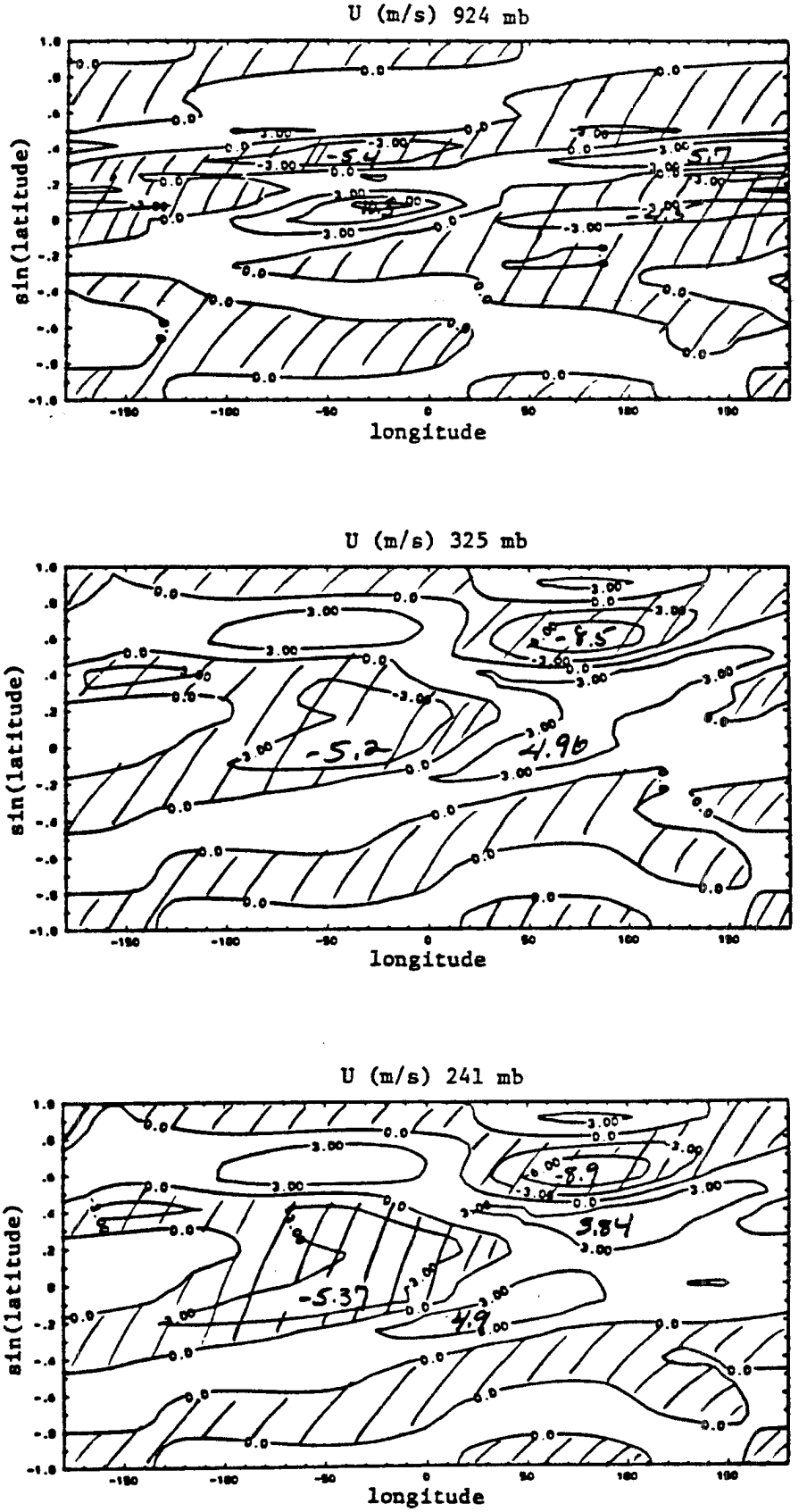

Fig. 5-23a. As in Fig. 5.22a except with a basic state consisting of a mean winter zonal wind.

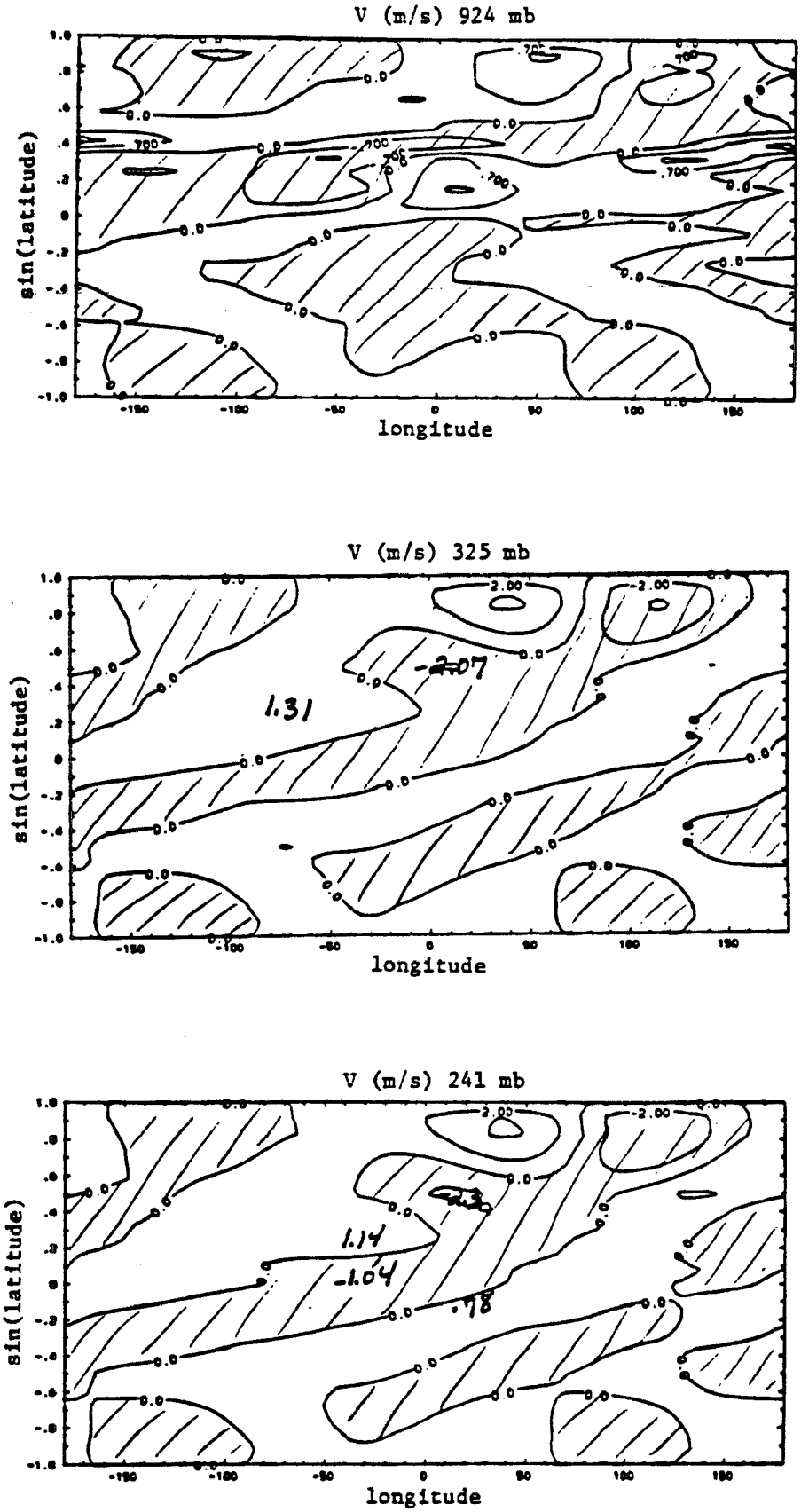

Fig. 5-23b. As in Fig. 5.22b except with a basic state consisting of a mean winter zonal wind.

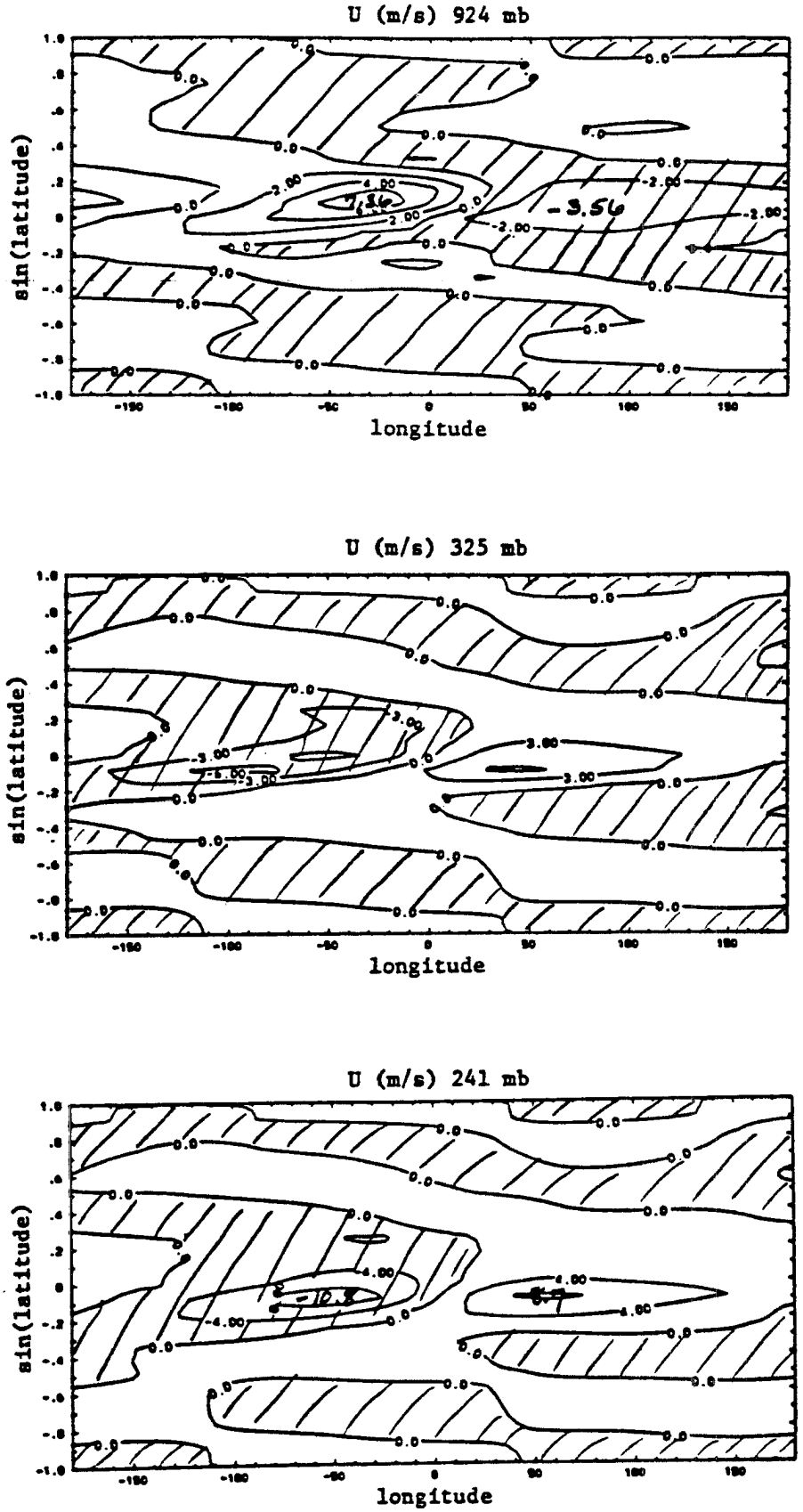

Fig. 5-24a. As in Fig. 5.22a except with a basic state consisting of a mean summer zonal wind.

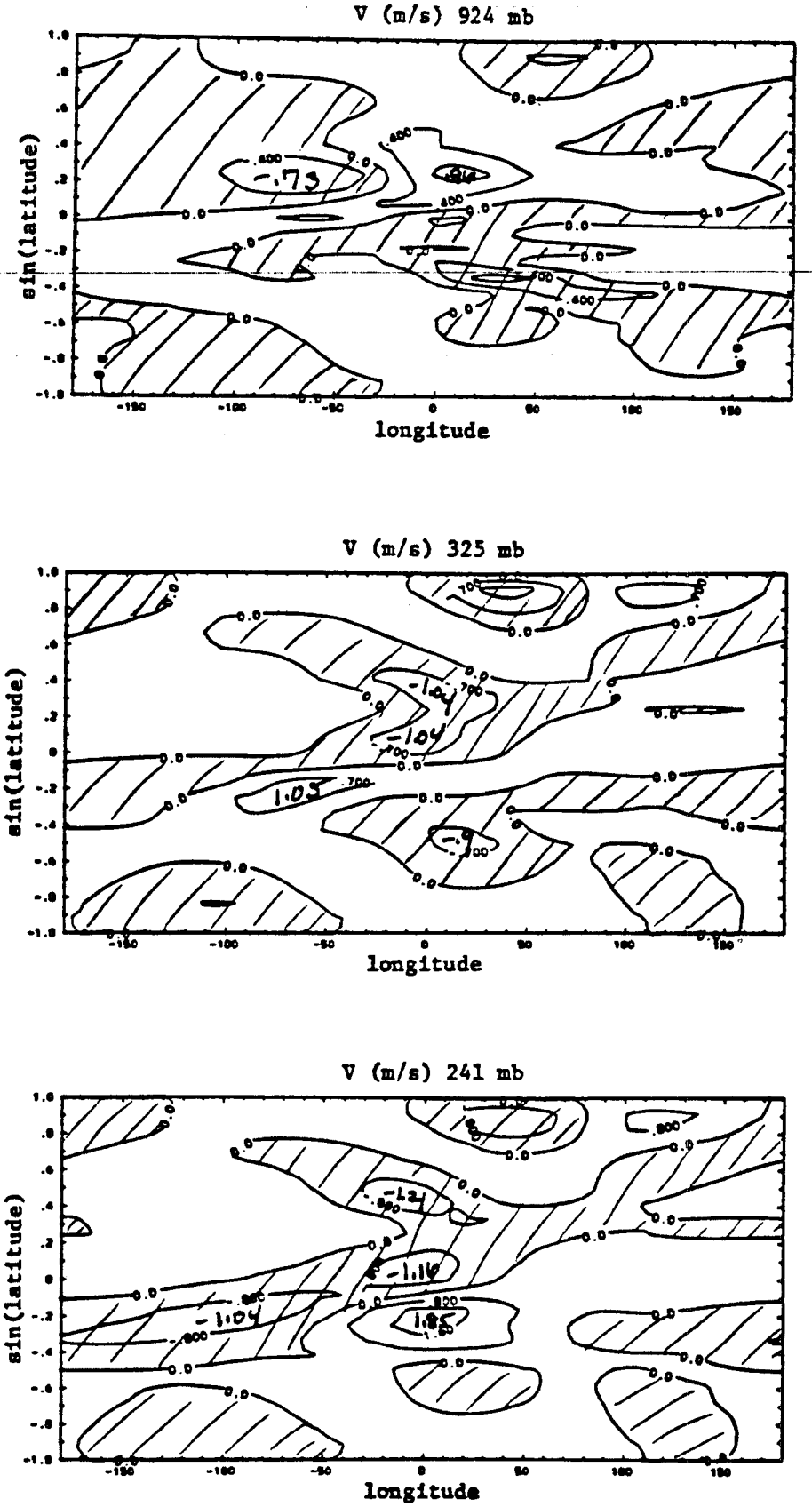

Fig. 5-24b. As in Fig. 5.22b except with a basic state consisting of a mean summer zonal wind.

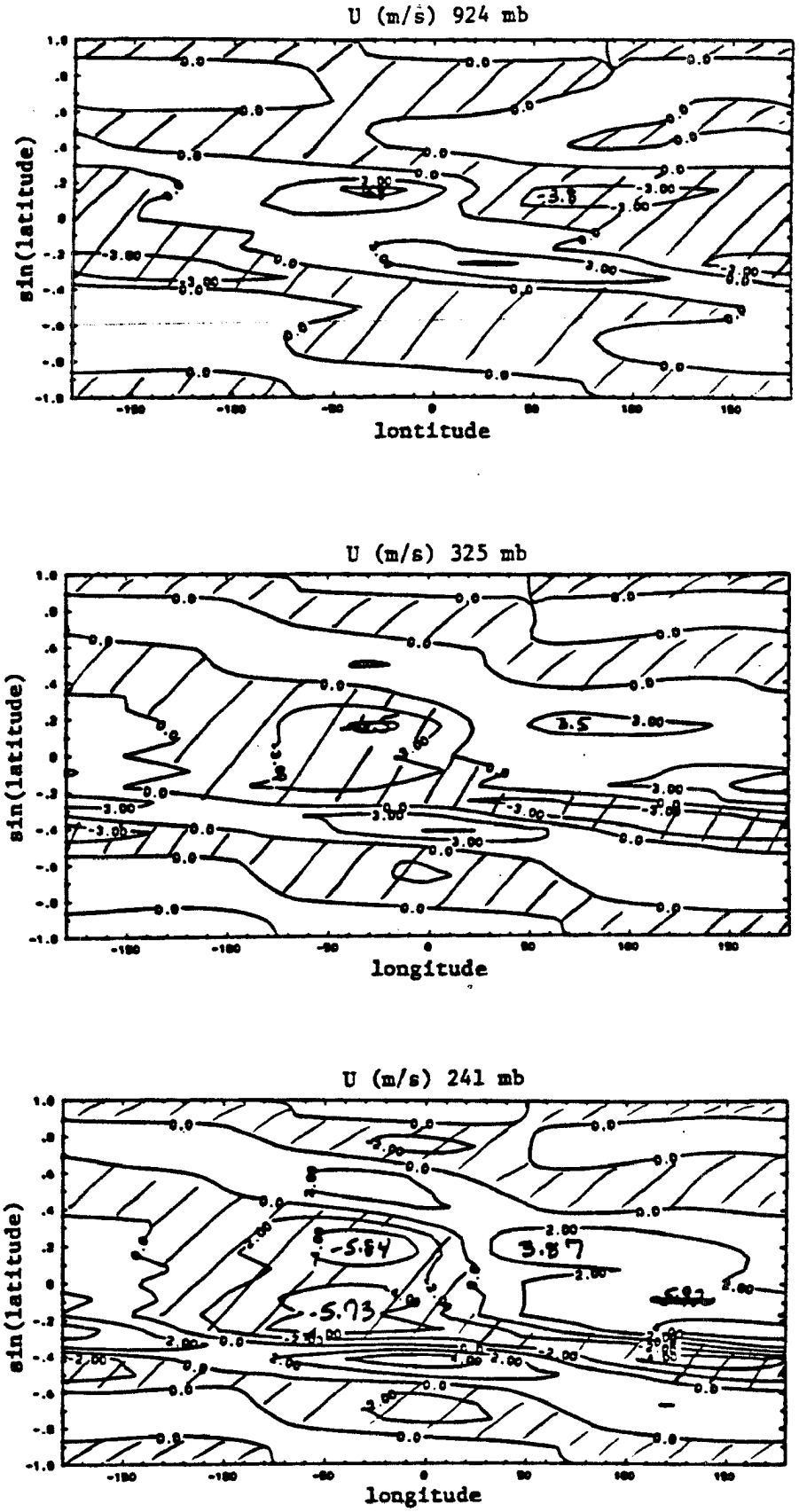

Fig. 5-25a. As in Fig. 5.22a except with a basic state consisting of a mean summer zonal wind and a Hadley cell centered at 9°N.

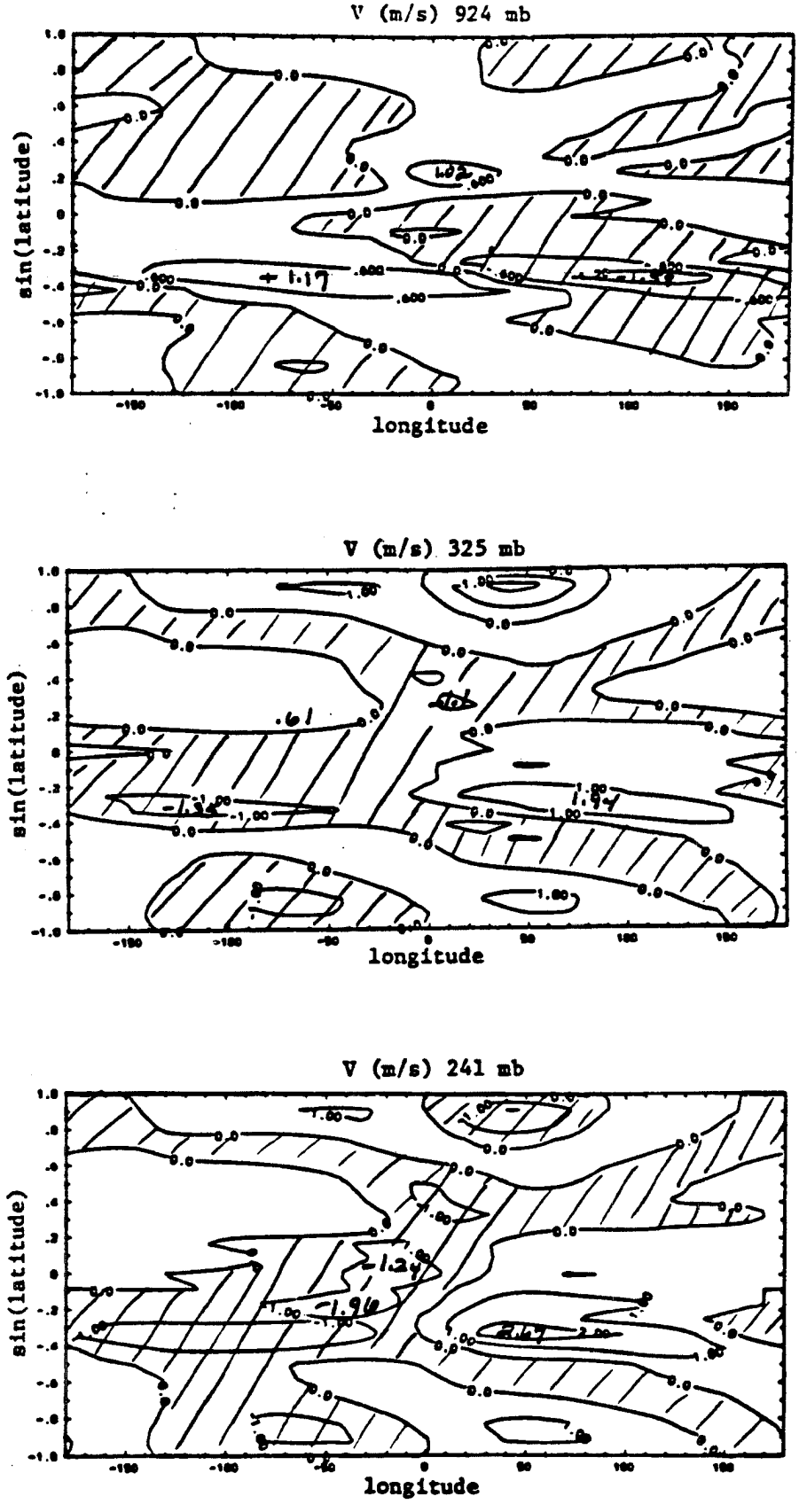

Fig. 5-25b. As in Fig. 5.22b except with a basic state consisting of a mean summer zonal wind and a Hadley cell centered at 9°N.

west of the heating as was the case for the equatorial heating. In the v field, there is a strengthening of the meridional circulation in the southern hemisphere when compared with the run with no Hadley cell. The presence of the mean Hadley cell seems to increase the area which is influenced by the heating more so for the 9° N heating than for the equatorial heating. This is probably due to the mean zonal wind fields being used for each case. For the equatorial heating, run 1d, a mean winter zonal wind was used because in the northern hemisphere winter, the mean Hadley cell tends to be centered near the equator. However, the mean Hadley cell tends to be centered in the northern hemisphere in the summer, so a mean summer zonal wind structure was used for the off-equator heating, run 2d. Therefore, when the mean Hadley cell was centered on the equator, the mean zonal winds were weak easterly in the lower levels turning to westerly above 300 mb with a significant amount of the heating in westerlies above 600 mb. However, for the basic state with a mean Hadley cell centered at 9° N, mean easterlies existed to the model top. When a tropical heating is entirely embedded in easterlies without a Hadley cell, the response tends to be equatorially trapped. When the heating is partially in mean westerlies, a higher latitude response is seen. For the run with the heating on the equator, a larger portion of the heating lies in mean westerlies than for the 9° N run, so that a significant response is seen outside of the tropics even without a mean Hadley cell. However, when the heating is placed at 9° N with the mean summer zonal winds, most of the heating is confined within mean easterlies, and the main response is limited to the tropics. The addition of a mean Hadley cell provides a means for the heating to influence areas outside of the band of easterlies. Advection by the

mean wind therefore appears to be more important for instances where the heating lies exclusively in mean easterlies than when some of the heating lies in mean westerlies.

The effect of moving the heating to 9° N on the Walker circulation can be seen by comparing the u fields at the heating centers. The resulting east-west circulation at 9° N (Fig. 5.26) is quite similar to the equatorial heating for the cases with a motionless basic state. The off-equator heating produces a stronger circulation at the heating center for the summer zonal basic state. The circulations are of similar magnitudes for the winter zonal basic state in the upper levels while slightly weaker near the surface. When the u field on the equator is examined (Fig. 5.27), it can be seen that the east-west circulation is stronger than for the equatorial heating for the three basic states which do not include a Hadley cell. The two runs which do include a Hadley cell cannot be compared because they use entirely different basic states. However, as was the case for the equatorial heating, including a basic state Hadley cell raised the level of zero wind.

5.4 Summary

We have come to two main conclusions from this study of the sensitivity of the model response to different basic states. The first conclusion is that in order to see a mid-latitude response to a tropical heating, a mean zonal wind which allows some of the heating to lie in mean westerlies must be included. When our model was forced with a tropical heating in a resting basic state, we found the response was restricted to the tropics. This coincides with the results of Gill (1980). However, when a mean zonal wind was included, we found that if

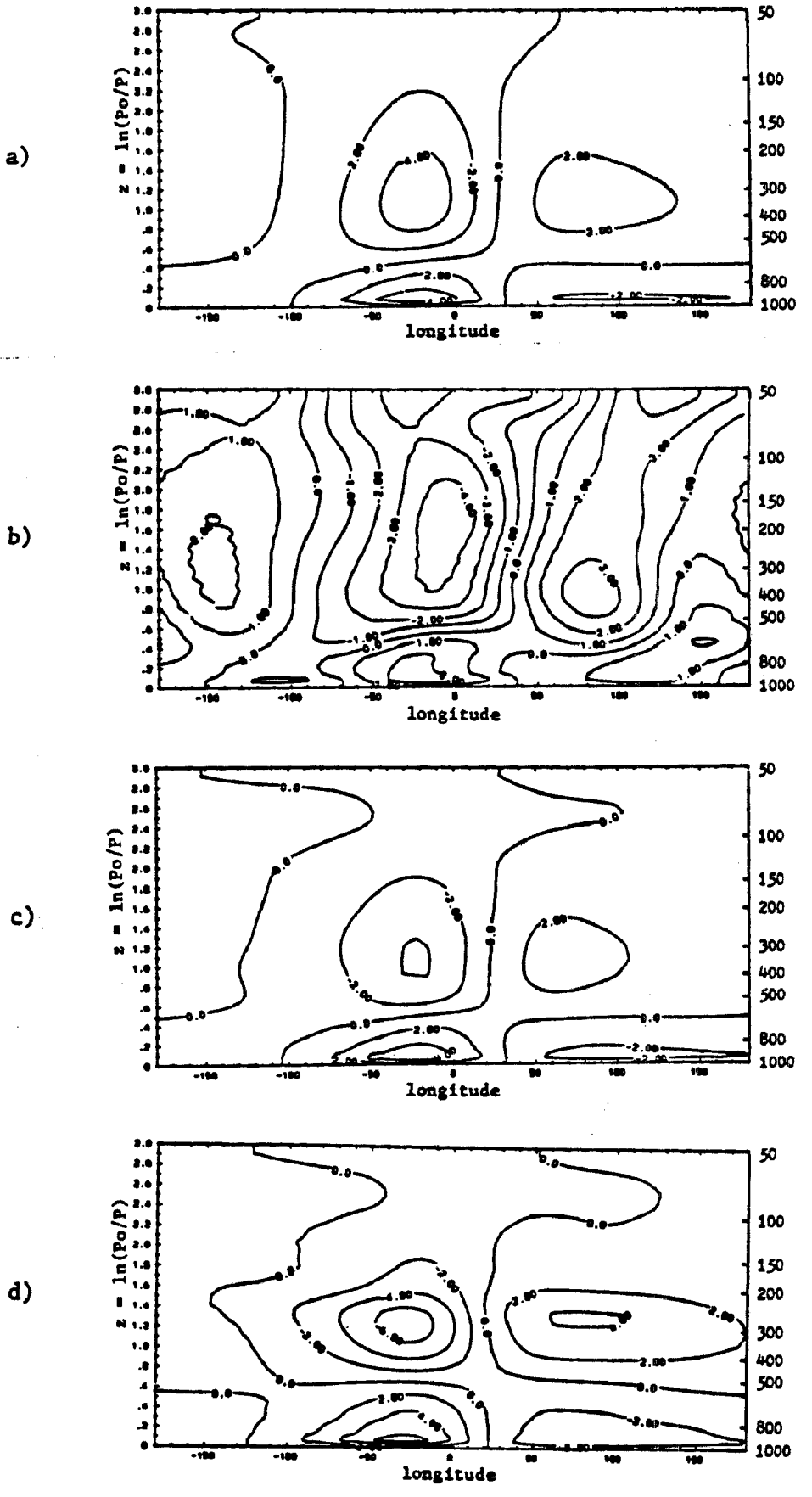

Fig. 5-26. Perturbation u field at 9°N with the heating centered at 9°N for a motionless basic state (a), a mean winter zonal wind basic state (b), a mean summer zonal wind basic state (c), a mean summer zonal and a Hadley cell centered at 9°N basic state.

a)

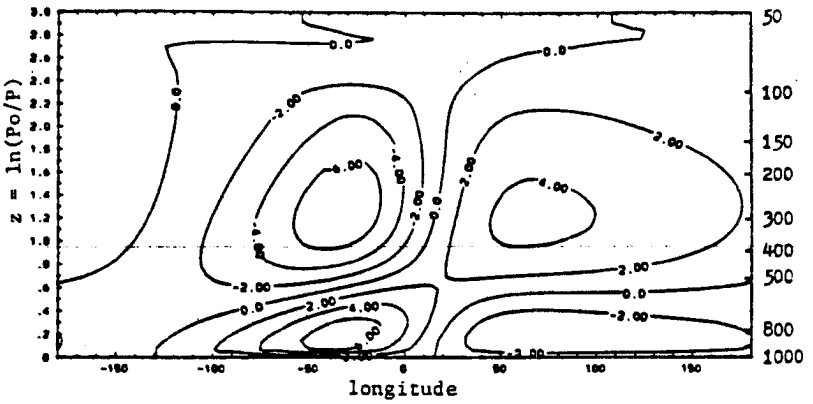

b)

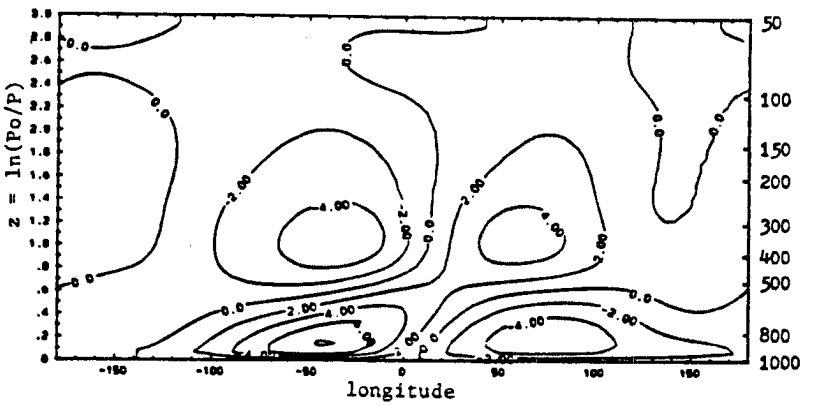

c)

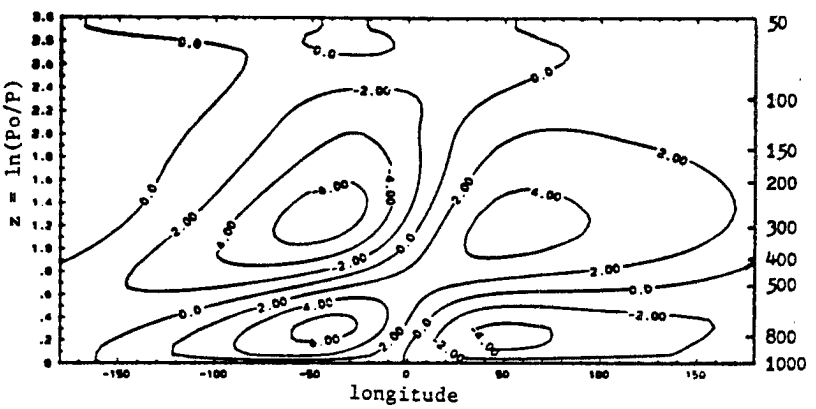

d)

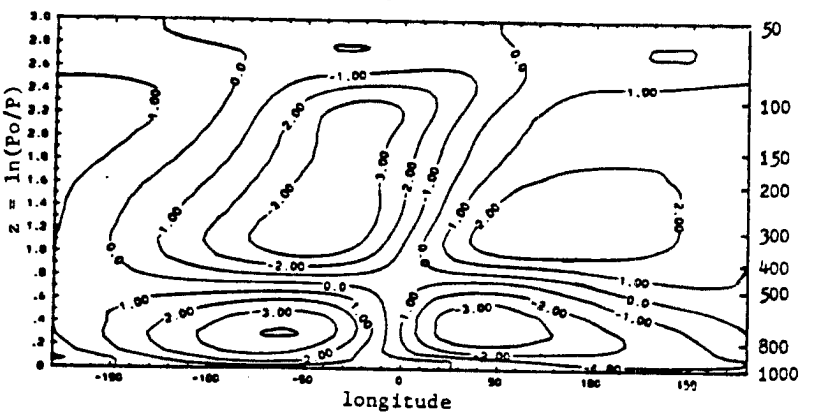

Fig. 5-27. As in Fig. 5.26 except at the equator.

any of the heating was in weak westerlies, there was a higher latitude response. This agrees with the findings of Webster (1982) and Lindzen et al. (1982).

The second conclusion of this sensitivity study is that if a cumulus parameterization is included in a linear model, a mean Hadley cell should also be included in the basic state. When the terms in the u-momentum equation are examined, we find that advection by the mean vertical velocity field tends to be of similar magnitude but opposite sign from the largest magnitude cumulus friction term. Including the mean Hadley cell also tends to cause a rise in the level of zero wind in the Walker Circulation which makes it appear more like the observed circulation. In addition, the inclusion of a mean Hadley cell with a summer mean zonal wind basic state which consists of deep easterlies in the tropics, brings about an enhanced mid-latitude response. Advection by the mean Hadley cell seems to transmit information about a tropical heating to higher latitudes.

6. Inclusion of the wavenumber zero response

Up to this point, the wavenumber zero response has not been considered in any summations. This has been done because of the definition of the Walker Circulation as the deviation of the wind wind field from the zonal average (Newell et al., 1974). It would then be the response to a deviation of precipitation from the zonal average and therefore, there would be no mean or wavenumber zero response. However, the perturbation heating profile used for this study is actually fairly broad. For the cases when wavenumber zero is not considered, the positive anomaly covers roughly one quarter of the distance around the globe. Although over the entire globe there is no net heating, in the region where the Walker Circulation occurs, there is a net positive heating. It may be that the response we are relating to the observed Walker Circulation actually has a wavenumber zero component. The wavenumber zero response will take the form of a pair of Hadley cells. In the study of Gill (1980), he found that for his symmetric heating, the east-west circulation is about five times that in each Hadley cell, or, for the heating used, the Walker Circulation response dominates.

In order to see how the character of the response differs when wavenumber zero is included, four cases will be considered and compared to similar cases without wavenumber zero. For these additional summations, the distribution of the perturbation heating will be as given for the equatorial heating cases discussed previously except the

amplitude of the heating will give a precipitation rate of 1.6 m/yr. This added onto a mean precipitation rate of 2.6 m/yr will give a maximum of 4.2 m/yr as was used for the summations that did not include the wavenumber zero response. The four cases to be compared will include a run a motionless basic state and no cumulus friction, a motionless basic state with cumulus friction, a mean winter zonal flow, and a mean winter zonal flow with a mean Hadley cell centered on the equator. These cases are summarized in Table 6.1.

Table 6.1. Experiments including wavenumber zero

Run	Basic State	Dissipation
A	rest	$\alpha_R^{-1} = \alpha_N^{-1} = 20$ days, no $\bar{M}_c$
B	rest	$\alpha_R^{-1} = \alpha_N^{-1} = 20$ days, $\bar{M}_c$
C	winter zonal flow	$\alpha_R^{-1} = \alpha_N^{-1} = 20$ days, $\bar{M}_c$, M_c'
D	winter zonal flow equatorial Hadley cell	$\alpha_R^{-1} = \alpha_N^{-1} = 20$ days, $\bar{M}_c$, M_c'

When the upper level flow for the case without cumulus friction, experiment A, is compared with the flow for the similar summation excluding wavenumber zero (Fig. 6.1), three differences are apparent. The first is that the divergence of the perturbation u field is decreased from that of the run summing wavenumbers one through ten. This is entirely due to the change in amplitude from 2 m/yr precipitation for the case excluding wavenumber zero to 1.6 m/yr when it is included because the amplitude of the u' response for wavenumber zero is identically zero on the equator. The second significant difference is the presence of a westerly jet near 20° for the case including wavenumber zero. This is exclusively a wavenumber zero response. The third

a)

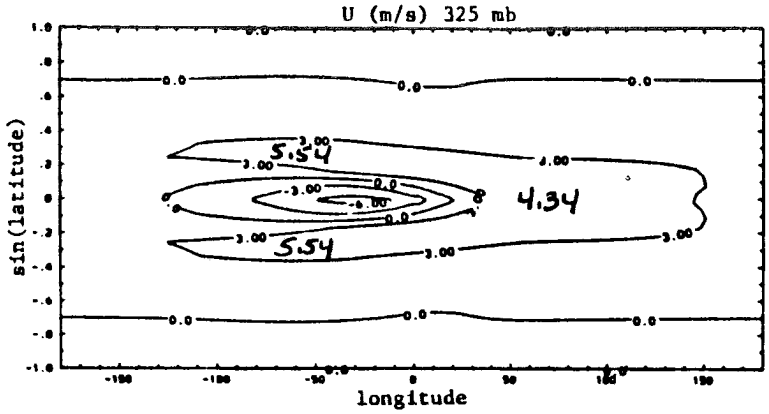

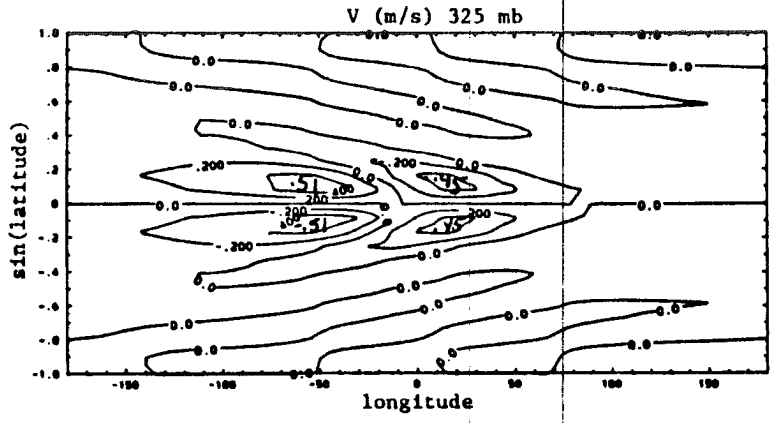

b)

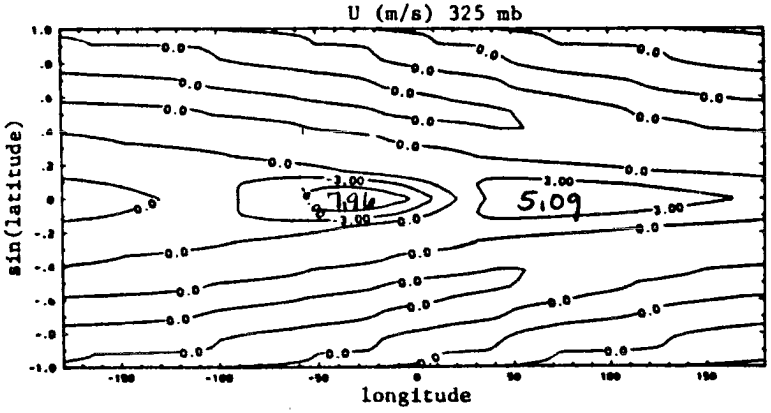

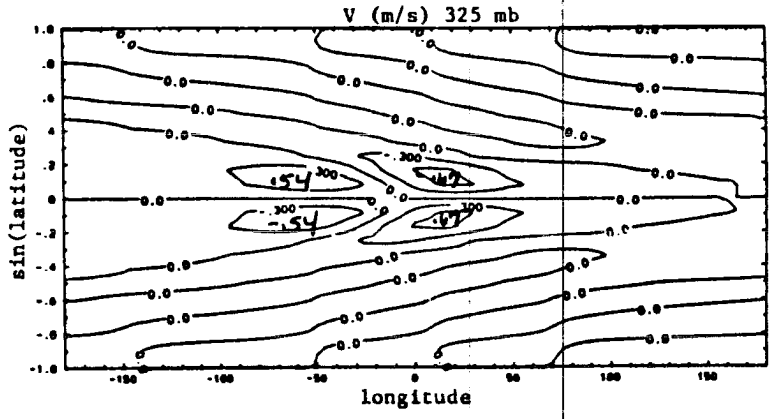

Fig. 6-1. Perturbation wind response for a motionless basic state with no cumulus friction for a summation of wavenumbers 0-10 (a), and for a summation of wavenumbers 1-10 (b).

major difference is that the meridional overturning to the east of the heat source which acts contrary to a Hadley cell is weakened and covers a smaller area. This resulting circulation between 11° N and 11° S resembles somewhat the circulation Gill (1980) obtained in his study. This circulation consists of a predominately zonal wind response to the east of the heating and two antisymmetric circulations on a constant pressure surface centered just to the west of the heating center on either side of the equator.

An examination of the other cases considered yields essentially the same conclusion. For the run with a motionless basic state which includes cumulus friction, experiment B, again there is no wavenumber zero response on the equator (Fig. 6.2) so the changes in the magnitude of the zonal wind divergence are due entirely to the change in the amplitude of the perturbation heating. The jets that did exist near 20° are strengthened and the meridional overturning east of the heating is weakened. These same differences also hold for the run with a mean zonal wind, experiment C, and the run which includes a mean Hadley cell with the mean zonal wind, experiment D (Fig. 6.3).

With the 40° e-folding width perturbation heating used here, the wavenumber one response dominates. However, if the heating is of a broader longitudinal extent, the wavenumber zero response will become more important. A broader heating field would be expected in the Pacific during an El Niño event when the sea surface temperatures in the eastern Pacific are significantly warmer than normal. Presumably, by some mechanism not well understood, this sea surface temperature information would be transmitted to the atmosphere and cause increased cloudiness and rainfall, thereby heating the atmosphere through condensational processes. With this broader heating, we would expect to see

a)

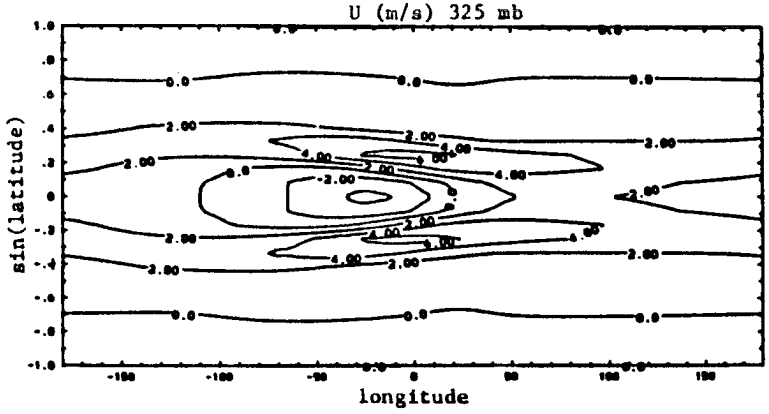

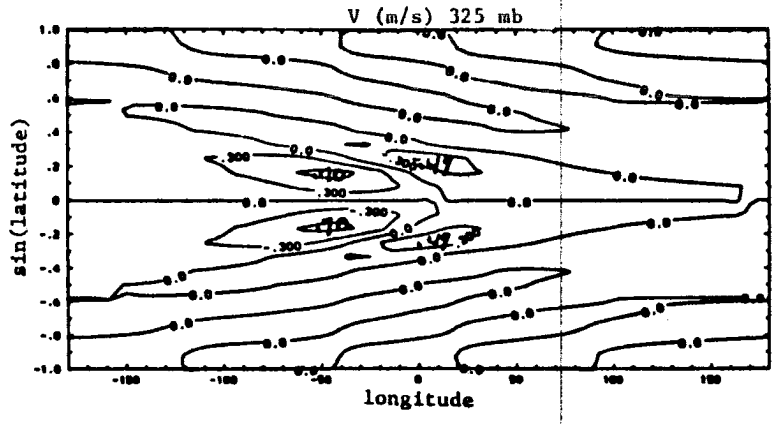

b)

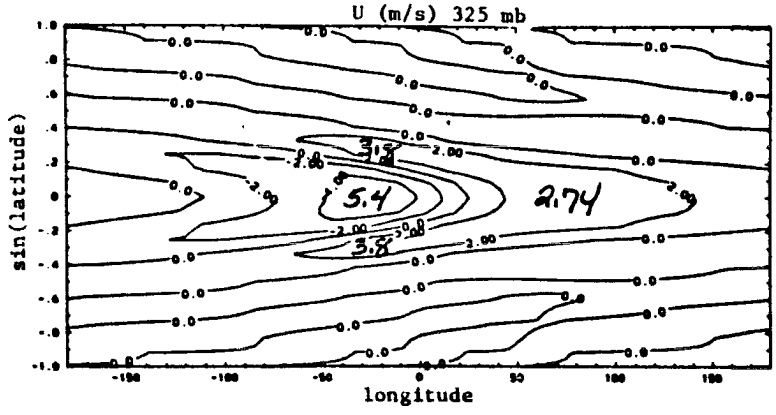

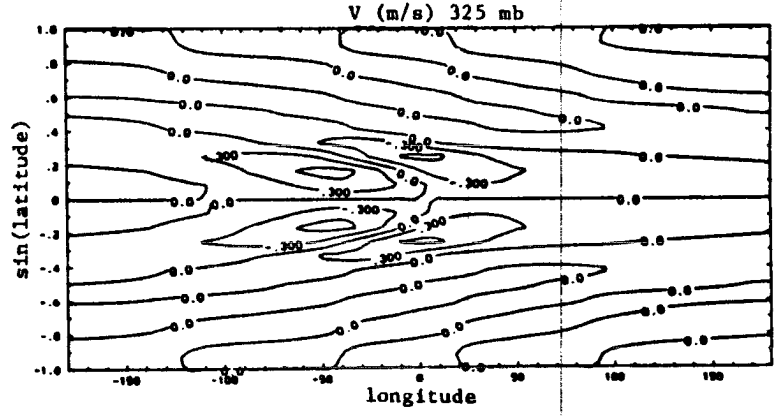

Fig. 6-2. As in Fig. 6.1 for a motionless basic state including cumulus friction.

a)

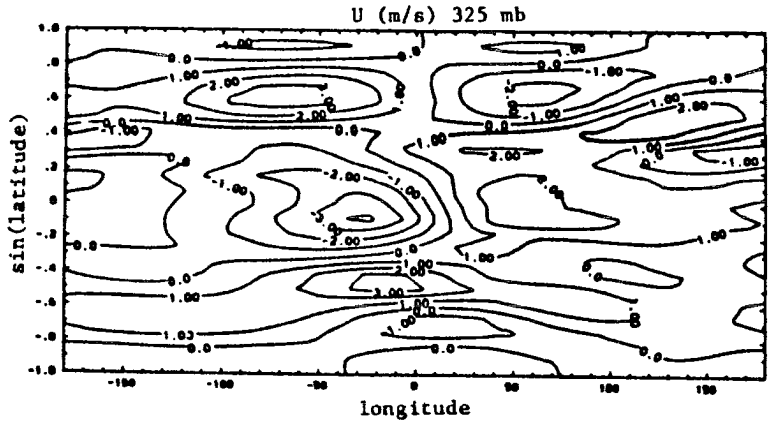

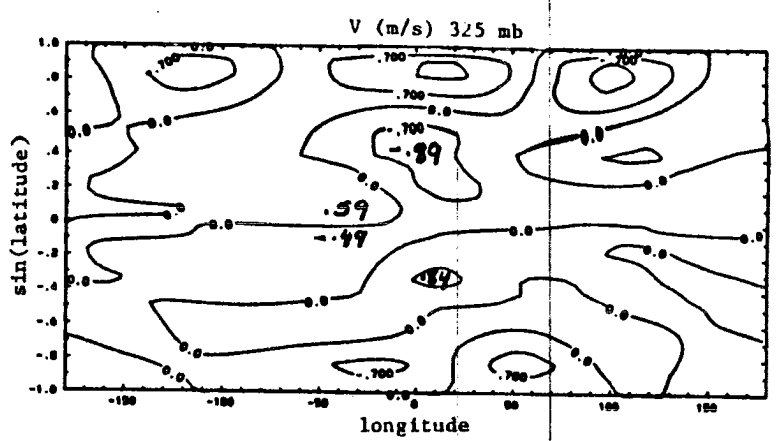

b)

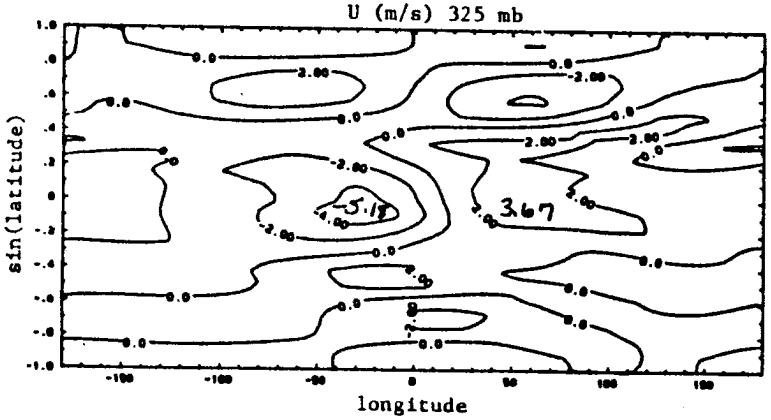

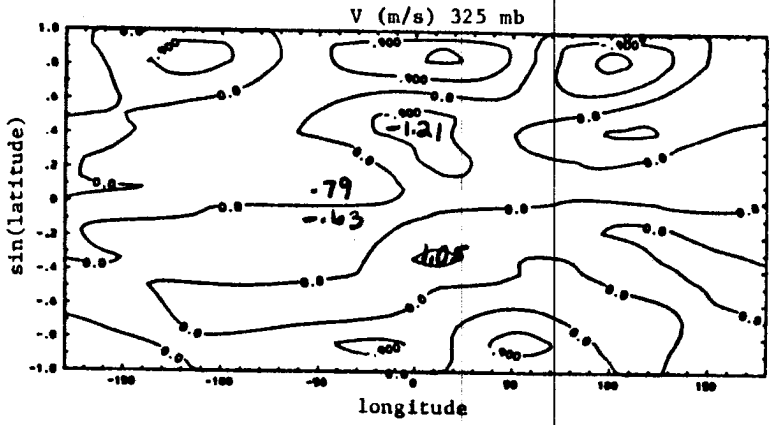

Fig. 6-3. As in Fig. 6.1 for a basic state consisting of a mean winter zonal wind and a Hadley cell centered on the equator.

less of Walker Circulation response and more of a Hadley cell type response.

In a run with our model where the e-folding width was changed to 80°, it was found that the region of positive vertical velocities on the equator nearly doubled, going from 105° to 180°, while the region of sinking in the subtropics increased. If we assume the center of the heating is on the western edge of the Pacific, that would mean that the perturbation vertical velocity is positive over 70% of the equatorial Pacific. There also exists perturbation westerlies in a band from 10° to 45° latitude above 500 mb. These are approximately 65% stronger than for the narrower heating.

Bjerknes (1966) observed that during a period of time with anomalously warm sea surface temperatures along the equatorial Pacific, there were record intensity westerlies in the eastern north Pacific. He hypothesized that a warmer than normal equatorial ocean over a broad range of longitude would intensify the Hadley circulation in that region. This would in turn transport westerly absolute angular momentum to the subtropical jet stream at a faster than normal rate which would create stronger mid-latitude westerlies.

In this present study we find that with a broad heating, the strongest intensification of the upper level westerlies would occur in the western Pacific at about 20° latitude in the winter hemisphere. However, we also find some pertubation westerlies in the eastern Pacific. The greatest intensification in the upper level westerlies occurs about 40° east of the largest pertubation meridional velocity response that acts in the sense of a Hadley cell and at the same longitude of the maximum vertical velocity response. This then supports

Bjerknes' theory that an increase in the Hadley cell can bring about an increase in higher latitude westerlies. However, for our case this occurs where the perturbation heating is a maximum. Since we consider the center of the perturbation heating to be in the far western Pacific where precipitation is observed to be a maximum, we find the phenomena Bjerknes (1966) refers to occuring in the western Pacific much more so than in the eastern Pacific. However, in the case of an El Niño event the heating center is farther to the east (Shukla and Wallace, 1983), so our findings might coincide with Bjerknes' theory. Regardless, to find these results at all, the wavenumber zero response is critical.

In summary, we find that as the perturbation heating becomes of broader longitudinal extent, the wavenumber zero response becomes more important. Thus, in order to model the effects on the Walker Circulation and higher latitude responses due to a broad tropical heating such as would occur during an El Niño event, the wavenumber zero response must be considered in a linear model.

7. Conclusions

The main intent of this study has been to assess the effects changes in the basic state will have on the response of a linear, spherical, primitive equation model forced with a tropical heat source. In reality, the phenomena being studied is probably not adequately represented by linear assumptions. However, the simplicity of a linear model allows us to better understand what causes our results and permits us to compare our results with previous linear studies.

The heat source used for this study was chosen to give a model circulation that can be compared to the observed Walker Circulation. Regardless of the mean state used, the model produces a response that qualitatively resembles a Walker circulation. That is, there is a maximum rising motion over the maximum heating and a convergence of the zonal wind in lower levels with an associated divergence of the zonal wind in upper levels. The circulation produced to the east of the heating in our model is of broader longitudinal extent than that to the west of the heating. This parallels what has been observed in other linear studies (Gill, 1980; Geisler, 1981), and compares favorably with the observed circulation. Gill (1980) interpreted this result in terms of Kelvin and Rossby waves. If the heating is turned on at an initial time, Kelvin waves would move rapidly eastward at a rate roughly three times that of the fastest moving westward Rossby waves. This would create a broader region of perturbation easterlies to the east of the

source, and a narrower region of perturbation westerlies west of the heat source. Our model runs which include wavenumber zero resemble Gill's (1980) results. The inclusion of wavenumber zero reduces the perturbation meridional velocity east of the equator so that it appears more like a Kelvin wave.

The zonal flow consisting of the summation of wavenumbers one through ten east of the heating tends to be weaker than that west of the heating. The model circulation east of the heating is weaker more so than occurs in the observed circulation pictured in Newell et al. (1974). In addition, although the observed circulation is of broader longitudinal extent east of Indonesia, the ratios between the longitudinal size of the perturbation easterlies to that of perturbation westerlies is smaller than for the model circulation. In fact, the resulting model response covers most of the globe while the observed Walker circulation does not.

In reality, there are other local maxima in precipitation around the globe which would in turn be accompanied by heating maxima not included in this model study. If a complicated heating function was used to adequately model the observed precipitation in the tropics, there would undoubtedly be changes in the longitudinal extent covered by the east-west circulation produced. Other factors, such as influences of topography and nonlinear interactions, may act to give the observed Walker Circulation its exact appearance. A recent study by Chervin and Druyan (1984) using a coarse-mesh climate model showed that the removal of South America and its associated convective activity caused significant changes in the resulting circulation. However, we conclude, as previous researchers have done, that a circulation similar to that of

the observed Walker circulation is produced by an Indonesian heat source.

Although a Walker-type circulation is produced when forcing a resting basic state with a tropical heat source, there are differences in response when different basic states are included. Two major differences can be noted. The first is that in order to see a mid-latitude response with a tropical heating in a linear model, mean zonal winds must be part of the basic state. When a mean zonal wind is included, we find there are subtle changes in the model Walker Circulation, while there are significant changes in higher latitude responses. Including a mean Hadley cell brings about a second major change in response. The inclusion of a mean Hadley cell lifts the level of zero perturbation zonal winds on the equator in runs which also include a mean cumulus mass flux. In fact, an examination of the magnitude of terms in the u-momentum equation shows that advection by the mean vertical velocity field is a major term and of opposite sign from the largest magnitude cumulus friction term, $-\frac{g}{p}\frac{\partial}{\partial z}(\bar{M}_c u')$. In addition, including a mean Hadley cell when the zonal wind in which the tropical heating is embedded consists primarily of easterlies, we find an enhanced mid-latitude response.

When cumulus friction is included without including a mean vertical velocity in a linear model, effectively half of the process we are trying to parameterize is left out. Because observations indicate that between cloud subsidence is small, it is unlikely that there would be a mean cumulus mass flux without a mean vertical velocity in the ITCZ. Thus, to obtain realistic model results when a cumulus mass flux parameterization is used, a basic state which includes a mean vertical velocity should also be used.

Another effect that is produced as a result of including cumulus friction is that the winds tend to be damped in the vicinity of the heating. In fact, a westerly jet response in the upper levels occurs about 20° of latitude away from the heating center. This does not occur when a constant Rayleigh friction is used throughout the model domain. These significant differences produced using different dissipation parameterizations indicate that perhaps more research needs to be done on the adequacy of different friction parameterizations.

The attempt in this study to create a model Hadley cell using an analytical stream function is very simplistic. Ideally, there needs to be a model Hadley cell that is a response to a mean heating and a mean cumulus mass flux that is computed at the same time which is consistent with the mean vertical velocity field. However, our simplistic Hadley cell gives a result that shows the advective processes of a mean Hadley cell are important in the atmospheric response to a tropical heat source. Specifically, we find that when a mean Hadley cell is not included in the basic state, the zero wind level of the model Walker Circulation is much lower than observed. We also find that when a mean Hadley cell is included for the case of a heating embedded in mean easterlies, an enhanced mid-latitude response occurs.

References

Anderson, J.R., 1984: Slow motions in the tropical troposphere. Atmospheric Science Paper No. 381, Colorado State University, Dept. of Atmos. Sci., Fort Collins, CO, 142 pp.

Bjerknes, 1966: A possible response of the atmospheric Hadley circulation to equatorial anomalies of ocean temperature. Tellus, 18, 820-829.

_____, 1969: Atmospheric teleconnections from the equatorial Pacific. Mon. Wea. Rev., 47, 163-172.

Chervin, R.M., and L.M. Druyan, 1984: The influence of ocean surface temperature gradiant and continentality on the Walker Circulation. Part I: Prescribed tropical changes. Mon. Wea. Rev., 112, 1510-1523.

Cornejo-Garrido, A.G., and P.H. Stone, 1977: On the heat balance of the Walker Circulation. J. Atmos. Sci., 34, 1155-1162.

Geisler, J.E., 1981: A linear model of the Walker Circulation. J. Atmos. Sci., 38, 1390-1400.

Gill, A.E., 1980: Some simple solutions for heat induced tropical circulations. Quart. J. Roy. Meteor. Soc., 106, 447-462.

Hartmann, D.L., H.H. Hendon, and R.A. Houze, Jr., 1984: Some implications of the mesoscale circulations in tropical cloud clusters for large-scale dynamics and climate. J. Atmos. Sci., 41, 113-121.

Julian, P.R., and R.M. Chervin, 1978: A study of the Southern Oscillation and the Walker Circulation phenomena. Mon. Wea. Rev., 106, 1433-1451.

Lau, K., and H. Lim, 1982: Thermally driven motions in an equatorial β-plane: Hadley and Walker circulations during the winter monsoon. Mon. Wea. Rev., 110, 336-353.

Lindzen R.S., T. Asu, and D. Jacquim, 1982: Linearized Calculations of stationary waves in the atmosphere. J. Met. Soc. Japan, 60, 66-77.

_____, and H.O. Kuo, 1969: A reliable method for the numerical integration of a large class of ordinary and partial differential equations. Mon. Wea. Rev., 97, 732-734.

Newell, R.E., J.W. Kidson, D.G. Vincent, and G.J. Boer, 1972: The general circulation of the tropical atmosphere and interaction with extratropical latitudes. Vol 1, MIT Press, 258 pp.

_____, 1974: The general circulation of the tropical atmosphere, Vol. 2, MIT Press, 371 pp.

Rowntree, P.R., 1972: The influence of the tropical east Pacific ocean temperatures on the atmosphere. Quart. J. Roy. Meteor. Soc., 98, 290-321.

Shukla, J., and J.M. Wallace, 1983: Numerical simulation of the atmospheric response to equatorial Pacific sea surface temperature anomalies, J. Atmos. Sci., 40, 1613-1630.

Stevens, D.E., and P.E. Ciesielski, 1984: A global model of linearized atmospheric perturbations: Model description. Atmospheric Science paper No. 377, Colorado State University, Dept. of Atmos. Sci., Fort Collins, CO, 86 pp.

_____, R.S. Lindzen, and L.J. Shapiro, 1977: A new model of tropical waves incorporationg momentum mixing by cumulus convection. Dyn. Atmos. Oceans, 1, 365-425.

U.S. Standard Atmosphere Supplements, 1966, U.S. Government Printing Office, Washington, D.C., 289 pp.

Webster, P.J., 1972: Response of the tropical atmosphere to local steady forcing. Mon. Wea. Rev., 100, 518-541.

_____, 1981: Mechanisms determining the atmospheric response to sea surface temperature anomalies. J. Atmos. Sci., 38, 554-571.

_____, 1982: Seasonality in the local and remote atmospheric response to sea surface temperature anomalies. J. Atmos. Sci, 39, 41-52.

APPENDIX A

LIST OF SYMBOLS

CD	surface drag coefficient
C_p	specific heat of air at constant pressure
H	$\frac{RT}{g}$, scale height
M_c	cumulus mass flux
Q	diabatic heat source
R	gas constant for dry air
T	temperature
T_o	surface temperature (300°K)
V	horizontal velocity vector
V_o	gustiness factor (8 m/s)
a	mean radius of the earth (6.37×10^6m)
f	$2\Omega\sin\theta$, coriolis parameter
g	gravitational acceleration
p	$p_o e^{-z}$, pressure
p_o	surface pressure (1000 mb)
s	longitudinal wavenumber
t	time
u	$a\cos\theta \frac{d\lambda}{dt}$, zonal velocity component
u_c	u-component of the wind at the base of the momentum detrainment layer
v	$a \frac{d\theta}{dt}$, meridional velocity component

v_c v-component of the wind at the base of the momentum detrainment layer

w $\frac{dz}{dt}$, vertical velocity component

y $\sin(\theta)$

z $\ln (P_o/p)$, vertical coordinate

z_c height of the base of the momentum detrainment layer

Ω angular speed of rotation of the earth

α_N Newtonial cooling coefficient

α_R Rayleigh friction coefficient

θ latitude

κ R/C_p

λ longitude

$\mu^\dagger$ dynamic coefficient of viscosity

$\hat{\mu}^\dagger$ dynamic coefficient of thermal diffusion

ν $\frac{\mu\dagger}{\rho}$, kinematic coefficient of viscosity

$\hat{\nu}$ $\frac{\hat{\mu}}{\rho}$ kinematic coefficient of thermal diffusion

p density

σ angular frequency

ϕ geopotential height

Ψ stream function